UNIVERSITÀ DEGLI STUDI DI PADOVA

Head Office: Università degli Studi di Padova

Department of Biology

---

Ph.D. COURSE IN: Biosciences

CURRICULUM BIOCHEMISTRY AND BIOTECHNOLOGY

SERIES XXXIV

# The mitochondrial nucleoid-binding protein WHIRLY2 plays a key role in plant development and stress responses.

**Coordinator:** Prof. Ildikò Szabò

**Supervisor**: Prof. Michela Zottini

**Ph.D. Student**: Yuri Luca Negroni

# Table of Contents

# Summary

During the three years of PhD, I investigated the WHIRLY2 function and impact during plant growth. WHY2 is among several mitochondrial proteins involved in mtDNA replication and in non-homologue recombination avoidance and repair (e.g. OSB1, OBD1, SSB1, MSH1). The redundancy of these proteins is an indication of the importance of the control on these processes. Recent studies are unveiling a more complex role for them, having an impact not only on DNA replication but also on some aspects of plant development and in environmental sensing.

Mitochondrial ss-DNA binding proteins seem not involved in plant growth when the primary root, rosetta and flower development parameters have been analysed. A more detailed analysis reported a high transcriptional expression of *WHY2* during the early stages of embryo development as well as during the development of pollen. Furthermore, it has been observed that the absence of WHIRLY2 can cause problems during developmental phases in which high cell replication rate and high-energy demand are required.

To allow proper mitochondrial division, mtDNA replication is increased during these stages in order to provide organelles with a complete and organized genetic endowment. We reported that the knockout of WHY2 is enough to cause an increase in embryonic abortion and failure in germination.

The function of this protein under normal growth conditions was investigated by comparing WT to mutant lines, in which disorganization at the level of the mitochondrial nucleoid was observed. In addition, an increase in mtDNA damages, not supported by an increase in mtDNA copy number was reported when WHY2 knock-out lines were exposed to a genotoxic agent. On the other hand, in stressful conditions when mitochondrial activity becomes fundamental as main energy source and as stress sensing, the absence of WHY2 causes an increase in aberrant mtDNA products, in the disorganization of the nucleoids and also in mtDNA copy number. This mechanism could be part of the signal communication system between the mitochondrion and the nucleus. The importance of WHY2 has been confirmed by observing knock out plant growth during prolonged salt stress: there show a delay in the primary root growth, in germination and in plant survival.

In addition, we hypothesized a second role for WHY2 as a possible player in retrograde signalling (RS). Several factors involved in this communication mechanism were analysed in plants exposed to salt stress, comparing the response of WT and mutant lines. Our results highlighted a delay in the RS response in mutant line, and consequently an increase in the intracellular ROS accumulation and in oxidative damage mirrored by a stronger induction of the ROS-regulated genes (*mtHSC70-1* and *WRKY15*). A misperception of salt stress and ROS (and thus an inefficient response) is further supported by enzymatic activity and energy production assays. More and more recent studies are hypothesizing the involvement of WHIRLY proteins in the retrograde signalling pathway, this work indeed shows that *WHY2* role is not restricted to the organelle DNA replication and repair.

In conclusion, mitochondria and mitochondrial proteins are required during the entire plant life cycle and during stress responses, playing fundamental in several processes.

Increasing knowledge in this research field will become more and more relevant in the next future for its possible applications in crop production and yield increase.

# Abstract

In the last few years, the importance of organelles as central coordinators of plant responses to internal/external stimuli has become increasingly important. Mitochondria have a fundamental role in energy production, but play also a role as stress sensors of environmental stimuli, being a component of a complex communication network between organelles and nucleus. WHIRLYs are plant-specific proteins that have been characterized as ssDNA-binding proteins because of a characteristic conserved DNA-binding domain. In *Arabidopsis*, the WHIRLY family includes three members: WHIRLY1, WHIRLY2 and WHIRLY3, presenting specific target sequences that localize them in the plastids and nucleus (WHIRLY1, WHIRLY3) or in the mitochondria (WHIRLY2). WHY2 among the proteins involved in mtDNA repair is the most abundant and evidences suggest an important role of it in mitochondrial genome replication necessary to complete mtDNA activity. Recent results on WHY2 show a link between mtDNA stability and proper mitochondrial morphology, dynamics and functionality, indicating a fundamental role of this protein in mitochondrial activity during development and stress responses. Failure in maintaining the mitochondrial genome stability results in the accumulation of mutations and genomic rearrangements that can become deleterious. In the present work data are reported showing the relationship between mtDNA maintenance, high levels of WHY2 and the response to abiotic stress. Evidences show that WHY2 plays a role in the response to different abiotic stresses. Our results also suggest an involvement of WHY2 protein in retrograde signalling in response to abiotic stresses. The study of mitochondrial proteins, as WHY2, contributes to open up a new conception of the role of mitochondria as a stress response centre and to unveil molecular mechanisms underlying the communication between mitochondria and nucleus in response to stress.

# Introduction

## 1.1 Plant bioenergetic organelles

Plants are unique organisms provided with different intracellular organelles: unlike animals their cells contain not only mitochondria, the centre of energy production (ATP), but also chloroplasts as main organelles. Mitochondria have a multitude of roles and are fundamental not only for providing the cell with the energy required for their functioning, but also for allowing a proper response to a wide range of stresses and environmental stimuli. In addition, they play a role in deciding the fate of the cell by regulating programmed cell death. Chloroplasts are organelles in which photosynthesis takes place, converting lights (photons) energy into complex molecules such as sugars, used in ATP-producing metabolic pathways like glycolysis and the Krebs cycle. Chloroplasts and mitochondria cooperate in basic energy producing processes and both contribute to retrograde signalling (a communication mechanism between organelles and nucleus) during high energy-demanding growth phases and in response to stress (Crawford et al., 2018). This unique system of plant cells provides the opportunity to study intraorganellar communication mechanisms between nucleus and organelles and a possible communication mechanism between mitochondria and chloroplasts. Photosynthesis and respiration are, in fact, interrelated processes as well as mitochondrial and chloroplasts functionality and their biogenesis is dependent on each other.

These two intracellular organelles have evolved from bacteria through endosymbiosis, a process in which an organism evolves to live in symbiosis inside its host. This endosymbiosis process likely originated as an initial fusion of two prokaryotic cells, probably between a bacterium and an archaea, turning into a close living relationship after a long period of metabolic interconnection between the two cells. Biochemical and structural analyses suggest mitochondria descended from an α-proteobacterium-like ancestor that invaded or was engulfed by an archaeal-like host 1.5 billion years ago or earlier. Subsequently, there was a second colonization of these new eukaryotic cells with prokaryotes containing chlorophyll, which, over the time, became the current chloroplasts. Mitochondria and chloroplasts have their own genome and have the ability to maintain genetic information across generations. Over time the retention of the organellar genome has changed. During the co-evolution period, most of the protein-coding genes have been transferred from the mitochondria to the nucleus, that is now carrying the wider part of organellar genetic information. Nowadays, plant organelle genomes are severely reduced, in fact, more than 95% of organelle proteins are encoded by nuclear-located genes. For instance, *Arabidopsis thaliana* mitochondrial DNA (mtDNA) encodes 32 proteins, 3 ribosomal RNAs (5S, 18S and 26S rRNAs) and 22 tRNAs (Unseld et al., 1997; figure 1.1), a very small number when compared to the 1500 proteins localized in mitochondria (Woodson and Chory, 2008). The same process happened for chloroplasts during evolution. The chloroplast genome contains 112 unique genes, 16 of which are duplicated in the

inverted repeat (figure 1.1). Of the 112 unique genes, 78 are predicted protein-coding genes, 4 are ribosomal RNA genes and 30 are tRNA genes (Supriya and Priyadarshan, 2019).

Chloroplasts are composed by an envelope of two membranes which encompass a third complex membrane system, the thylakoids, including grana and lamellae. Their dimension goes from 5-10 µm to 3-4 µm. The chloroplast movements should be appropriately regulated by environmental signals, such as light. Chloroplasts change their position in response to light, moving towards weak light to capture light efficiently (Suetsugu et al., 2016) and escape "chloroplast avoidance" in response to high light.

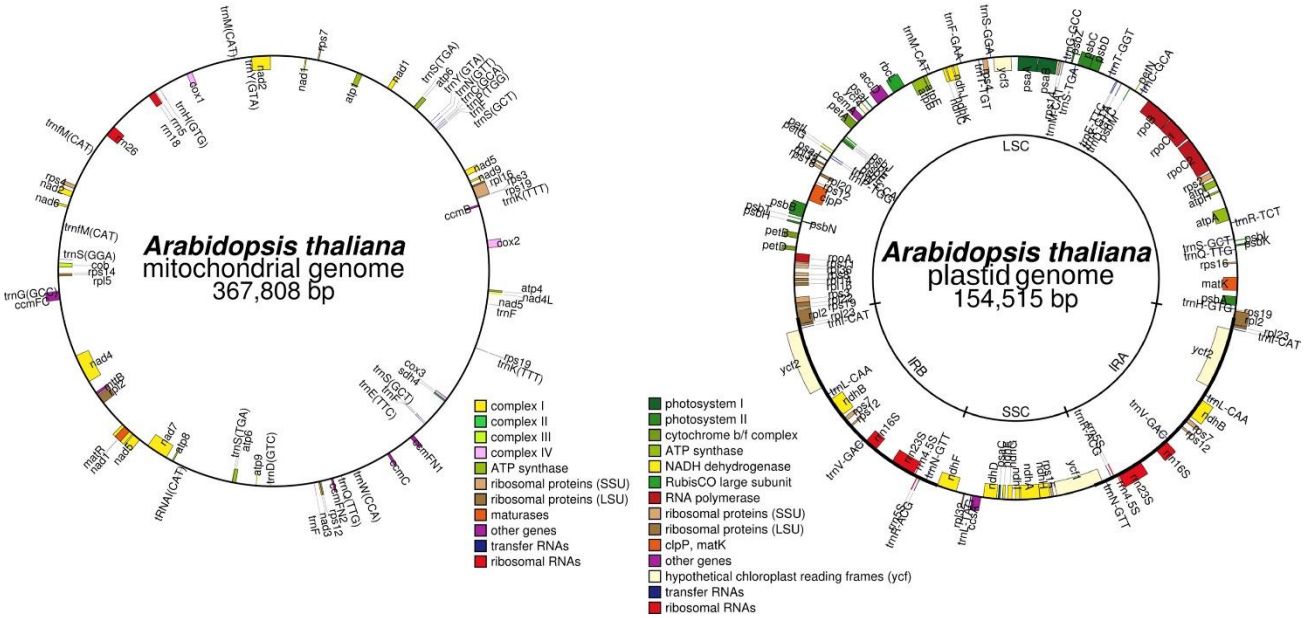


**Figure 1.1:** Organelles genomes in Arabidopsis. **(A)** Circular mapping of mtDNA (NCBI NC_037304), encoding some (not all) subunits of Complexes I–IV, ATP synthase, the mitochondrial ribosome, tRNAs, and rRNAs. The genome is much larger than the familiar 16 kb mammalian mtDNA, with large non-coding regions. **(B)** Circular mapping of ptDNA (NCBI KX551970), encoding some (not all) subunits of photosystem complexes, electron transport chain proteins, the plastid ribosome, tRNAs, and rRNAs. The genome is divided into large and small single copy regions (LSC and SSC) separated by inverted repeat regions IRA and IRB. From Johnston 2019.

Mitochondrial genome of animals and fungi is much smaller (around 16.5 kb in animals) and more packed than that of the plant, that is larger (from 200 kb to 11.3 Mb) and structurally more complex (Backert et al., 1997; Cupp and Nielsen, 2014; Taanman, 1999). In angiosperms mtDNA size is between 200 and 750 kb (Kubo et al., 2008).

Mitochondria in plants are 1-2 µm long and usually spherical with fast dynamics (figure 1.2): a high rate of fission and fusion is required to maintain functional mitochondria and to allow the sharing of proteins, metabolites and mtDNA (Paszkiewicz et al., 2017). The dynamic exchange and movement also allow the fast positioning of mitochondria in the areas of the cell where their functions are especially required and organellar proximity is needed in several metabolic pathways (Jones, 1986; Chustecki et al., 2021). Mitochondria can form dynamic, interconnected networks, regulated by an equilibrium of fusion and fission events that, in turn, determine the organelle number, size, shape, dynamics, and, most importantly, functionality. Alterations of the dynamics

and shape of mitochondria can be detrimental to the organism and strongly linked to genome instability (Hoppins, 2014; Prevost et al., 2018).

Given their origin, the intercommunication mechanism between nucleus and organelles must be tightly regulated to ensure the proper functioning of the intertwined system and to ensure no imbalance.

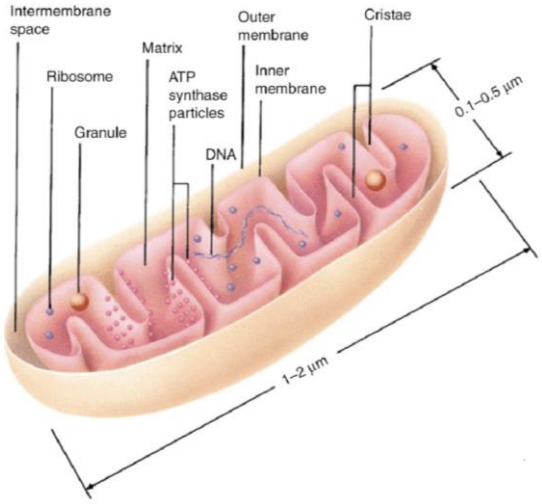


**Figure 1.2:** The internal structure of mitochondria. Mitochondria structure that comprises outer membrane, inner membrane, intermembrane space and matrix. From Frey and Mannella, 2000.

## 1.2 Mitochondrial DNA and its maintenance in plants

Like chromosomes, mtDNA is packed into discrete mtDNA-protein complexes referred to as nucleoids. In addition to its role as a mtDNA shield, nucleoid-associated proteins play a role in mtDNA maintenance and gene expression through either temporary or permanent association to mtDNA or other nucleoid-associated proteins (Doimo et al., 2020; Lee and Han, 2017). Nucleoids (nucleoproteins-DNA complexes, figure 1.3) are the sites where mitochondrial genome is packed and where replication, repair and transcription take place.

The mtDNA varies highly in plant cells: the length and its complex organization and structure can differ a lot between mitochondria of different tissues or developmental phases, and even in the same cell (Preuten et al., 2010). Moreover, there is often less than one copy of mtDNA per mitochondria, meaning that not all mitochondria contain DNA (Preuten et al., 2010). The mtDNA forms a mix of loop and linear-branches, rosette-like structures, and head-to-tail concatemers and can accordingly be found in many different structures (Backert et al., 1996; Bendich, 1996; Oldenburg and Bendich, 1996, 2001; Backert and Borner, 2000). Large repeated sequences appear to mediate high frequency, reciprocal DNA exchange that can result in subdivision of the genome into a multipartite configuration. In plant mitochondrial genome, where multiple pairs of repeats

are present, the recombination activity produces a complex, inter-recombining population of heterogeneous molecules (Fauron et al., 1995).

In plants, mitochondrial DNA replication is completely different compared to animals. Different populations of mtDNA co-exist in the same plant: this is caused by recombination events that happen between different DNA molecules on large repeats (usually interconvertible by homologue recombination) and by ectopic recombination between microhomology sites that are usually unreversible (Woloszynska et al., 2009). These events modulate the plasticity of plants mtDNA.

Given its complex organization and structure, the maintenance of correct replication and division of organellar DNA is one of the roles of the organelle itself, and it is crucial for the correct functioning. The replication process is recombination-dependent, and it particularly relies on homologue recombination driven by a high number of repeated sequences. The exact mechanism of plant mtDNA replication remains unclear. Plants most likely utilize multiple strategies in tandem to replicate their mitochondrial genomes (Cupp and Nielsen, 2014). Some of these mechanisms include recombination dependent replication (RDR) and/or a rolling circle mechanism similar to bacteriophage T4 DNA replication (Backert and Borner, 2000), as well as traditional bi-directional replication from specific origins of replication. The mtDNA can be observed as 'rosette' structures, these structures are due to a high frequency of recombination and replication that originate from recombination sites. Incorrect replication of mitochondrial DNA would damage mitochondrial dynamics and functionality creating aberrant sequences and molecules. For this reason, there is a redundancy in DNA repair proteins that localize into the mitochondria, like Organellar DNA-binding Protein 1 (ODB1), Organellar Single-stranded DNA-binding protein 1 (OSB1), MUTL protein Homolog 1 (MSH1), Single Strand DNA binding protein (SSB1), Whirly2 (WHY2). Among them, WHY2 was found to be the most abundant protein in *A. thaliana* mitochondria (Fuchs et al., 2019; figure 1.3).

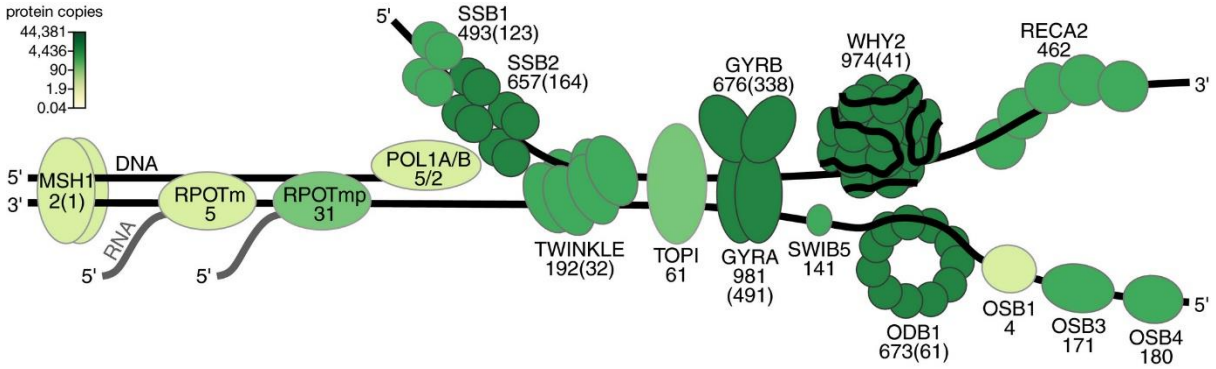


**Figure 1.3:** Proteins involved in plant mitochondrial nucleoids. RecA homolog 2 (RECA2); MutS homolog 1 (MSH1); organellar DNA-binding protein 1 (ODB1); organellar single-stranded DNAbinding protein (OSB1, OSB3, OSB4); T3/T7 bacteriophage-type RNA polymerase, mitochondrial (RPOTm); T3/T7 bacteriophage-type RNA polymerase, mitochondrial/plastidial (RPOTmp); Mitochondrial single-stranded DNA-binding protein (SSB1, SSB2); SWI/SNF protein complex B protein 5 (SWIB5); Type-IA DNA topoisomerase (TOPI), Twinkle-like DNA primase-helicase (TWINKLE); Whirly 2 (WHY2). From Fuchs et al., 2019.

The process of mitochondrial division is of particular importance since mitochondria cannot be created *de novo*, and must, therefore, be formed by the division of an existing organelle (Scott et

al., 2006). Mitochondrial fission and fusion, mtDNA replication, repair and homologue recombination are fundamental processes that allow a proper division and replication of mtDNA.

Mitochondrial fusion provides another opportunity for the exchange of mtDNA fragments whose integration occurs through recombination during the replication of mtDNA (Arimura, 2018). These processes are important for mitochondrial inheritance and for the maintenance of mitochondrial function.

A high degree of mitochondrial replication activity is linked to an increase in mtDNA structural complexity caused by the different mtDNA replication methods, that reflect an increase in mtDNA content per organelle. Mitochondria have to ensure a perfect expression of organellar DNA-binding proteins involved in the repair system to avoid non-homologue recombination that can generate aberrant and incomplete DNA products (Cheng et al., 2017). Massive mitochondrial fusion (MMF) plays an important role in plants, mainly during specific growth phases, for example flowering, in the embryo development and germination (figure 1.4), mixing the mitochondrial population and allowing proper mtDNA replication. MMF, in fact, ensures genome repair and a proper distribution of mtDNA between mitochondria, to secure a functional mitochondrial genome in each of them (Ray et al., 2021).

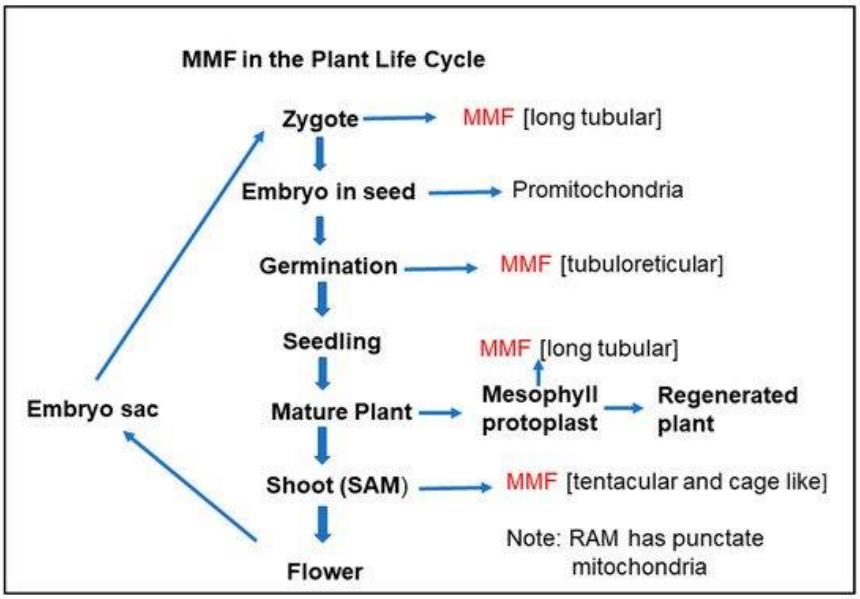


**Figure 1.4:** Massive mitochondrial fusion (MMF) in plant life cycle. From Ray et al., 2021.

There are many factors that can induce mtDNA damage. During growth, a high rate of mtDNA replication is required and it may lead to the formation of aberrant products, if not properly helped by the cell repair system. Environmental stresses may also impact on mtDNA integrity. Oxidative molecules (particularly Reactive oxygen species (ROS) such as peroxides and free radicals) can react with DNA bases causing mutations or strand breakage. Thus, an active DNA recombination system is crucial and allows the cell to correct mutations. In particular, high-frequency homologous recombination (HR) and base excision repair (BER) systems are required for efficient DNA repair in mitochondrial environment (Gualberto et al., 2014). In plants, HR has a fundamental role in many

processes, like primary DNA repair, mtDNA replication and segregation. Defects of such a system can lead to malfunctions of all these processes. Failure in maintaining the stability of mitochondrial genome results in the accumulation of mutations and in genomic rearrangements that, if not properly repaired or removed, can become deleterious for the whole organism (Gualberto and Kühn, 2014; figure 1.5). Aberrant mitochondrial DNA can cause the formation of aberrant genes that, in some cases, were found to lead to male sterility and other plant growth impairments (Chen and Liu, 2014).

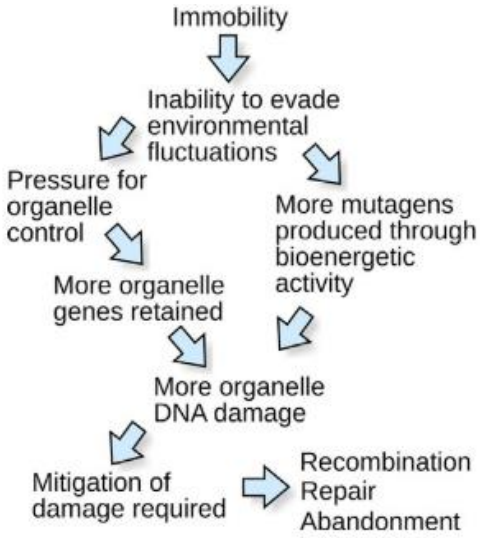


**Figure 1.5:** Plants are immobile and thus subject to greater environmental fluctuations than motile organisms. These fluctuations are hypothesized to lead to increased potential for organelle DNA damage through redox activity (ROS), and an increased pressure to retain organelle genes for CoRR or alternative sensing and control. From Johnston 2019.

In animal systems it has been suggested that the shape of mitochondria is strictly dependent on its DNA organization and integrity that are, in turn, reliant on many proteins and complexes involved in different nucleoids functions, structural and not (Ban-Ishihara et al., 2013). Moreover, in mammals it has already been proved that the organization of cristae strongly depends on the integrity of mtDNA/nucleoids (Ban-Ishihara et al., 2013). In plants such relation has only been speculated but not yet shown. Generally, the swelling of mitochondria can be explained by an impairment in the recruitment of fission proteins involved in the organelle division, while an elongated shape can be ascribed to an imbalance between fission and fusion (Yan et al., 2019). Moreover, in plants, mitochondrial dynamics are closely related to both organellar shape and DNA state: ongoing fusion and fission events, that reshape organelle morphology, are an important feature for maintaining mitochondrial plasticity and to provide a way for promoting recombination of DNA fragments (Arimura, 2018). MMF is likely to facilitate nucleoid transmission, mtDNA recombination, and the homogenization of mitochondrial components, thus providing a sort of quality control for mitochondrial populations (Rose and McCurdy, 2017).

## 1.3 Mitochondria in plant development

Organelles have a major role in intracellular energy production, that is the very foundation of all plant cells processes. Mitochondria occupy a central spot in the metabolic network of eukaryotic cells: they house many essential metabolic processes and several other pathways fundamental during plant development. In the last few years, the importance of these organelles is increased more and more: they are known not only as major energy producers but also to allocate resources, metabolites, and signals throughout the cell, becoming central coordinators of several responses such as plant development, metabolic pathways, and stress responses.

In plants, high motility of mitochondria is required to meet the changing energy requirements of the cells throughout different developmental stages and environmental conditions (Zottini et al., 2006). The regulation of mitochondrial network dynamics is critical for energy homeostasis, allowing the plant to respond rapidly and directly to acute metabolic perturbations balancing energy demand and production (Yu and Pekkurnaz, 2018). Indeed, this is more evident in those phases of plant life when high mitochondrial activity is particularly required, such as seed germination. In fact, early plant developmental phases are highly energy demanding, needing functional mitochondria to provide ATP. It has been observed that in tissues where a high cell division occurs (germinating seeds, embryo development, shoot apical meristems and pollen development), characterized by an active mtDNA synthesis, mitochondria have an elongated shape due to the dominance of the fusion over the fission process (Seguı´-Simarro et al., 2008; Paszkiewicz et al., 2017; Mogensen and Rusche, 1985; Mogensen et al., 1990).

The mitochondrial isoform of Muts homolog1 participates in DNA recombination surveillance in *A. thaliana*. Its absence results in enhanced mitochondrial genome recombination at the level of numerous repeated sequences. As a consequence, unusually large-sized mitochondrial shapes and compromised dynamics are detected (Xu et al., 2011). The absence of some mitochondrial nucleoids proteins are linked to alterations of mitochondria morphology and functionality during plant development. In conclusion, mitochondrial morphological changes can be induced by the cell itself to meet specific metabolic needs but can also be due to mutations and other detrimental processes, causing physiological and developmental alterations.

## 1.4 Mitochondria in stress response

Mitochondrial fission and fusion rate can be altered not only by a high energy demand during developmental phases but also by various stimuli related to stresses, as for example low oxygen, UV light and dark (Ramonell et al., 2001; Jaipargas et al., 2015; Gao et al., 2008). Under stress conditions, mitochondria clustering can be observed associated to mitochondrial reorganization and replication as well as to the sharing of compounds fundamental in mitochondrial activity necessary

to achieve stress acclimation. Under these circumstances, a reduced motility is observed while mitochondrial expansion is promoted (Pan et al., 2014). The clustering of fused mitochondria not only permits a reorganization of mtDNA, but also allows protein exchange to optimize ATP supply, needed in different zones of the cell. For example, during exposure to high NaCl concentrations, high cytosolic $Na^+$ causes a depolarization of mitochondrial membranes (affecting the transport of metabolites across the inner mitochondrial membrane) and induces the production of Reactive Oxygen Species (ROS) (Che-Othman et al., 2017). The negative membrane potential of functional mitochondria means that $Na^+$ in the cytosol will be drawn to accumulate inside the organelle, leading to excessive ROS production in mitochondria and loss of mitochondrial outer membrane potential caused by oxidative modification of the permeability transition pore. A high level of $Na^+$, in addition to causing osmotic stress, is also highly toxic to the cell: it affects TCA cycle (tricarboxylic acid cycle), several metabolic pathways and proteins functionality. For example, $Na^+$ competes with $K^+$ which is a co-factor of different enzymes, but also affects the mitochondrial activity caused by the membrane potential depolarization. During salt stress, ATP and reducing molecules are essential to drive reactions in the cell to prevent or reduce the severity of salt toxicity. Mitochondria fill this storage-and-supply role during stress response to cover the need for ATP and reducing molecules required for ion transport, compatible solutes biosynthesis (sugars and amino acids), and ROS detoxification in different compartments of the cell (Che-Othman et al., 2017).

In response to salt stress, tissue tolerance is achieved by regulating the cellular and intracellular $Na^+$ homeostasis, through ion exclusion and compartmentation, induced by the salt overly sensitive (SOS) pathway (Manishankar et al., 2018). During stress response, intracellular $Ca^{2+}$ homeostasis is altered generating a cytosolic signal defined as “calcium signature” that varies in frequency, amplitude and shape depending on the nature of the stimulus (Dodd et al., 2010). Calcium-dependent protein kinases (CDPKs), translate the information from $Ca^{2+}$ signatures into phosphorylation of specific target proteins and are therefore classified as sensor responders. Their function is to alter downstream target activities via $Ca^{2+}$-dependent protein-protein interaction. Calcineurin B-like proteins (CBLs) also have a role in mediating the output of calcium ion fluxes: upon calcium binding, they interact with a family of serine/threonine protein kinases designated as CBL-interacting protein kinases (CIPKs). CBL-CIPK complexes modulate the phosphorylation state of target proteins and could be considered as bimolecular sensor responders. In response to salt stress, the cytoplasmic $Ca^{2+}$ concentration has been shown to increase rapidly after plants salt exposure, as a consequence of $Na^+$ intracellular accumulation. This $Ca^{2+}$ fluctuation later results in $Ca^{2+}$ uptake from the apoplast and other intracellular compartments (Hasegawa, 2013). One of the early signalling pathways induced during salt stress response in plants is the $Ca^{2+}$/SOS cascade (Roy et al., 2014). The salt overly sensitive (SOS) signalling pathway is the most studied CBL-CIPK induced pathway and comprises the proteins SOS3, SOS2, and SOS1. The increase in cytoplasmic $Ca^{2+}$ originated after salt stress activates the $Ca^{2+}$ binding protein SOS3 (also called CBL4) allowing it to interact with the protein kinase SOS2 (CIPK24). This SOS2/3 complex then activates several

downstream processes: vacuolar sequestration of $Ca^{2+}$ and $Na^{+}$ by the calcium exchanger, vacuolar $Na^{+}/H^{+}$ antiporter (NHX), and extrusion of excess sodium in the apoplast through the activity the $Na^{+}/H^{+}$ antiporter SOS1, located on the plasma membrane (Qiu et al., 2003; Qiu et al., 2004). SOS1 and NHX1 are considered to be fundamental in controlling ion homeostasis in the cytoplasm during salinity stress. The SOS pathway not only mediates cellular signalling under salt stress, but also aids the cell in maintenance of calcium and sodium homeostasis. These processes require ATP to actively drive ion transport through the membrane against the ionic potential, making functional mitochondria fundamental during salt stress response.

Moreover, mitochondria have an important function in abiotic and biotic stress responses as first stress sensors. Under stress conditions, there are different intracellular candidate molecules that could play a role in the activation of mitochondrial stress perception, for example ROS and calcium ions. Cellular and mitochondrial redox homeostasis and signalling induce two distinct communication pathways between nucleus and mitochondria: retrograde and anterograde signalling (figure 1.6), which rely on signal molecules rapidly passing information from around the cell (organelles) to the nucleus, and back.

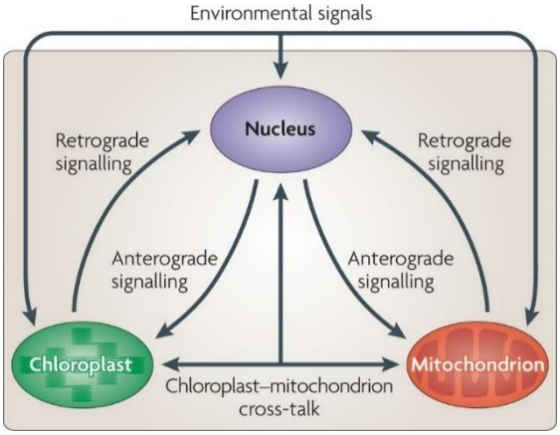


**Figure 1.6:** An overview of genome co-ordination between the nucleus and intracellular organelles. From Woodson and Chory, 2008.

## 1.5 Anterograde signalling pathway

The anterograde signalling is moving in the opposite direction compared to the retrograde signalling: this mechanism coordinates gene expression from the nucleus to chloroplasts and mitochondria, and it can control transcriptional and posttranslational events (Ng et al., 2013; figure 1.6). The anterograde response is activated to instruct the organelles on their effector role and the signals that control gene expression for this type of signalling can be developmental, hormonal, or environmental (Leister, 2005).

Mitochondrial biogenesis and function are tightly controlled through proteins encoded by nuclear genes (more than 1000), forming a nucleus-to-mitochondria regulatory system. Signals directly regulate nuclear gene expression to adjust the protein composition of mitochondria to the needs of

the cell under different stresses or developmental phases. The transcriptional networks that control nuclear-encoded mitochondrial genes still remain to be fully understood. The anterograde signalling from the nucleus to chloroplast is better understood and comprises a class of proteins called Regulators of Organelle Gene Expression (ROGEs), which include the sigma proteins and other factors required for plastidial genes transcription. Among the targets of these proteins, there is a large number of posttranscriptional regulatory factors such as the pentatricopeptide repeat (PPR) proteins and other classes of RNA-binding proteins that control RNA metabolism. Finally, there are also nuclear-encoded posttranslational factors (for e.g. tetratricopeptide repeat (TPR) proteins) that facilitate protein–protein interactions but also influence protein stability and degradation (Chi et al., 2012; Adam, 2007). In plants, one of the main aims of the anterograde signalling is the adjustment of photosynthetic capacity in response to varying environmental conditions and during development, a fundamental process for plant survival.

## 1.6 Retrograde signalling pathway

Retrograde signalling (RS) is a communication pathway that starts from organelles and goes to the nucleus (Woodson and Chory, 2008). It takes place in response to changing conditions and allows to modulate anterograde regulatory pathways to affect the functioning of organelles (Pesaresi et al., 2007). The organelles sense the stress first and, accordingly, induce in *primis* retrograde signalling. Thus, the signal reaches the nucleus that acts through transcription factors regulation and changes in the gene expression profile. The response is firstly aimed to face the stress, and, secondly, to allow the plant to endure it and later on to recover from the damage. There is evidence of another existing communication pathway, the chloroplast-mitochondrion crosstalk, but this still needs to be studied further (Woodson and Chory, 2008).

The network communication among intra-cellular compartments is crucial for the integration of complex and finely regulated signalling pathways triggered by external stimuli. Moreover, it is necessary to coordinate energy production and molecule supply coming from organelles with the stress-specific requirements. RS is a complex network that is still mostly unknown in plants, to get an insight in this process it is important to identify the molecular players involved, in particular, the molecules and the communication mechanisms involved in the signalling from mitochondria to the nucleus. In this perspective, it is of great interest to investigate in detail retrograde signalling (RS) factors, focusing, in particular, on the molecular mechanisms involved in the coordination between organelles and nucleus. In addition to stress, nuclear expression of several genes is influenced by signals originating from mitochondria and chloroplasts during high-energy demand growth phases (Wang et al., 2020).

To meet the complex metabolic needs throughout the cell, organelles have to receive appropriate stimuli, and that is achieved through modulation of gene expression and by the exchange of

metabolites and smaller molecules. ROS and other molecules, or ions such as calcium, can diffuse or be transported through different compartments. As a consequence, transcriptional changes are induced along with alterations of cytosolic homeostasis of different molecules and ions, leading to different responses based on the type of stimulus perceived. Moreover, redox metabolites like ascorbate/dehydroascorbate can take part in this communication network thanks to the redox fluctuations between the reduced and oxidized form of the ascorbate. Dehydroascorbate reductase (DHAR) is a key enzyme involved in the recycling of ascorbate, which catalyses the glutathione (GSH)-dependent reduction of oxidized ascorbate. As a result, DHAR regenerates a pool of reduced ascorbate and detoxifies reactive oxygen species (Do et al., 2016). ROS, in particular, have been proposed as possible candidates in retrograde signalling and organelles communication, because they are short-lived molecules and produced in different compartments, (like chloroplasts and mitochondria) of metabolically active cells (Apel and Hirt, 2004). One proposed mechanism of communication triggered by ROS involves post-translational protein-thiol modifications in a chain reaction that can extend to the whole cell (Pesaresi et al., 2007).

Chloroplasts act as central metabolic hubs in leaves cells. In fact, they are not only the site where photosynthesis takes place but also house the *de novo* biosynthesis of fatty acids, the production of fatty-acid-derived metabolites, and hormonal metabolisms. To safeguard these core processes against frequent challenges, chloroplasts work not only as central metabolic hubs but also as environmental sensors (perceiving stress) and produce retrograde signals to coordinate nuclear-encoded adaptive responses (De Souza et al., 2017). Chloroplast-specific retrograde signalling has been extensively studied: some proteins like Genomes Uncoupled 1 (GUN1) and the phosphatase SAL1 are known to be the first ones activated in the plastid following biotic and abiotic stresses. These two proteins induce signalling cascades in the cytosol by modulating Mitogen-activated Protein Kinase 3 and 6 (MPK3/6), 3'-phosphoadenosine 5'-phosphate (PAP), chloroplast envelope-bound PHD transcription factor (PTM) and possibly other molecules. Later on the signal reaches the nucleus (through translocation of proteins and other mechanisms) allowing the modulation of transcriptional factors by regulating effector genes. The activated response is involved in all cellular processes like photosynthesis, senescence, transcription factor cascade, hormones, and starch synthesis (De Souza et al., 2017; Wang et al., 2020; figure 1.7). Instead, regarding mitochondrial-specific retrograde signalling less is known, and the intercommunication mechanisms and the involved molecules and ions (e.g. calcium) are only hypothesized so far. Figure 1.7 shows a diagram of the retrograde signalling in plants from chloroplasts and mitochondria to the nucleus and the possible link between the two organelles retrograde communication mechanisms.

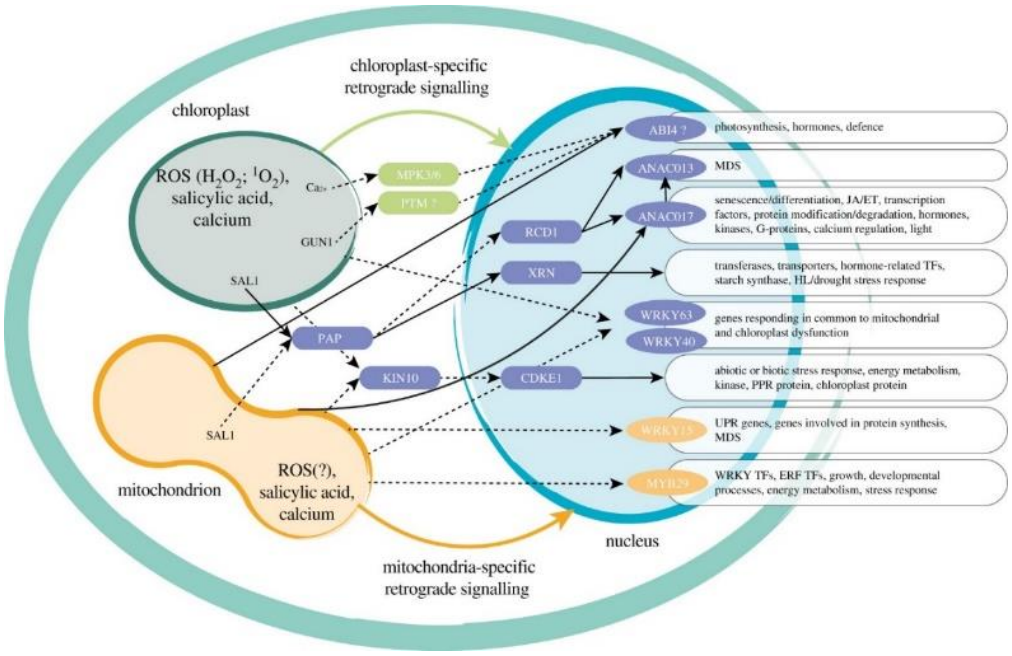


**Figure 1.7:** "Linking mitochondria and chloroplast retrograde signalling in plants". From Wang et al., 2020.

In the last few years, the awareness that chloroplasts and mitochondria work in concert in retrograde signalling has become stronger and stronger (Wang et al., 2020). Despite the close interdependence of the organelles, only few components of the pathways are known, further studies are needed to clarify the molecular details responsible of organelle and nuclear genome coordination.

### 1.6.1 Mitochondrial retrograde signalling

Many stresses activate the mitochondrial RS, such as exposure to high light, drought, and salt (ionic and osmotic stress). Key regulation mechanisms about mitochondrial retrograde signalling remain still unclear, but many studies are beginning to shed light on several aspects of this pathway in the last years. Once the stress or stimulus reaches the organelle, a change in intra-mitochondria redox homeostasis is perceived and this equilibrium disruption starts a signalling pathway that triggers the release of different mobile signal molecules or ions like ROS, calcium and hormones (SA and ABA) (Wang et al., 2020). These metabolites move through active or passive transport and allow the communication from mitochondria to the nucleus to induce an adaptative response.

ROS are highly reactive chemicals that include: peroxides, superoxide, hydroxyl radical, singlet oxygen, and alpha-oxygen. These molecules are well-known for having a dual role as destructive and constructive species: they function in cells as signalling molecules, but are also toxic by-products of aerobic metabolism, and this is the reason why the balance between production and detoxification is so crucial. They are primarily produced in different intracellular compartments, including mitochondria. Here, an over-accumulation of ROS leads to an unbalance in the membrane potential: these molecules directly react with proteins, lipids and nucleic acids, damaging the

electron transport chain (mtETC), impairing the activity of different enzymes, inducing lipid peroxidation, and causing DNA breakage and damage (Sachdev et al., 2021). A fine balance between ROS production/removal is at the basis of the ROS signalling network determining the overall response of the cell to a particular stimulus (Mittler et al., 2017; figure 1.8).

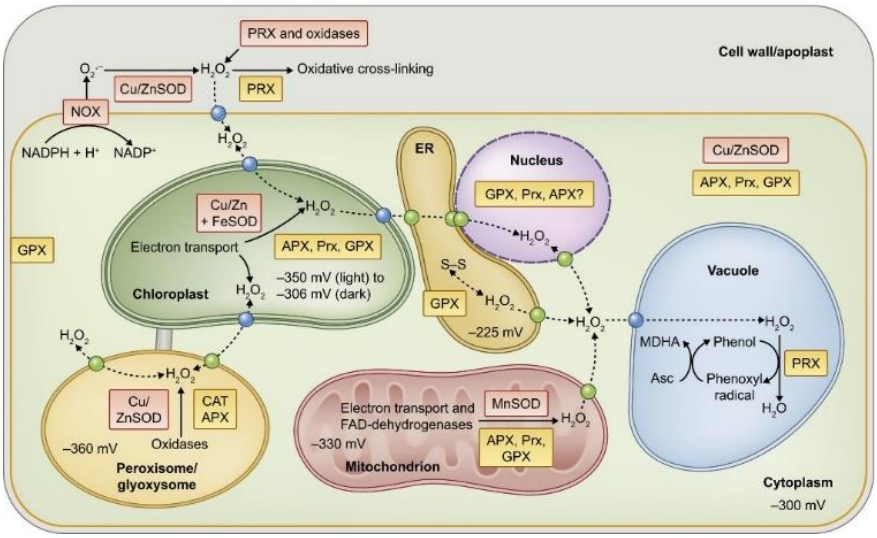


**Figure 1.8:** Sites of hydrogen peroxide ($H_2O_2$) production, scavenging and transport. The diagram shows the main sites of $H_2O_2$ production and scavenging in a typical plant cell. $H_2O_2$ transport from chloroplast to nucleus is shown via the endoplasmic reticulum (ER), but could be more direct. The normal glutathione redox potential (mV) in each compartment is also indicated (Schwarzlander et al., 2008). Asc, ascorbate; APX, ascorbate peroxidase; CAT, catalase; FAD, flavin adenine dinucleotide; GPX, glutathione peroxidase; MDHA, monodehydroascorbate radical; NOX, NADPH oxidase; PRX, type III peroxidase; Prx, peroxiredoxin; SOD, superoxide dismutase. From Smirnoff and Arnaud, 2018.

Another player in the context of mitochondrial RS is $Ca^{2+}$ which appears to be involved in early signalling of plant responses to environmental stimuli: cytosolic $Ca^{2+}$ concentration varies as a consequence of changes in intra or extra cellular conditions, determining the "calcium signature", specific for each different stimulus (figure 1.9). $Ca^{2+}$ functions as a universal messenger in all eukaryotes including plants, playing an essential role in the network of signalling pathways (Kudla et al., 2018). $Ca^{2+}$ ions are present throughout the cell but can be accumulated and released by intracellular compartments such as vacuoles and ER. $Ca^{2+}$ fluxes are regulated by membrane selective channels that allow or not the passage of the ion, depending on their specific regulation.

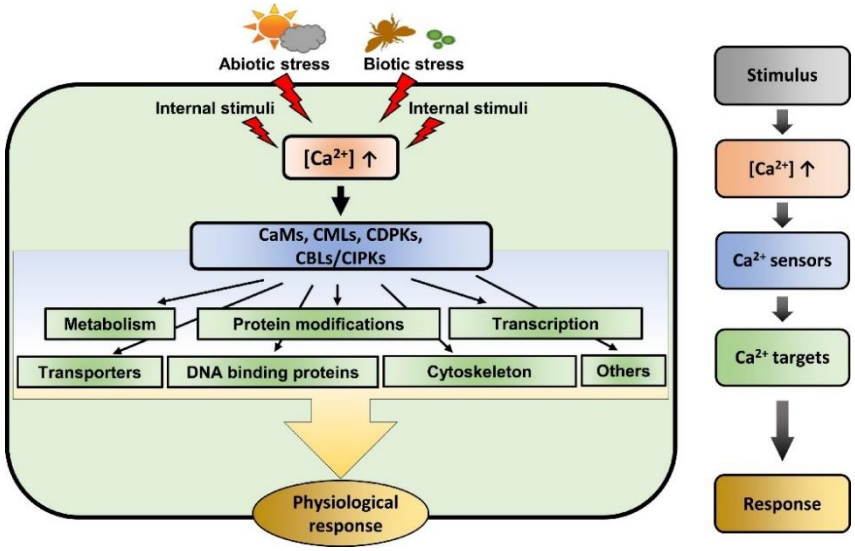


**Figure 1.9:** The $Ca^{2+}$ signalling network in plant cells. From Pirayesh et al., 2021.

In plants, cell-to-cell communication is mainly mediated by hormones, such as auxins, cytokinins, gibberellins, abscisic acid (ABA), ethylene, brassinosteroids, and jasmonates. These compounds are involved in various aspects of plant growth regulation including defence responses, meristem organization, self-incompatibility, root growth, leaf-shape regulation, nodule development, and organ abscission. Plant hormones travel, mostly, via the vascular tissue and cell-to-cell via plasmodesmata. ABA is an isoprenoid phytohormone synthetized in plastids. It has a role in many plants developmental processes, such as dormancy and seed development. Indeed, many genes that respond to ABA are expressed in the late stages of embryogenesis, during the development of seeds (Yamaguchi Shinozaki and Shinozaki, 1994). ABA is also involved in the control of organ size and stomatal closure and plays a major role in the response to environmental stresses, including drought, soil salinity and cold. The increase in ABA levels leads to the activation and assembly of its specific receptor complexes that are present in both cytoplasm and nucleus. Once activated, ABA signalling pathways lead to the regulation of many ABA-responsive genes: downregulated genes are mostly related with growth while there is an induction in the expression of stress tolerance-related genes, such as regulatory proteins (transcription factors, protein kinases, phosphatases), enzymes required for phospholipid signalling and detoxifying enzymes of reactive oxygen species (Fernando and Schroeder, 2016). Regarding mitochondria, ABA signalling induces the expression of Alternative Oxidase1a (*AOX1a*) by removing the repressor APETALA2 (AP2)-type transcription factor (ABI4) from *AOX1a* promoter (Giraud et al., 2009; figure 1.10). ABI4 was found to be a regulator of AOX1a in mitochondrial retrograde signalling (Finkelstein et al., 1998). Plant AOXs are encoded by a small nuclear multi-gene family composed by two distinct subfamilies: AOX1 and AOX2. *AOX1* genes are highly responsive to abiotic and biotic stresses, whereas *AOX2* genes are expressed in a constitutive or developmentally regulated way (Polidoros et al., 2005, Polidoros et al., 2009). AOX is located in mitochondria and competes for electrons with the standard cytochrome (Cyt) pathway at the terminal end of ETC (figure 1.10) directly reducing $O_2$ to $H_2O$. Alternative ETC does not generate proton motive force for ATP synthesis but acts as an antioxidative strategy to control mitochondrial redox state and prevent excessive ROS production (Mur et al. 2008; Derevyanchuk et al., 2015). Therefore, AOX needs to be tightly regulated on various levels to guarantee cellular energy balance, but also needs to be activated to counteract oxidative stress. Among *AOX* genes, *AOX1a* is expressed at levels 10 to 100 fold greater than other *AOX* genes, and its expression is affected in a variety of cell-signalling mutants (Ho et al. 2008). *AOX1a* expression is triggered by the inhibition of the ETC, and its transcript abundance can be induced in response to mitochondrial stresses, highlighting its role in stress sensing and response. Thus, *AOX1a* is by far the most reliable marker to study and identify mitochondrial retrograde signalling (Ng et al., 2014). WHIRLY2 (WHY2), a ss-DNA binding protein involved in the mtDNA maintenance, has been recently hypothesised to play a function in the retrograde signalling, showing its over expression line an increase in the expression of *AOX1a* (Zhao et al., 2018). AOX1a RS induces a cascade response in

which several nuclear transcription factors are involved along with the mitochondrial unfolded protein response (mtUPR), important for mitochondrial and cellular adaptation to stress.

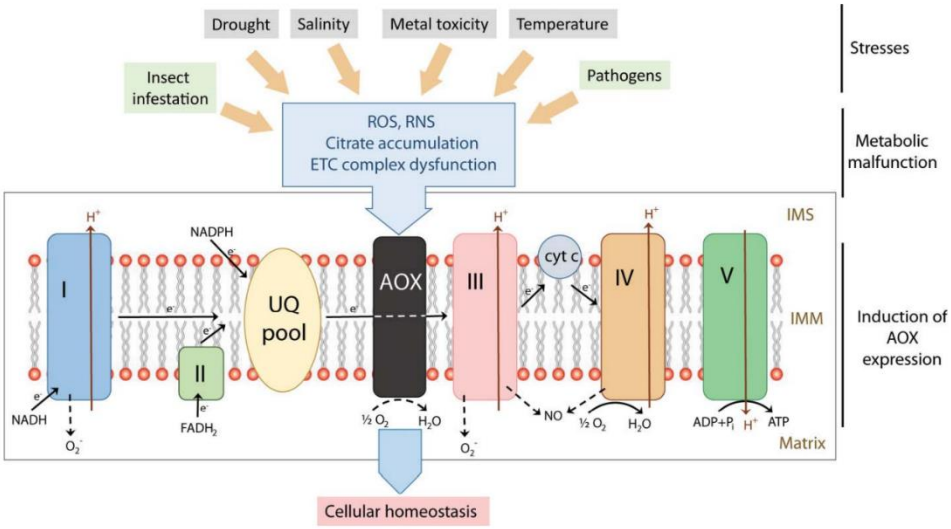


**Figure 1.10:** Schematic representation for AOX induction under stress and response of the plant Electron Transport Chain (ETC). Under unstressed condition NADH oxidation by complex I is coupled to proton transport from matrix to inter-membrane space (IMS), whereas oxidation of FADH2 and NAD(P)H doesn't lead to such fate. Similar is the electron flow from ubiquinol to complex III and then to complex IV which is additionally associated with reduction of $O_2$ to $H_2O$. Proton transport across the membrane generates a proton motive force which is dissipated by complex V to produce ATP. But under stress due ETC complex dysfunction, citrate accumulation there is electron leakage from complexes as ROS and RNS (shown in dotted lines) which induces AOX. AOX puts a branch in ETC after ubiquinol pool and directly reduces $O_2$ to $H_2O$ with production of heat. I, II, III, IV, V: Complex 1–5; IMS: Inter Mitochondrial Space; IMM: Inner Mitochondrial Membrane. From Saha et al., 2016.

Two interesting genes involved in mitochondrial retrograde signalling are *WRKY15* and *mtHSC70-1*, whose expression is induced by *AOX1a* and ROS. WRKY15 is a transcription factor (AtWRKY15) that modulates several nuclear genes involved in plant growth and salt/osmotic stress responses (figure 1.11). The relevant role in RS of AtWRKY15 is underlined by the fact that in *A. thaliana* overexpressing plants, a reduced *AOX* expression was observed, leading to an increased susceptibility to osmotic stress (Vanderauwera et al., 2012; figure 1.11). It has been proposed that WRKY15 $Ca^{2+}$-dependent CaM-binding domain mediates $Ca^{2+}$ flux sensing triggering the mitochondrial retrograde cascade (Wang et al., 2020). Thus, WRKY15 might function as a reporter of mitochondrial retrograde regulation (MRR) (Wang et al., 2020). mtHSC70-1 is a mitochondrial heat shock protein that plays an important role in redox homeostasis in mitochondria (Wei et al., 2019). *mtHSC70-1* induction is strictly related to mitochondrial ROS increase which causes proteins unfolding and affects ETC functionality. The loss of mtHSC70-1 functions resulted in an increased level of ROS, abnormal mitochondria and alterations to respiration because of an inhibition of the cytochrome c oxidase (COX) pathway and the activation of the alternative respiratory pathway (Zhai et al., 2020).

In conclusion, several aspects have been uncovered in the last years, but still much has to be investigated. Retrograde signalling is a communication mechanism that includes different interconnected pathways necessary to control the cell response exposed to different stimuli. It would be important to understand better how plants sense the environment and manage to adapt and recover from different stresses.

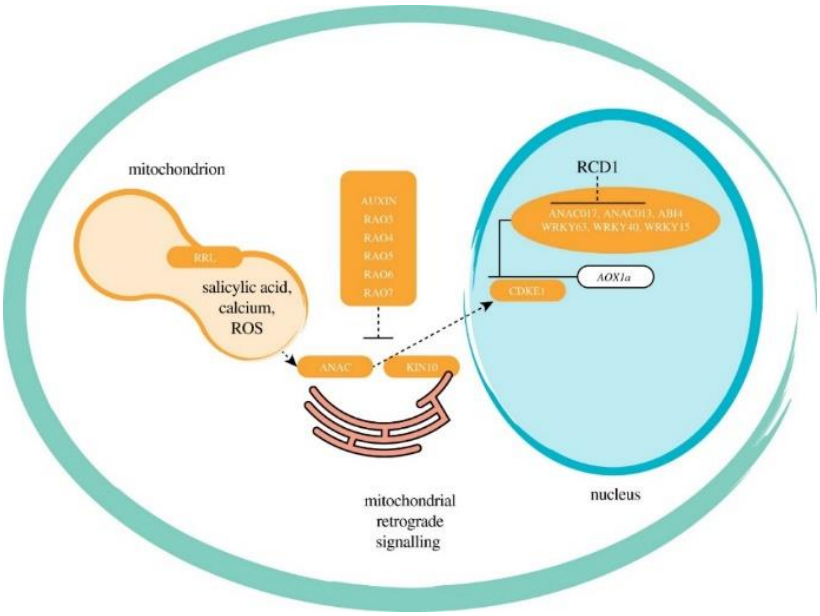


**Figure 1.11:** Retrograde regulation of AOX1a. A number of components that regulate the expression of AOX1a have been identified. Upon mitochondrial dysfunction, activation of a number of ER-bound ANAC transcription factors occurs, with ANAC017 being the master regulator regulating the expression of a number of other transcription factors. Other positive regulators identified include WRKY63 and ANAC013. CDKE1, a subunit of the kinase module of the Mediator complex, was also shown to be required for the induction of AOX1a, and interacts with KIN10. The latter has been shown to dynamically move between the ER and the nucleus. A number of negative regulators, including ABI4, WRKY40 and WRKY15, have also been identified. Other negative regulators include MYB29, components involved in auxin signalling (RAO3, 4, 5, 6 and 7) and RCD1. Finally, it has been shown that a dual-targeted protein, called RETARDED ROOT LIKE (RRL), is required for the translation of AOX1a and accumulation of AOX1a. ROS, reactive oxygen species; RRL, RETARDED ROOT GROWTH-LIKE protein; RAO, Regulator of Alternative Oxidase 1A; ANAC, the membrane-bound NAC transcription factors; KIN10, SNF1-related protein kinase; CDKE1, CYCLIN-DEPENDENT KINASE E1; RCD1, RADICAL-INDUCED CELL DEATH PROTEIN 1; ABI4, ABA INSENSITIVE 4; WRKY63, WRKY DOMAIN PROTEIN 63; WRKY40, WRKY DOMAIN PROTEIN 40; WRKY15, WRKY DOMAIN PROTEIN 15; AOX, Alternative Oxidase. From Wang et al., 2020.

## 1.7 WHIRLY family proteins

WHIRLY family proteins have been discovered in potato and in *A. thaliana*, they are organized in tetramers and are active in binding ssDNA. All members of the family share a highly conserved WHIRLY domain that includes the KGKAAL motif implicated in binding promoter regions thus allowing modulation of gene expression (Desveaux et al., 2005; figure 1.12).

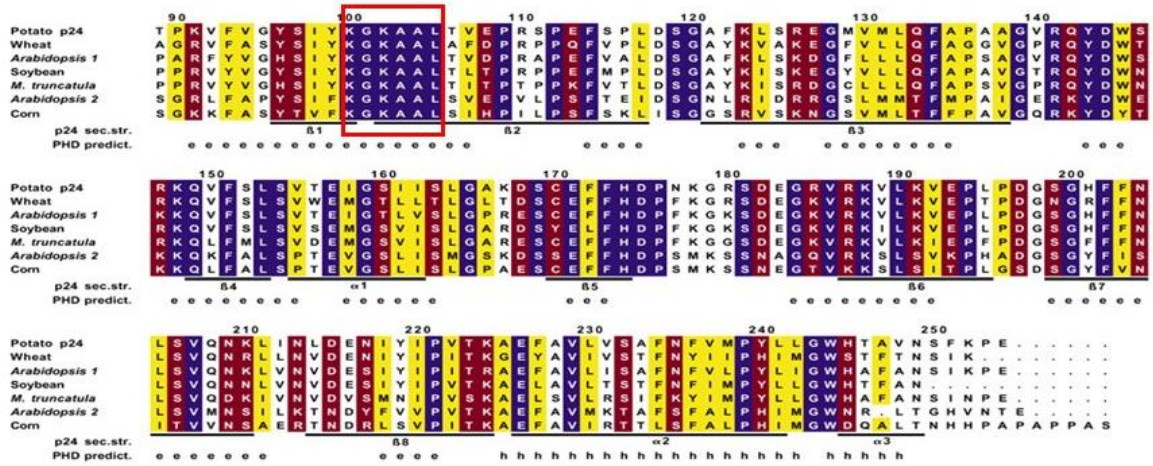


**Figure 1.12:** Structural conservation of Whirly proteins. Sequence alignment of seven Whirly proteins from various plant species. The red square represents the KGKAAL motif. From Desveaux et al., 2002.

While most plants own two WHIRLY proteins, *Arabidopsis thaliana* and other members of the Brassicaceae family have three WHIRLY proteins: WHIRLY1 (At1G14410), WHIRLY2 (At1G71260) and WHIRLY3 (At2G02740), that localize in different sub-cellular compartments and present specific targeting sequences for either plastids (WHIRLY1, WHIRLY3) or mitochondria (WHIRLY2) (figure 1.13).

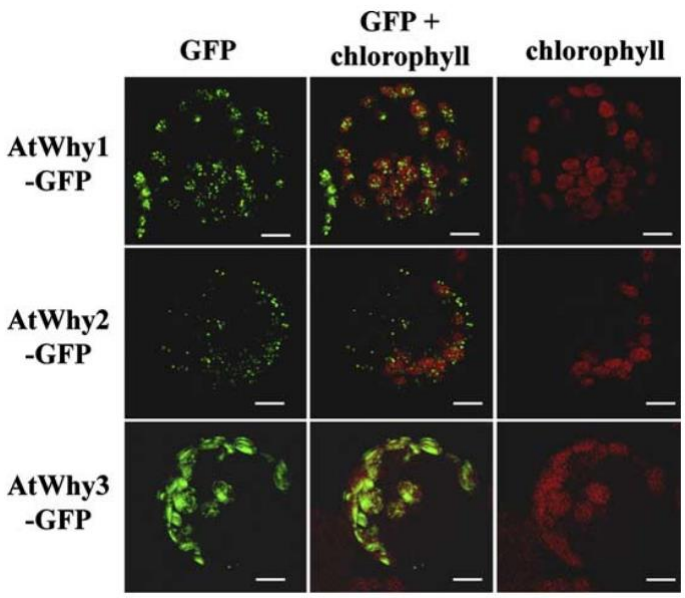


**Figure 1.13:** Subcellular localisation of AtWhy1-GFP, AtWhy2-GFP and AtWhy3-GFP fusion proteins in potato protoplasts. Confocal images of GFP fluorescence and chlorophyll autofluorescence are shown in the left and right columns, respectively. The middle column depicts the merged images. Each scale bar represents 8 µm. From Krause et al., 2005.

Transient expression analyses showed that WHY1 and the N-terminal part of WHY3 are targeted to chloroplasts, while WHY2 is imported into mitochondria (Krause et al., 2005; Maréchal et al., 2008). Regarding the evolution of the family, it could be assumed that a duplication of the ancestral *why* gene happened very early during angiosperms evolution, before the separation between monocotyledonous and dicotyledonous plants. A second duplication event might have happened more recently restricted to members of Brassicaceae as *A. thaliana*. The sequence homology between AtWHY1 and AtWHY3 is around 77%, while AtWHY2 and the plastidic AtWHY1 and AtWHY3 share around 34% of the sequence. Crystal structure of WHIRLY domain has been determined by X-ray diffraction analysis (Cappadocia et al., 2010 and 2013; figure 1.14) and such analysis revealed that tetrameric WHIRLYs bind to ssDNA in a sequence unspecific manner.

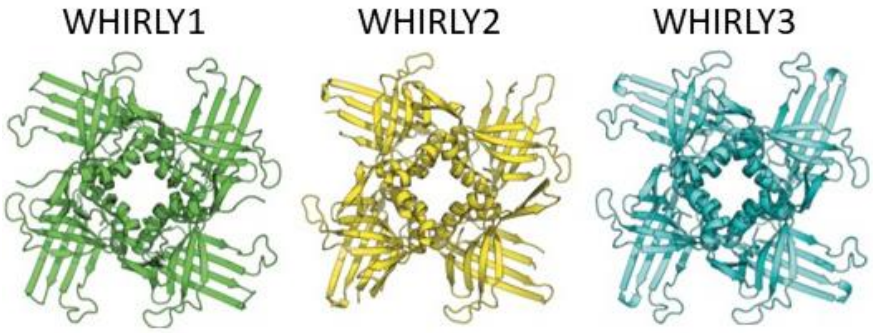


**Figure 1.14:** Tetramers of (a) WHY2, (b) WHY1 and (c) WHY3 in cartoon representation. WHY2 tetramers are present in the asymmetric unit. Tetramers of WHY1 and WHY3 were generated by applying the appropriate crystallographic symmetries. From Cappadocia et al., 2013.

Throughout atomic force microscopy, it has been shown that hexamers of WHY2 tetramers assemble into 24-meric higher order structures upon binding long DNA molecules, whereby the interactions between the tetramers depend on K67 residue within the KGKAAL motif (Cappadocia et al., 2013; figure 1.12). The structure of WHYRLY domain is highly conserved, even among different plant species, as revealed by a 3D structure analysis (Akbudak and Filiz, 2019). WHY2, together with other organellar ssDNA binding proteins, plays a key role in the maintenance of integrity of mitochondrial DNA that is an absolute requirement for cell survival, growth and proliferation.

There are evidences that WHIRLY proteins modulate DNA repair in chloroplasts and mitochondria by binding ssDNA and interacting with other DNA repair proteins to retrieve them in specific spots (Cappadocia et al., 2013; Cai et al., 2015; figure 1.15). WHIRLY proteins are indeed involved in the maintenance of organellar genome stability. *A. thaliana* plants, lacking either plastidial or mitochondrial WHIRLY proteins, accumulate higher levels of microhomology-mediated DNA rearrangements (MHMRs) than wild-type (Maréchal et al., 2010; Cappadocia et al., 2010 and 2008).

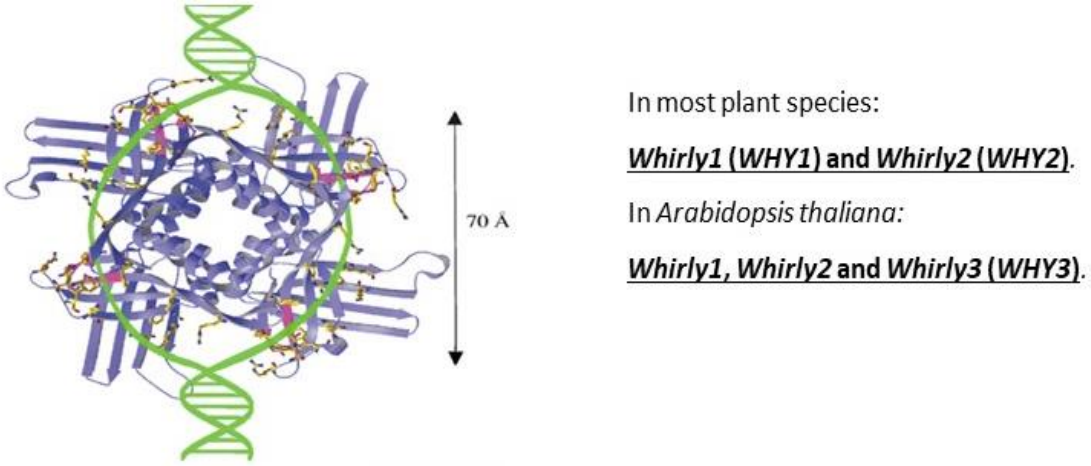


**Figure 1.15:** Binding of p24 (potato homologue of WHIRLY proteins) to melted dsDNA. DNA is represented as a green ribbon with horizontal bars indicating base pairs. Side chains of aromatic and basic amino acids that lie along the proposed DNA-binding surface are also indicated. The C4 symmetry of PBF-2 readily accommodates binding to melted dsDNA as depicted. From Desveaux et al., 2002.

In immature leaf cells, where an active chloroplasts biogenesis occurs, high level of WHY1 transcript is detected, thus suggesting a role of WHY1 as a key component in the maintenance of the chloroplast nucleoid structure and functionality (Krupinska et al., 2014). Experimental evidences suggest a role of WHY1 in controlling the flow of signalling information in and out of the plastids, both during development and stress conditions (Krupinska et al., 2014). The whirly1KO mutants show a reduced sensitivity towards salicylic acid (SA) and ABA during germination (Isemer et al. 2012) two hormones that are typically synthetized within plastids. There is evidence that a kinase, functionally similar to the mammalian protein kinase C, could be involved in the signal transduction events that lead to WHIRLY activation following a biotic stress (Desveaux et al., 2005). During a pathogenic infection, an upregulation of WHY1 induced by SA induces the expression of pathogenesis-related (PR) genes in the nucleus (Desveaux et al., 2004). Since the three different WHIRLY proteins are localized in different sub-cellular compartments (mitochondria and plastids), it has been proposed that WHIRLY proteins are ideal candidates as central coordinators of the

retrograde signalling pathway (by mediating organellar interactions). Supporting this role, WHY1 was detected also in the nucleus making it an ideal candidate to exchange information between the two compartments (Isemer et al., 2012, Foyer et al., 2014). Foyer et al (2014) also suggests a schematic model of the WHIRLY1-dependent perception and involvement in the retrograde signalling (figure 1.16).

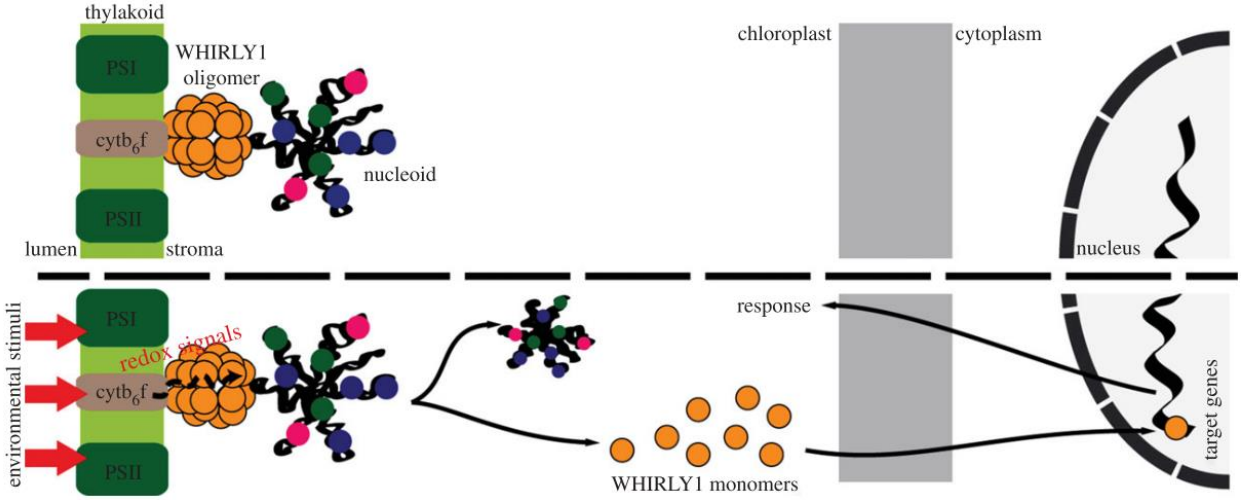


**Figure 1.16:** Schematic model of the WHIRLY1-dependent perception and transduction of redox signals originating from the photosynthetic apparatus. Under control conditions WHIRLY1 forms 24-oligomers which form a bridge between the thylakoid and the nucleoid. In response to environmental stimuli, the redox state of the photosynthetic apparatus is altered and this induces a monomerization of WHIRLY1. From Foyer et al., 2014.

Recently, it has been reported pieces of evidence on the involvement of WHY1 in the retrograde translocation pathway in plastids. Moreover, it has been demonstrated that, in mitochondria of WHY2 knock-out plants, WHY3 is present also in mitochondria (Golin, Negroni et al., 2020; Negroni unpublished data), underlining the role of WHIRLY proteins and the importance of their presence in organelles. For these reasons it would be interesting to investigate a possible subcellular re-localization induced by developmental or environmental stimuli of WHY2, being highly similar to WHIRLY1 gene, but with a different subcellular localization (mitochondria).

### 1.7.1 WHIRLY2

WHIRLY2 is a ssDNA-binding protein found in plant mitochondrial nucleoids (Desveaux et al., 2002). Plants lacking WHY2 do not show differential growth and development compared to the WT, even if seeds germination resulted compromised. By analysing the expression profile of WHIRLY genes in WT plants, the level of WHIRLY2 results lower than the one of WHIRLY1 and WHIRLY3 in shoots (Figure 1.17), but the opposite is observed in seeds, a phase in which heterotrophic metabolism prevails and the energy requirements are provided by mitochondria, since functional chloroplasts are not yet formed (Golin, Negroni et al., 2020).

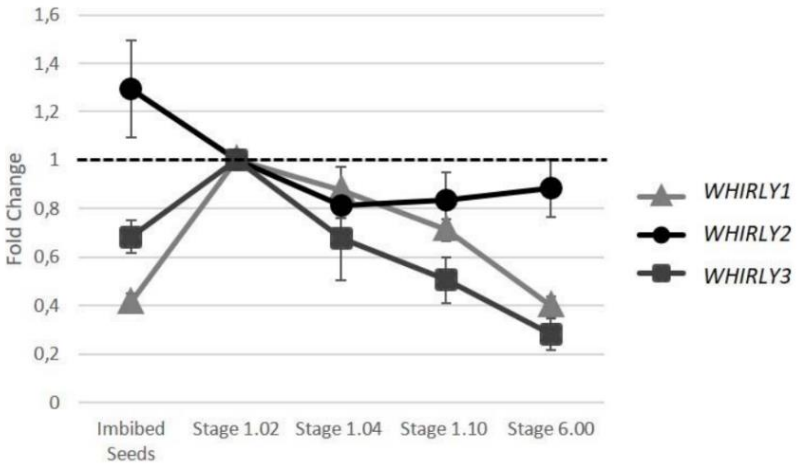


**Figure 1.17:** Expression profile of WHIRLY genes in WT plants and seeds. The expression was analysed in 24 hours imbibed seeds and in plants at 1.02, 1.04, 1.10 and 6.00 stages of growth. The expression was measured in the entire plant (shoot and root). From Golin, Negroni et al., 2020.

The impact of WHY2 absence is mostly appreciated when mitochondrial DNA replication occurs, such as in highly dividing cells and during germination, when high levels of ATP are required (Arimura, 2018; Cheng et al., 2017). During germination, cells undergo a metabolic re-organization: in this context, a higher expression of WHY2 was observed in wild-type imbibed seeds after the reactivation of cellular and mitochondrial metabolism (Paszkiewicz et al., 2017).

The mtDNA is fundamental to provide part of the genetic information needed for mitochondrial functionality but also for aiding the structural organization of the whole organelle. Therefore, its replication must occur in a very controlled and regulated way, particularly in those phases when mitochondria are the organelles that mostly sustain cell metabolism. Such process has not been studied in detail in plants. In plants, mtDNA replication probably takes place in a recombination-dependent manner, resulting from double-stranded homologous recombination breakage or from double- or single-stranded break repair, mechanisms that might involve the presence of the DNA-binding protein WHY2 (Cheng et al., 2017). WHY2 is, in fact, the most abundant among the proteins involved in mtDNA repair, and some evidence suggest its important role in mitochondrial genome replication and stability, allowing the maintenance of mtDNA integrity (Fuchs et al., 2020). Recent insights show a link between mtDNA stability and proper mitochondrial morphology, dynamics, and functionality, underlining the fundamental role of WHY2 in mitochondrial activity (Golin, Negroni et al., 2020). Failure in the maintenance of mitochondrial genome stability results in the accumulation of mutations and genomic rearrangements that can become deleterious (figure 1.18).

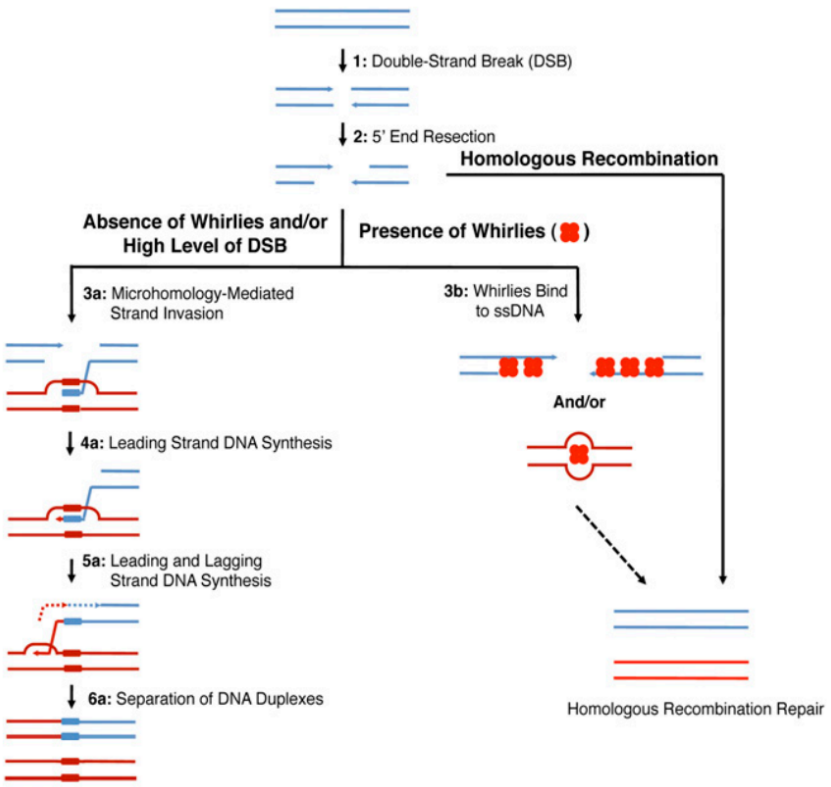


**Figure 1.18:** Model for the Repair of Organellar Double-Strand Breaks in the Absence or Presence of Whirly Proteins. Upon formation of a DSB (1), the 59 end of the broken DNA molecule is resected from the break, exposing a 39 tail (2). At this step, the break can be repaired through homologous recombination in a Whirly-independent manner. Alternatively, if the Whirlies are absent or the repair machinery is overloaded due to numerous DSBs, the 39 tail can anneal to any exposed ssDNA through microhomologies (3a). A D-loop forms and DNA polymerization proceeds from the microhomology junction (4a). A replication fork is established and lagging strand synthesis initiates while leading strand synthesis continues (5a). DNA synthesis continues until the end of the chromosome is reached (6a). Alternatively, if the Whirlies are present and the DSB level is low (3b), Whirlies could bind and protect ssDNA (either the 39 tail and/or any exposed ssDNA), thereby promoting homologous recombination and accurate DNA repair. Arrowheads represent 39 ends; a box symbolizes the microhomology between broken and unbroken DNA molecules; dashed arrows in tandem represent lagging strand synthesis. From Cappadocia et al., 2010.

García-Medel PL et al, proposed that WHY2 limits microhomology-mediated end-joining during double-stranded breaks in mtDNA repair process, thus preventing the accumulation of abnormal mtDNA molecules (García-Medel et al., 2019). Cappadocia et al., (2010) discovered that if the *why2-1* mutant plants were exposed to different concentration of ciprofloxacin, a genotoxic agent that induces double mtDNA breaks, the number of aberrant products increase abruptly.

At morphological level, similarly to what has been observed in chloroplasts of WHY1 knockdown barley plants (Krupinska et al., 2014), mitochondria of *why2-1* mutants house a peculiar translucent area that contains filamentous mtDNA, coinciding with a reduced packaging of nucleoids (Figure 1.19). Young leaves of *why2-1* mutants show swollen mitochondria with aberrant structure characterized by unpacked and disorganized nucleoids, a reduced number of cristae and a low matrix density (Golin, Negroni et al., 2020), confirming the nucleoid localization of WHIRLY2 and also supporting a structural role in nucleoid organization, with an impact on mitochondrial activity and dynamics.

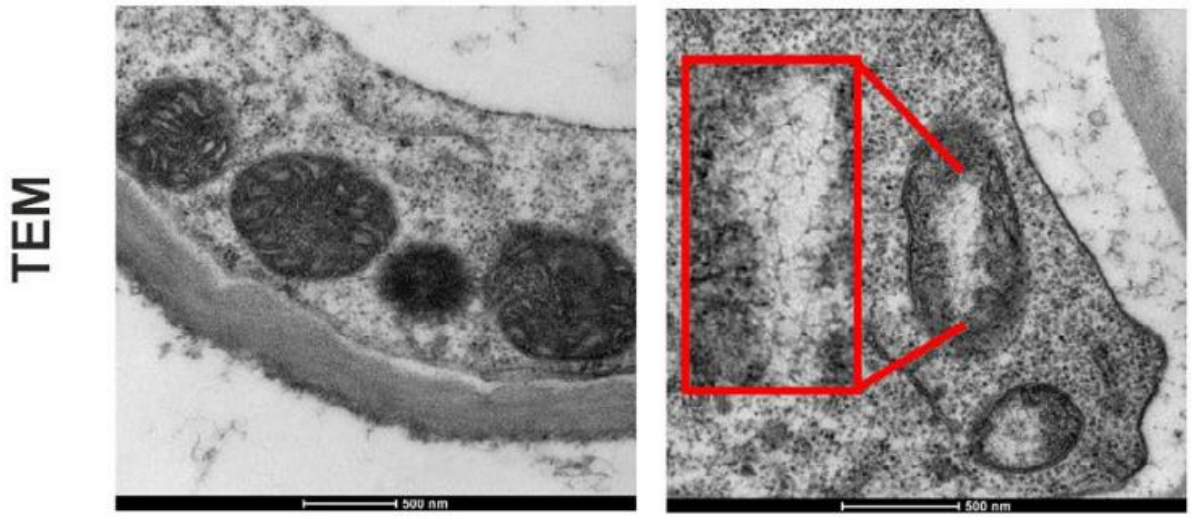


**Figure 1.19:** Transmission electron microscope images of mitochondria from suspension cell cultures at 5 days after subcultures. From Golin, Negroni et al., 2020.

On the other hand, an overexpression of *WHY2* in *A. thaliana* shows a reduction of the total mitochondrial transcripts levels and mtDNA content, causing a lower activity of the respiratory chain complexes as well as precocious senescence (Maréchal et al., 2008). Tissues owning low levels of mtDNA, such as mature pollen, have a lower transcription level of WHY2 (Cai et al., 2015). However, overexpression of WHY2 in pollen vegetative cells, induce a slower growth of pollen tubes, an increase of mtDNA content in pollen, and accumulation of ROS (Cai et al., 2015).

To sum up, it seems that WHY2 has a role in the maintenance of the copy number of mtDNA, which is controlled differently at different developmental stages. Beyond its role in the maintenance of the integrity and replication of mtDNA and organellar gene expression, it is not known whether WHY2 could play a specific role in the mitochondrial metabolism.

Zhao et al. (2018) studied more in deep the involvement of SlWHY2 (*Solanum lycopersicum* WHIRLY2) in stress response and the effects of its overexpression in *Nicotiana tabacum* (tobacco). They observed a strong induction of SlWHY2 after treating WT tomato plants with $H_2O_2$ and salt (figure 1.20)

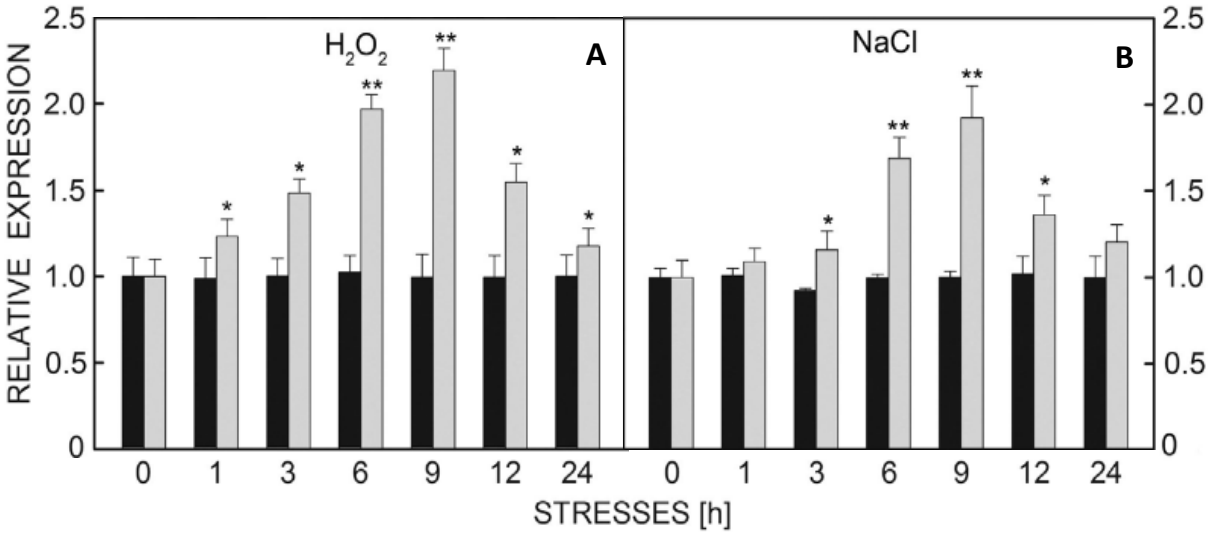

**Figure 1.20:** Relative expression of tomato SlWHY2 in different conditions: **(A)** effect of 200 mM NaCl and of **(B)** 20 mM $H_2O_2$. The control was watered with Hoagland's solution without additives. In grey WT in control condition, in black WT treated. From Zhao et al., 2018.

The authors later produced tobacco plants overexpressing SlWHY2 and studied their behaviour in drought conditions and after *Pseudomonas solanacearum* infection. In both seedlings and adult plants, an increased tolerance to drought stress was observed, partly due to a stronger antioxidative intracellular response. Moreover, overexpressors exhibited only mild or partial signs of disease after bacterial infection and were characterized by a high expression level of pathogen responsive genes 1 and 2 (PR1 and PR2). This work highlighted the possible role of SlWHY2 as a mediator of many different stress-related responses.

In conclusion, WHY2 in addition to having a central role in the maintenance and repair of mtDNA seems to play a fundamental role in stress conditions. This could be linked either to the function of WHY2 at the mtDNA level or to its possible involvement in retrograde signalling.

# Aim of the thesis

One of our biggest challenges as humanity is the increase of global food production, climate changes further undermine crops yield by making the environment more hostile for plant growth and by triggering stress mechanisms with a significant impact on food quantity and quality. Mitochondria are fundamental organelles, they are the energy production centre in plants, but they also play a fundamental role in sensing endogenous and exogenous stimuli, during plant development and stress response. Different stimuli induce different responses in plant cells that require energy, ATP is a key compound during these intracellular changes, for that reason mitochondria play a central role during plant life. Organelles have their own genome, but present-day organelle genomes are severely reduced, in fact, most proteins that are found in mitochondria are encoded in the nucleus. The compartmentalization of genomes requires coordination of gene expression among different subcellular compartments in order to guarantee the cell homeostasis. For all these reasons it is of crucial importance to study the proteins involved in the maintenance of the mitochondrial genome. Among those, WHIRLY2 is one of the most abundant being involved in mitochondrial genome replication and repair (Fuchs et al., 2020; Cappadocia et al. 2010). WHIRLY proteins own a characteristic DNA binding domain (Desveaux et al. 2002) and are involved in the maintenance of mitochondrial and plastids genome stability (Maréchal et al. 2010; Cappadocia et al. 2010). There is indeed evidence that WHIRLY proteins exert their effect by binding ssDNA and retrieving other proteins involved in DNA repair (Cappadocia et al. 2013; Cai et al. 2015). WHIRLY family in *Arabidopsis* includes three different members: WHIRLY1, WHIRLY2 and WHIRLY3, localized in different sub-cellular compartments and presenting specific targeting sequences for either plastids (WHIRLY1, WHIRLY3) or mitochondria (WHIRLY2) localization (Krause et al. 2005; Maréchal et al. 2008). The aim of this PhD project is to investigate a possible link between WHY2, mtDNA stability and proper mitochondrial functionality, exploring the possibility of its involvement in mtDNA replication during development and stress responses. WHIRLY family proteins due to their localization, are ideal candidates for mediating/regulating inter-organelle crosstalk during stress response. For this reason, in this thesis work will be also investigated the possible role of WHY2 in retrograde signalling triggered in plants upon exposure to environmental stress. The study of mitochondrial proteins is opening up to a new conception of the role of mitochondria as a stress response hub and WHY2 could be a fundamental element involved in this mechanism.

# Materials and Methods

## 2.1 Plant material

All experiments were performed on *Arabidopsis thaliana* plants, ecotype Columbia (Col-0). As *whirly2* knock-out mutants, the following lines were used: *why2-1* (SALK mutant; SALKseq_118900.0 purchased from the European Arabidopsis Stock Centre (NASC)), *why2-3* and *why2-4* (CRISPR/Cas9 lines, obtained in collaboration with Prof. Karin Krupinska). The line *pWHY2:GUS* (Cai et al., 2015) was used for GUS assay.

The WT mt-YFP (Col-0, mitochondrial YFP line (mt-yk; CS16264)) were purchased obtained from NASC and the double mutant has been obtained by crossing WT mt-YFP with *why2-1* line.

Wild-type seeds of *Arabidopsis thaliana* (accession Columbia, Col-0) harbouring the ATeam (cytosolic line; De Col et al., 2017) genetically encoded biosensor, were used for the ATP homeostasis assays (provided by Markus Schwarzländer, University of Münster). This mutant was crossed with *why2-1* line to obtain the knock-out lines harbouring the biosensor.

Line expressing the biosensor Yellow Cameleon 3.6 NES (cytosolic line; NES YC 3.6) already available in the lab (Loro et al., 2012), was crossed with the line *why2-1* to produce the knock-out line harbouring the biosensors.

*WHY2 knock-out mutants*

In order to study the role of WHY2 in *Arabidopsis thaliana* we selected three different *WHY2* mutant lines: the first, obtained from the European *Arabidopsis* Stock Centre and called *why2-1* (SALKseq_118900.0; Cappadocia et al., 2010), is a SALK line with a T-DNA insertion in the last intron of *AtWHY2*, and two others CRISPR/Cas9 lines generated in the Krupinska's lab (University of Kiel) and then selected and characterized in Zottini's lab.

**Genomic sequence and binding sites:**

AtWHY2:

```
2521  AATCATAAAA CCTCAGAAGT CGGAAGACCT CAAGTGATGC TTTTTACTCG AGACAGAAGA
       K  S  ~   N  L  R  S   R  K  T   S  S  D   A  F  Y  S   R  Q  K
2581  AGATGATGAA GCAAGCCCGC TCTTTGCTCT CCAGGTTACT TCAGTTCCTC TCAAAATTCA
                  PAM PS1       PS1
       K  M  M   K  Q  A  R   S  L  L   S  R  L   L  Q  F  L   S  K  F
        >>............exon 1.............>>
2641  GATTTTAGAT TTCATTACTC TTAAAATGGC TTCTCTGGGT TGGTTTGTTT TTGTTAAAGC
       R  F  ~   I  S  L  L   L  K  W   L  L  W   V  G  L  F   L  L  K
2701  AGGAGCCTTT GTGACCAAAG TAAGTCACTT TTCGAAGCTT CGACGTTGCG TGGTTTTGCA
       Q  E  P   L  ~  P  K   ~  V  T   F  R  S   F  D  V  A   W  F  C
        >>.........................exon 2.........................,>
2761  AGCTGGTCAA ATTCTTCAAC CCCTGGACGT GGATTCCCTG GTAAAGGTAA GAACTTGGTT
                                        PS2        PAM PS2
       K  L  V   K  F  F  N   P  W  T   W  I  P   W  ~  R  ~   E  L  G
      >.....................exon 2.....................,>>
2821  TGTTTCCGTT TCGTCAGTTT AAGTGTACTT GCCCTAATTT TGTTTGCTTG ATTTGAGAAG
       L  F  P   F  R  Q  F   K  C  T   C  P  N   F  V  C  L   I  ~  E
```

**Figure 2.1:** Genomic sequence of WHY2, in red the target sequence and in blue the PAM sequence for the CRISPR/Cas9 technology. In green is represented the amino acid sequence and the 1 and 2 exons of the gene.

The two CRISPR/Cas9 mutants were generated by choosing the first and second exon of *WHY2* as target sequences. PS1 represents the sequence chosen to generate the mutant line *why2-3* and PS2 the one for *why2-4* (figure 2.1).

The transformed lines were isolated through hygromycin screening and the absence of Cas9 was confirmed by PCR. Then, the resistant lines not bearing Cas9 were chosen for sequencing and brought into homozygosity confirming the mutations by sequencing. Two insertional knock-outs were isolated, both with an additional thymine in the target sequence (*why2-3* and *why2-4;* Figure 2.2).

From NASC:

- *why2-1* (*why 2-1;* T-DNA insertion mutant)

Collection Salk_118900 (T-DNA in last intron)

Collaboration with Prof. Dr. Karin Krupinska:

- *why2-3* (CRISPR/CAS9 mutant)
- *why2-4* (CRISPR/CAS9 mutant)

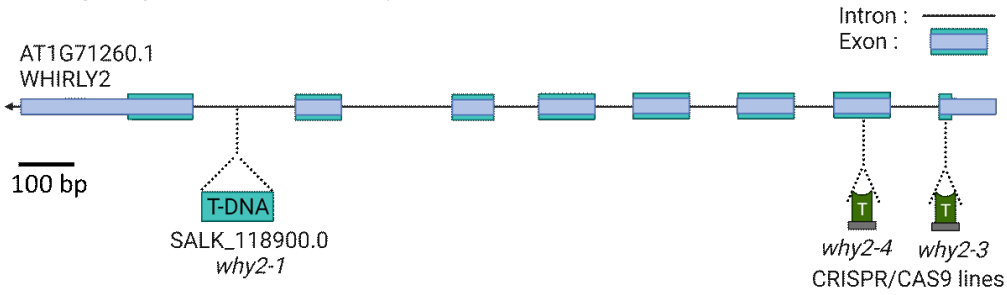


**Figure 2.2:** Schematic representation of the mutations in the 3 knock-out lines used: *why2-1, why2-3* and *why2-4.*

To further confirm the absence of functional WHY2 we checked the new predicted reading frame of its amino acidic sequence: as it is shown in figure 2.3, upon the thymine insertion several premature STOP codons originated, implying a correct deletion of the WHY2 protein.

Whirly2 WT

5'3' Frame 1

**Met Met** K Q A R S L L S R S L C D Q S K S L F E A S T L R G F A S W S N S S T P G R G F P G K D A A K P S G R L F A P Y S I F K
G K A A L S V E P V L P S F T E I D S G N L R I D R R G S L **Met Met** T F **Met** P A I G E R K Y D W E K K Q K F A L S P T E V G S
L I S **Met** G S K D S S E F F H D P S **Met** K S S N A G Q V R K S L S V K P H A D G S G Y F I S L S V N N S I L K T N D Y F V V P V
T K A E F A V **Met** K T A F S F A L P H I **Met** G W N R L T G H V N T E A L P S R N V S H L K T E P Q L E L E W D K **Stop**

*why2-3*
(T insertion in the 1 exon)

5'3' Frame 1

**Met Met** K Q A R S F A L Q E P L **Stop** P K **Stop** V T F R S F
D V A W F C K L V K F F N P W T W I P W **Stop** R C R K
A **Stop** W S I V R T L F Y L Q R K S C S L C **Stop** T C S S Q F
H **Stop** N R F G K S S D R S S W I L N D D F Y A C Y
W **Stop** A **Stop** V R L G K E T E I C F V T Y **Stop** S W I L
N **Stop** H G F Q R Q L R V F P **Stop** P F H E I K **Stop** C W S
S Q E V T V S **Stop** A P R R W **Stop** R L L H L I E
R **Stop** Q **Stop** H P Q N Q **Stop** L F C G S C H K S **Stop** I C S
D E D S F **Stop** F C S S T H H G L E S V N W S
R **Stop** Y **Stop** S S A V E E C F S S K D **Stop** T T V R A G V
G **Stop** **Met**

*why2-4*
(T insertion in the 2 exon)

5'3' Frame 1

**Met Met** K Q A R S L L S R S L C D Q S K S L F E A S T L R G
F A S W S N S S T P G R G F P G **Stop** R C R K A **Stop** W S I
V R T L F Y L Q R K S C S L C **Stop** T C S S Q F H **Stop** N R F
G K S S D R S S W I L N D D F Y A C Y W **Stop** A **Stop** V R L
G K E T E I C F V T Y **Stop** S W I L N **Stop** H G F Q R Q L R V
F P **Stop** P F H E I K **Stop** C W S S Q E V T V S **Stop** A P R R
W **Stop** R L L H L I E R **Stop** Q **Stop** H P Q N Q **Stop** L F C
G S C H K S **Stop** I C S D E D S F **Stop** F C S S T H H G L E S
V N W S R **Stop** Y **Stop** S S A V E E C F S S K D **Stop** T T V R
A G V G **Stop** **Met**

**Figure 2.3:** WT and new aminoacidic sequence of *why2-3* and *why2-4* lines.

In *WHY2* mutant, WHY2 protein was not detected by using specific antibodies raised against a WHY2 peptide as reported by Huang and collaborators (Huang et al., 2020).

## 2.2 *Arabidopsis* plant growth conditions

For phenotyping experiments, *Arabidopsis* unsterilized seeds were grown in pots on soil profi-substrat (Gramoflor). The pots were stratified for 48h and then put in a growth chamber under a long daylight period: 16 h light and 8 h dark at 22°C, with a light intensity of about 90-100 µmol $m^{-2}$ $s^{-1}$ and humidity was kept between 65 %.

For *in vitro* growth, seeds were mixed with 70 % (v/v) ethanol supplemented with 0.05% trytonx100 and vortexed for 1-2 min. Ethanol was removed by pipetting. Seeds were then mixed with 100% ethanol and vortexed for 1-2 min. Lastly, seeds were pipetted directly on sterile paper under the laminar-flow hood for drying. Surface-sterilized seeds were seeded on solid media using different methods. Plates were then sealed with 3M micropore to prevent the medium from drying out and to avoid contamination. Seeds were stratified for 48h at 4°C in the dark before placed under long daylight period in the growth chamber.

*Standard solid medium for Arabidopsis seedlings growth*

Solid medium for seedling growth was prepared by supplementing half-strength Murashige & Skoog medium including vitamins (Duchefa, Murashige and Skoog, 1962) with 1 % (w/v) sucrose, 0.5 g/L MES-KOH. pH was adjusted to 5.8 using KOH and solidified with either 0.8 % (w/v) plant agar or 1.5% (w/v) phyto agar.

*Solid medium for hygromycin selection*

Solid medium for hygromycin selection was prepared by supplementing Murashige & Skoog medium basal salt mix (no vitamins) (Duchefa, Murashige & Skoog, 1962) with 0.5 g/L MES-KOH. pH was adjusted to 5.8 using KOH and solidified with 0.8 % (w/v) phyto agar. Before solidifying, the medium was supplemented with 33.3 µg/mL hygromycin and poured in plates.

*Hygromycin selection*

Hygromycin selection was performed for the selection of both CRISPR/CAS9-edited why2KO lines. *Arabidopsis* seedlings (T1 generation) were sterilized and uniformly scattered on square plates on solid medium for hygromycin selection in sterile conditions under clean hood. Plates were sealed with 3M micropore and seeds were stratified for 2 days at 4°C in the dark. Plates were kept under light (intensity: 100 µmol $m^{-2}$ $s^{-1}$) for 6 h to induce germination, then they were wrapped with aluminium foil and incubated for 3 days at 22°C to stimulate elongation of the hypocotyl in hygromycin-resistant plants, according to Harrison et al., 2006 protocol. Resistant plants were

transferred on standard solid medium for an additional 2 days under long daylight period, before transferring them in soil.

*Germination assay*

Germination assays were performed in standard solid medium (0.8% plant agar) and under salt stress (standard solid medium supplemented with 100 mM NaCl), sowing the seeds with a sterile toothpick on square gridded plates (around 36 seeds per plate) and growing them horizontally. Images were acquired using a stereomicroscope (Leica MZ16F) to analyse the seeds abortion rate and the germination, taking into consideration the rupture of the seed testa and the emergence of the primary root at different time points. Each image was processed using a Fiji–ImageJ bundle software. The experiments were performed at least three times three biological replicates and each sample comprised 36 seedlings.

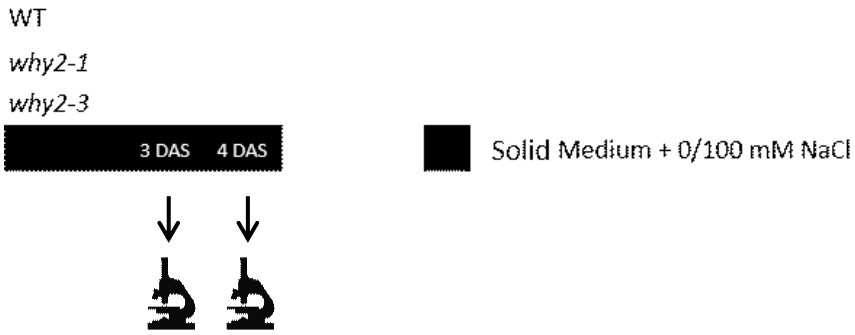


**Figure 2.4:** Experimental design for the germination assay in standard and salt stress condition.

## 2.3 Molecular biological techniques

*DNA extraction for phenotyping*

One or two leaves of collected samples were grinded with a pestle at room temperature in a 1.5 ml Eppendorf in 500 µl of TEN extraction buffer (100 mM Tris HCl pH8; 500 mM NaCl; 50 mM EDTA, pH 8). 30 µl of 20 % SDS were added to the samples, and they were incubated for 5 min at 65°C. To precipitate SDS and plant material, 130 µl of 5 M KCl were added, followed by an incubation of 5 min on ice. Samples were centrifuged for 10 minutes at full speed and supernatants were collected in a new tube containing 500 µl cooled isopropanol. The samples were incubated for 10 min at -20°C and then centrifuged for 10 min at maximum speed. DNA pellets were washed two times with 500 µl and 150 µl of 70 % ethanol, dried under the hood and resuspended in 50 µl of sterile nuclease-free water. DNA concentration was measured using Nanodrop ND-1000 spectrophotometer (Nanodrop Technologies, Rockland, DE, USA).

*PCR for genotyping, mtDNA fragmentation assay and why2KO ciprofloxacin assay*

For each PCR reaction 100 ng/µl of total DNA was used. PCR mix was prepared as follows:

| | |
|---|---|
| 1 µl | Template (concentration 100 ng/ul) |
| 0.25 µl | GOTaq Polymerase (Sigma) |
| 2.5 µl | 10 µmol forward primer (Sigma) |
| 2.5 µl | 10 µmol reverse primer (Sigma) |
| 1 µl | 10 mM dNTP mix (Sigma) |
| 10 µl | 5x GOTaq Buffer (Sigma) |
| 32.75 µl | dd$H_2O$ |

| **Step** | **Temperature (°C)** | **Time (seconds)** |
|---|---|---|
| Initial denaturation | 95°C | 120 s |
| Denaturation | 95°C | 30 s |
| Annealing | 59°C | 30 s |
| Elongation | 72°C | 60 s per kbp |
| Final extension | 72°C | 300 s |
| Hold | 4°C | ∞ |

35x

*Gel electrophoresis*

DNA was separated on 0.8 % (w/v) agarose gel prepared with 1x TAE-buffer (Tris acetate-EDTA Buffer 50x concentrate, Sigma) and supplemented with 6 µl of GelRed (Biotium). Typically, 8-10 µl of each sample were loaded alongside with 5 µl of DNA ladder (Gene Ruler 1kb, Thermo Fisher). DNA was separated by applying a current of 100 V in 1x TAE-buffer for 30 minutes. Images were taken using Elettrofor, Ruggero Massimo & C. S.a.s..

*DNA sequencing*

10-30 ng DNA were mixed with 1 µl of either forward or reverse primer (10 µmol) and lyophilised at 65°C. Samples were sent to BMR Genomics for sequencing (Sanger sequencing).

*Gel electrophoresis for mtDNA fragmentation assay and why2KO ciprofloxacin assay*

DNA was separated on 1.5 % (w/v) agarose gel prepared with 1x TAE-buffer and supplemented with 8 µl of GelRed. Typically, 5 µl of each sample were loaded alongside with 5 µl of DNA ladder. 2.5 µl of DNA were loaded for the housekeeping (*COX1*). DNA was separated by applying a current of 50-

60 V in 1x TAE-buffer for 2 hours at 4°C. Images were taken using ChemiDoc Touch Imaging System, Bio-Rad.

*RNA isolation and qRT-PCR*

100 µg plant material (seedlings, plants, other) of WTs and KOs was collected and grinded in liquid nitrogen with mortar and pestle. Total RNA was extracted using RNeasy® Plant Mini Kit (Quiagen) with an extra-protocol passage of 15 min of RNase-Free DNase (Quiagen) and resuspended in 30 µl of sterile nuclease-free water. RNA concentration was measured using a Nanodrop ND-1000 spectrophotometer (Nanodrop Technologies). First-strand cDNA synthesis was performed with SuperScript-IV Reverse Transcriptase kit (Invitrogen), using 2 µg of RNA and 1 µl of random primers (Sigma). qRT-PCR was performed in a 384 plate with 100 ng of cDNA per well using Taq® qPCR Master Mix (Promega) with SYBR Green technology in either QuantStudio 12K Flex or QuantStudio 5 (Thermo Fisher Scientific) instrument. Total volume of each reaction was 10 µl using 0.25 µl of primer mix (10 µmol). Sequences of used primers are reported in the table IV. The expression level of each gene was normalized to the level of the housekeeping gene Actin-2 (*ACT2*; At3g18780) and analysed using the ΔCt and ΔΔCt method (Livak and Schmittgen, 2001).

*mtDNA copy number quantification in standard condition*

WT, *why2-1* and *why2-3* lines were seeded on solid medium (1.5% phyto agar) and grown standard condition. The experiments were performed at 2 different developmental stages: 6 DAS old seedlings and 21 DAS old plants (1.10 growth stage plants Boyes DC et al., 2001). 6 DAS old seedlings were seeded by scattering around 75-100 seeds per plate and grown horizontally. 21 DAS old plants were sown with a sterile toothpick at 2 cm from the top edge, in line on square plates and grown vertically, each plate contained 6 plants. Samples were collected in sterile conditions. After 21 DAS, plants leaves were divided from the roots with a scalpel. Total DNA was isolated with High-Quality DNA extraction protocol (Bekesiova et al., 1999) from the whole seedlings (6 DAS) or the root and shoot segments (21 DAS). DNA concentration was measured by using Nanodrop ND-1000 spectrophotometer. qRT-PCR was performed according to the protocol with total DNA (100 ng) instead of cDNA as a template. The DNA amount of each mtDNA gene was normalized to the level of the single-copy number gene Rpotp and analysed using the ΔCt method. For mtDNA copy number quantification, 3 mitochondrial genes were used: *Q-COX1* and *orf170mito*. Primer sequences are reported in table III. The assays were performed at least on 3 biological replicates.

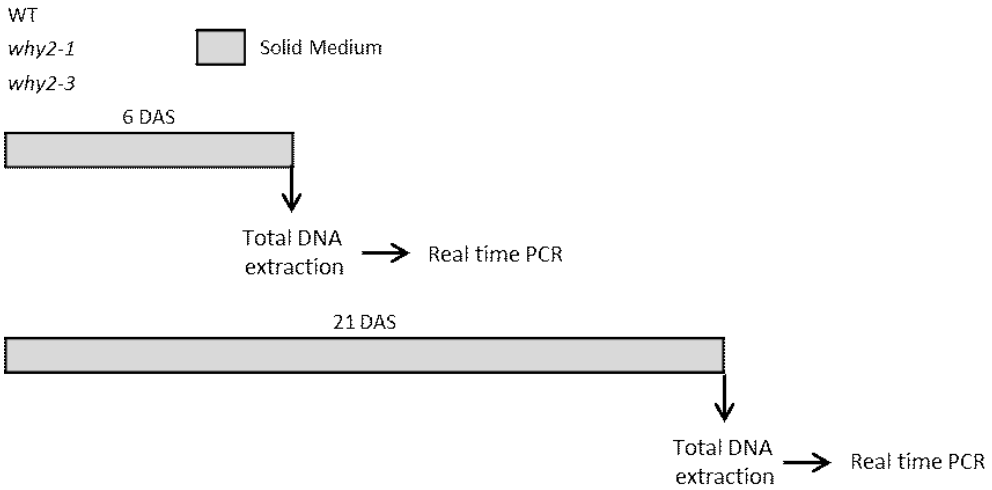


**Figure 2.5:** Experimental design for the mtDNA copy number quantification assay under standard condition.

## 2.4 Phenotyping Assays

Phenotyping was performed at different developmental stages, to highlight every possible growth impairment in different tissues: rosetta growth and size, flowering stem length and primary root length. Growth of knock-out mutants was compared to WT line (Col-0), the phenotyping of the rosetta and the flowering was performed in soil and for the primary root growth it was performed in standard solid medium (0.8% plant agar) placing the seeds vertically. At least 8 plants were used for the rosetta and flowering phenotyping. 20 plants and 3 biological replicates for each genotype for the primary root growth. Photos were taken every 2-3 days with a DSLR professional camera (Nikon D800) or using a Bio-Rad ChemiDoc Touch Imaging System (Flamingo setting).

## 2.5 Microscopy techniques

*Mitochondrial morphology and kinetics using mt-YFP line (Zeiss LSM700)*

Seedlings were grown vertically in square plates on standard solid medium (0.8% plant agar) for 5, 7 or 9 DAS. The analyses were performed on the primary root in the region where first root hairs arise, mainly in the external tissues. Zeiss LSM700 confocal microscope was used to capture images of seedlings with a 20x, 40x and 60x magnification. Samples were mounted onto a microscopy glass slide in imaging buffer (10 mM MES Tris base; 10 mM $CaCl_2$; 5 mM KCl pH 5.8) and excited at 513 nm (YFP absorption) and 614 nm (chlorophyll absorption). Emission was recorded between 520-550 nm (YFP emission) and 644-800 nm (chlorophyll emission). Each CLSM image was processed using a Fiji–ImageJ bundle software.

*Mitochondrial morphology with TMRM staining (Zeiss LSM700)*

Seedlings were grown vertically in square plates on standard solid medium (0.8% plant agar) for 5 DAS. Samples were incubated for 4 min in imaging buffer (10 mM MES Tris base; 10 mM $CaCl_2$; 5 mM KCl pH 5.8) supplemented with 200 nM tetramethylrhodamine methyl-ester (TMRM) and then washed with imaging buffer before being mounted on the slide. TMRM is a mitochondrial membrane potential indicator, a dye that permeates only in mitochondria with intact membranes and a negative inner membrane potential (coupled mitochondria). Excitation was set at 535 nm and emission at 562-800 nm. Samples were placed on the slide with 60 µl of imaging buffer and analysed setting the magnification at 20x, 40x and 60x. The experiments were performed in triplicates. We processed each single CLSM image using a Fiji–ImageJ bundle software.

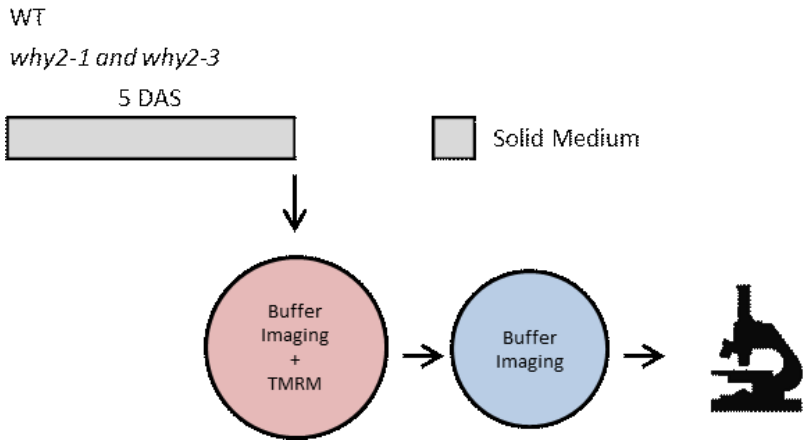


**Figure 2.6:** Experimental design for the Mitochondrial morphology with TMRM staining assay.

*Mitochondrial nucleoids with TMRM and picoGREEN staining (Zeiss LSM700)*

Seedlings were grown vertically in square plates on standard solid medium (0.8% plant agar) for 5 DAS. Samples were incubated for 4 min in imaging buffer (10 mM MES Tris base; 10 mM CaCl2; 5 mM KCl pH 5.8) with 200 nM TMRM and washed with imaging buffer, incubated for 10 minutes in imaging buffer containing 2% picoGREEN and finally re-washed in imaging buffer, before being mounted on the slide with 60 µl of imaging buffer. PicoGREEN is a dsDNA quantitation reagent that enters in mitochondria and intercalates in mitochondrial DNA. For TMRM signal acquisition parameters were set as described before, for picoGREEN excitation wavelength was set at 485 nm and emission peak at 520 nm. Samples were placed on the slide with 60 µl of imaging buffer and analysed setting the magnification at 20x, 40x and 60x. The experiments were performed in triplicates. We processed each single CLSM image using a Fiji–ImageJ bundle software and Volocity software.

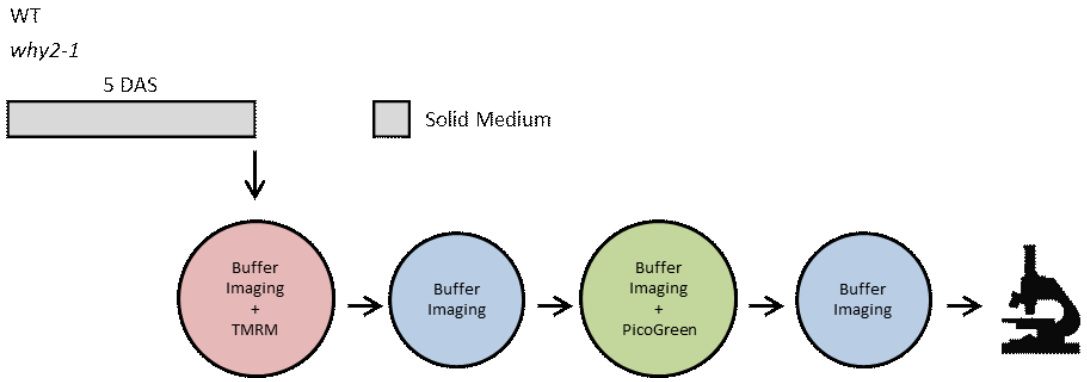


**Figure 2.7:** Experimental design for the mitochondrial nucleoids with TMRM and picoGREEN staining assay.

*ATP homeostasis assay (Leica 5000)*

Seedlings were grown vertically in standard solid medium (0.8% plant agar) in square plates. 5 DAS old seedlings were then exposed to salt stress for 24 h in standard liquid medium (MS-1/2, 1% sucrose, 0,5 g/l MES-OH pH5.8) with 0 and 150 mM NaCl. The experiments were performed on WT and knock-out lines expressing the biosensor ATeam (De Col et al., 2017) composed by the two fluorescent proteins mseCFP and cp173-Venus. Seedlings were dark-adapted for at least 30 min before image acquisition to minimize potential effects of active photosynthesis. The analyzed tissues of each plant were: cotyledon, hypocotyl, shoot-root transition (SRT)-shoot, SRT-root, root, and root-tip. Whole *Arabidopsis* seedlings were mounted onto microscopy glass slides with 40 µl of imaging buffer and pictures were acquired on Leica 5000 fluorescence upright confocal laser microscope setting the excitation at 458 nm and the fluorescence at 465-500 nm (mseCFP) and 526-561 nm (cp173-Venus), the magnification was set at 10x. The experiment has been repeated 2 times, the number of seedlings analysed for each treatment ranges from 6 to 9. Each single CLSM image was analyzed using Fiji–ImageJ bundle software.

*Analyses of $Ca^{2+}$ dynamics in Arabidopsis seedling roots assay (Nikon Ti-E)*

Plants were grown vertically in standard solid medium (0.8% plant agar) in square plates for 7 DAS. Samples were mounted on a perfusion chamber with 200 µl of imaging buffer (10 mM MES Tris base; 1 mM $CaCl_2$; 5 mM KCl pH 5.8) and a ISMATEC pump was used to administrate stimuli in continuous setting the flux at 3 ml/min; every stimulus was added to imaging buffer. The experiments on calcium homeostasis were performed on WT and knock-out lines encoding the biosensors Yellow Cameleon 3.6 NES (Krebs et al., 2012). Excitation was provided by fluorescent lamp equipped with a 436/20 nm filter, and emission signals were filtered at 483/32 nm for CFP and at 542/27 nm for cpVenus with a dichroic mirror (510 nm). Images were acquired using Nikon Ti-E epi-fluorescence microscope, the tissues analysed were the root tip region of primary root; for every sample at least 3 Region Of Interest (ROI) were taken, starting from the root tip. The experiment was repeated 3 times, each times analysing 5/6 biological replicates. As concern root analyses, data obtained by NIS element platform, we calculated the change in ratio Rt − R0 or ΔR, where R0 is the basal ratio before the application of the stimulus and Rt the ratio at a measured time point. The

FRET ratio was calculated using Fiji software (https://imagej.net/Fiji/). The intensities of CFP and cpVenus were measured from the single CFP and cpVenus images as pixel intensities expressed in arbitrary units. We normalized the ΔR to the basal ratio value (ΔR:R0) and plotted ratio graphs for each measurement.

### Samples prepared for microscopic analysis

*GUS assay*

For the GUS assays *pWHY2:GUS* line was used. Different tissues and developmental stages were analysed: flowers, embryos and pollen from plants grown on soil. Tissues were harvested or cut from the plants and put in small Petri dishes with 2.5 ml of GUS staining solution (2 mM X-Gluc; 0.05% of Triton X-100; 0.5 mM of $K_3(Fe(CN)_6)x3H_2O$; 0.5 mM of $K_4(Fe(CN)_6)x3H_2O$; 10 mM EDTA; 50 mM buffer phosphate pH 7). Samples were incubated at 37°C overnight (O/N) and the day after only non-green samples were washed in sterile distilled water. Green samples were washed for 15 minutes in 70% ethanol before washing them in water. After the incubation period and the washing, tissue samples were collected and placed on microscope slides with 70 µl of imaging buffer (10 mM MES Tris base; 1 mM $CaCl_2$; 5 mM KCl pH 5.8). For the embryo development analyses, flowers were manually pollinated and, after 1, 2, 3, 4 and 5 DAP the embryos were taken out of the silique before the photo acquisition by placing them on microscope slides with imaging buffer and pressing softly on the coverslip with tweezers until they are released (Jove protocol). Pollen was analysed during several anther maturation phases. For the acquisitions stereomicroscope Leica MZ16F was used, setting the magnification at 5x, 10x or 25x.

## 2.6 Transmission Electron Microscopy (TEM)

Seeds were sown with a sterile toothpick under hood in gridded square plates and grown horizontally, TEM analyses were performed on 5 and 23 DAS plants grown on standard growth medium (0.8% plant agar) with 0 or 100 mM NaCl. The imaging was performed on the *primary* root (portion in which the lateral root start to grow) and on the $5^{th}$ leaf of each plant. Tissue samples were fixed by incubating them overnight at 4°C in 2.5% glutaraldehyde plus 2% paraformaldehyde in 0.1 M sodium cacodylate buffer, pH 7.4. The samples were post-fixed with 1% osmium tetroxide for 2 h at 4°C. After 3 washes in water the samples were dehydrated in ethanol and embedded in Epon resin (Sigma). Ultrafine sections (60-80 nm) were obtained with a Leica Ultracut EM UC7 ultramicrotome, subsequently contrasted with 1% uranyl acetate and 1% lead citrate and visualized with a Tecnai G2 (FEI) transmission electron microscope operating at 100 kV. Images were captured with Veleta (Olympus Soft Imaging System) digital camera. Two biological replicates have been analysed for each condition.

## 2.7 Treatments

### Ciprofloxacin

*why2KO ciprofloxacin assay*

Seeds were scattered on square plates and were grown for 23 DAS on standard solid medium (0.8% plant agar) supplemented with 0, 0.25 and 0.75 µM ciprofloxacin. DNA was extracted using the protocol: Isolation of High-Quality DNA (Bekesiova et al., 1999). For each extracted DNA sample, a PCR and an electrophoresis gel were performed to appreciate the level of DNA fragmentation (5 µl sample were loaded and 2.5 µl for the housekeeping *COX1*). The assays were performed in triplicates and each sample contained around 30-35 seedlings.

### Salt stress

*Liquid medium for salt stress treatment*

Salt stress experiments were mostly performed in liquid medium composed by half-strength Murashige & Skoog medium including vitamins (Duchefa, Murasnige and Skoog, 1962) with 1 % (w/v) sucrose, 0.5 g/L MES-KOH. pH was adjusted to 5.8 using KOH without any addition of agar but with different concentrations of salt.

*Primary root growth*

Primary root growth experiment was performed under prolonged salt stress treatment. For the long salt stress treatment (figure 2.8), seeds were sown directly in standard solid medium (0.8% plant agar) with 0 or 100 mM NaCl using a sterile toothpick placing the seeds 2 cm from the top edge, in line in square plates, and were grown vertically. Plates were stratified for 2 days and starting from 5-6 DAS primary root growth was monitored. For each treatment 3 biological replicates (3 plates for each condition) were prepared, sowing around 20 seeds per replicates. The experiment was repeated at least two times.

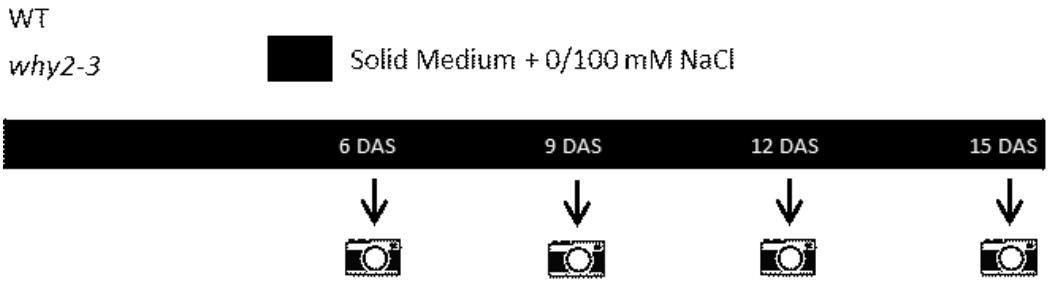


**Figure 2.8:** Experimental design for the long salt stress treatment.

Primary root growth images for each experiment were acquired using a Bio-Rad ChemiDoc Touch Imaging System (Flamingo setting) at different DAS and after the pulse stress. Images were processed using Fiji–ImageJ bundle software.

*Salt stress mtDNA fragmentation assay*

Plants were grown for 23 DAS in standard solid medium (0.8% plant agar) supplemented with 0, 100 and 150 mM NaCl, seeds were sown with a sterile toothpick under hood in gridded square plates and grown horizontally, around 36 seeds per plate. After 23 DAS some of the samples were collected while others were kept in culture for a recovery experiment. Recovery assay was performed by placing the seedlings for 10 days in a new plate containing standard solid medium (0.8% plant agar) without salt. After the recovery time the samples were collected for DNA extraction (Isolation of High-Quality DNA (Bekesiova et al., 1999). DNA concentration was measured using Nanodrop ND-1000 spectrophotometer. For each DNA sample a PCR was performed using opposite-direction primer and run on an electrophoresis gel to visualize the intensity of DNA fragmentation (7 µl sample were loaded). Primers have opposite direction mitochondrial sequences (figure 2.9.B): 180454For and 171214Rev; 80161For and 30001Rev. Primer sequences are reported in table II. The assays were performed 4 times and each sample contained around 30-35 seedlings.

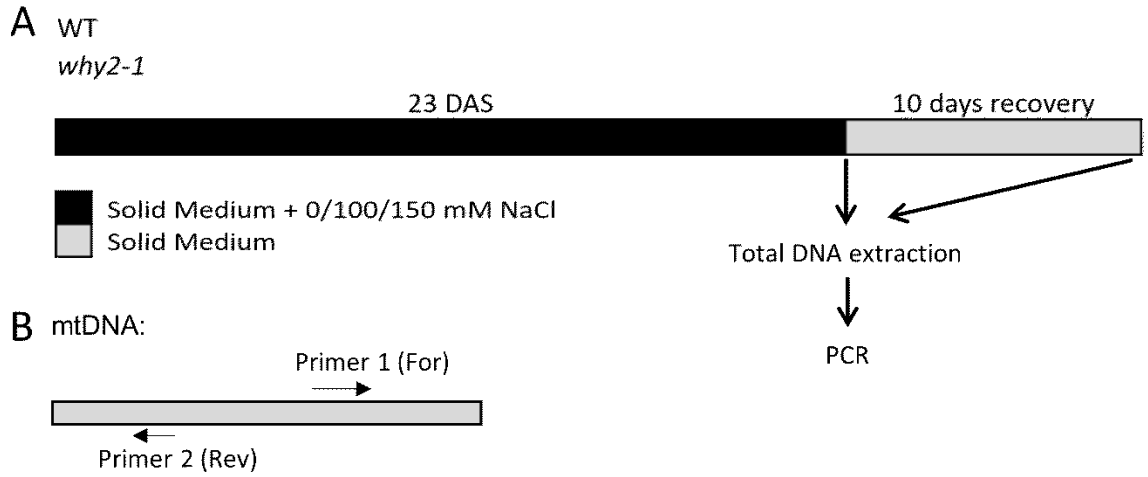


**Figure 2.9: (A)** Experimental design for the salt stress mtDNA fragmentation assay. **(B)** Primer design on the mtDNA to analyse possible DNA fragmentation.

*mtDNA copy number quantification under salt stress*

Plants were grown for 23 DAS in standard solid medium (0.8% plant agar) supplemented with 0, 100 and 150 mM NaCl, seeds were sown with a sterile toothpick under hood in gridded square plates and grown horizontally, around 36 seeds per plate. After 23 DAS some of the samples were collected while others were kept in culture for a recovery experiment. Recovery assay was performed by placing the seedlings for 10 days in a new plate containing standard solid medium (0.8% plant agar) without salt. After the recovery time the samples were collected for DNA extraction (Isolation of High-Quality DNA (Bekesiova et al., 1999). DNA concentration was measured using Nanodrop ND-1000 spectrophotometer. For each DNA sample a qRT-PCR was performed. The DNA amount of each mtDNA fragments were normalized to the level of the single-copy number gene Rpotp and analysed using the ΔCt method. For the mtDNA copy number quantification 3 mitochondrial genes were used:

*Q-COX1* and *orf170mito*. Primer sequences are reported in table III. The assays were performed at least 3 times and each sample contains around 30-35 seedlings.

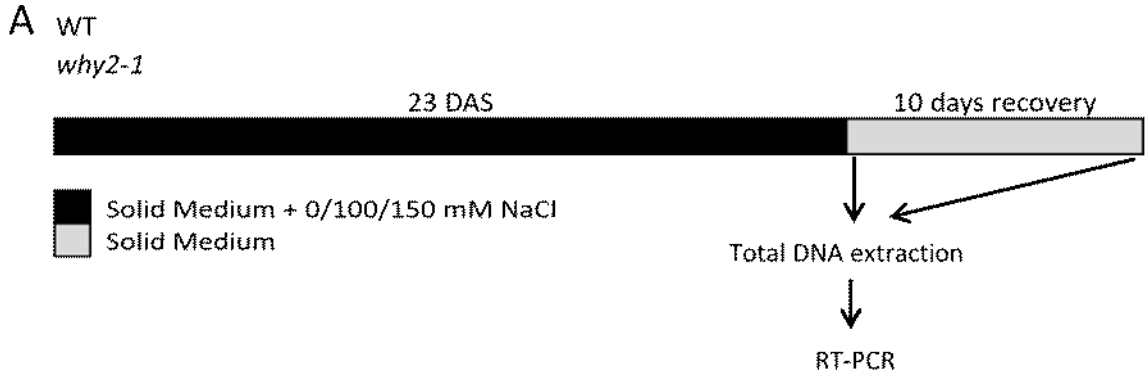


**Figure 2.10:** Experimental design for the mtDNA copy number quantification under salt stress.

## 2.8 Analysis of enzymatic and non-enzymatic antioxidants and determination of oxidative marker

Following experiments were performed in collaboration with the Lab of Prof. De Pinto (University of Bari). Samples were grown and treated in our lab and analysed in De Pinto Lab. Plants were grown for 14 DAS on standard solid medium and then exposed for 8 h to standard liquid medium with 0 and 150 mM NaCl. For every sample around 300 mg of fresh material were collected (all seedlings).

*Analysis of enzymatic and non-enzymatic antioxidants*

For the determination of non-enzymatic antioxidants, *Arabidopsis* seedlings were homogenized with four volumes of cold 5% (w/v) meta-phosphoric acid at 4°C in liquid nitrogen. The homogenates were centrifuged at 20000 g for 15 min at 4°C. Supernatants were used to determine contents and redox states of ASC and GSH according to De Pinto et al. (1999).

For the determination of enzymatic antioxidants activity, seedlings were ground in liquid nitrogen and homogenized at 4°C in a 1:8 (w/v) ratio with the extraction buffer (50 mM Tris–HCl pH 7.5, 0.05%cysteine, 0.1% bovine serum albumin, 1mM phenylmethanesulfonylfluoride-PMSF). For the determination of APX activity, 1mM ASC was added to the extraction buffer. Homogenates were centrifuged at 20000 g for 15 min, and the supernatants were used for spectrophotometric and electrophoretic analyses. Protein concentration was determined according to Bradford (1976), using bovine serum albumin as a standard.

Catalase (CAT, EC 1.11.1.6) activities was spectrophotometrically measured according to Paradiso et al. (2020), Ascorbate peroxidase (APX, EC 1.11.1.11), activities were determined according to De Pinto et al. (2000).

*Determination of oxidative marker*

The level of lipid peroxidation was evaluated in terms of malondialdehyde (MDA) content determined by the TBA reaction as described by Paradiso et al. (2008). The amount of MDATBA complex was calculated using an extinction coefficient of 155 $mM^{-1}$ $cm^{-1}$.

## 2.9 Primers list

*Table I Genotyping Primers*

| Gene | 5'->3' | Sequence | Function |
|---|---|---|---|
| *AtWHY2* | For | CCTCAGAAGTCGGAAGACC | *why2-3* and *why2-4* (CRISPR/CAS9 Mutants) |
| | Rev | TGCGAACAATCGACCACTAG | |
| *Cas9* | For | CAGCTCGTGCAGACCTACAAC | Presence of CAS9 |
| | Rev | TGCCTTCTAAGGATAGCGTG | |
| *AtWHY2* | Rev | GCATCCTCAAAACCAATGAC | *why2-1* (T-DNA insertional mutant) |
| | For | CATGATGTGTGGAAGAGCAA | |
| T-DNA | For | ATTTTGCCGATTTCGGAAC | |

*Table II mtDNA fragmentation assay Primers*

| Gene | 5'->3' | Sequence | Function |
|---|---|---|---|
| 171214REV0 | Rev | CATTCTAGCCCGAGAGGAACT | Possible mtDNA aberrant products (Cappadocia et al., 2010) |
| 180454FOR0 | For | ACCTACCAGCCCCATGTAAAC | |
| 30001REV0 | Rev | ACAGTCCACCAATAGCGGAAG | Possible mtDNA aberrant products (Cappadocia et al., 2010) |
| 80161FOR0 | For | ACGTGCAAGTTTCCCTGCATG | |
| *COX1* | For | GCTAGCTCATGGCAGGAAATC | Housekeeping (Cappadocia et al., 2010) |
| | Rev | GTAACGTCCGTTCCGTGATCT | |

*Table III mtDNA copy number Primers*

| Gene | 5'->3' | Sequence | Function |
|---|---|---|---|
| Q-*COX1* | For | GCCATGATCAGTATTGGTGTCTT | mitochondrial gene (mtDNA quantification) |
| | Rev | CTACGTCTAAGCCCACAGTAAACA | |
| *orf170mito* | For | CTTTAGCAACCAAGCGAGCC | mitochondrial gene (mtDNA quantification) |
| | Rev | TGATGCTCTCTCTCGGAACA | |
| *AtRpoTp* | For | TGGAAGCCGTCTGCTAGAACTA | Internal standard for mtDNA quantification (nuclear single copy gene) |
| | Rev | TGTCTGAATGCAGGTCGAAAC | |

*Table IV qRT-PCR Primers*

| Gene | 5'->3' | Sequence | Function |
|---|---|---|---|
| *WHY1* | For | ACTTCGAGAAGCAGAGGTTCGG | *WHIRLYs* genes |
| | Rev | TCTAGCAGGCAATCCTTCAGCAG | |
| *WHY2* | For | ACTGAAATCGATTCGGGAAA | |
| | Rev | CTGTTTCTTTTCCCAGTCGT | |
| *WHY3* | For | ACGATAGAACCACGAGCACCAG | |
| | Rev | GAATCTGGTGCGTTCAAGCTGACA | |
| *AtGA20ox3* | For | TCGTGGACAACAAATGGCA | Gibberellin 20-OXIDASE 3 (AT5G07200) |
| | Rev | TGAAGGTGTCGCCTATGTTCAC | |
| *MSH1* | For | AGCATTATTTTCCCATGCTTGT | MUTL protein homolog 1 |
| | Rev | TTTGCGCCCTCATCTAAACT | |
| *ODB1* | For | TCTTTGCCTTCTTGCCTCAGA | Organellar DNA-binding protein 1 |
| | Rev | ATTCCTTGACGGGTTTCATCAT | |
| *OSB1* | For | ACGATTGGTGGGACAACAGGAGAA | Organellar single-stranded DNA-binding protein 1 |
| | Rev | TCTGAGCAAAGCCAGAGAGCTTCA | |
| *mtSSB1* | For | ATCAAACCTCAACGACGTCG | mitochondrial SBB1 (Single strand DNA binding protein) |
| | Rev | GCTCCTACAAGCCTCTGAT | |
| *POLIB* | For | CCTGAATACCGTTCACGTGCCCA | mitochondrial polymerase I B (At3g20540) |
| | Rev | AGCCGCACTTCCCTGAACAGGA | |
| *mtHSC70-1* | For | GTCCAAATGGCTTCCGTATCTG | mitochondrial heat shock protein 70-1 |
| | Rev | CCAATAACATCATTCCCCACAG | |
| *WRKY15* | For | TCGTTGTCATTGCTCGAAGA | WRKY DNA-binding protein 15 |
| | Rev | CTTATCGCCGGAACCCTAAT | |
| *AOX1a* | For | GCCTACCGATTTGTTCTTCCAG | Alternative oxidase 1 a |
| | Rev | CAGTGTAGTAACATTCCTCCAACCA | |
| *ACT2* | For | AAGCTCTCCTTTGTTGCTGTT | Housekeeping gene |
| | Rev | GACTTCTGGGCATCTGAATCT | |

## 2.10 Statistics

All experiments were performed at least in three technical and biological replicates. The values are represented as the means ± standard deviation. Asterisks describe the level of significance: * = $p < 0.05$; ** = $p < 0.005$; *** = $p < 0.001$; **** = $p < 0.0001$. The statistical significance was demonstrated using GraphPad Prism, performing the following tests: Student's t-test method; two-way ANOVA; Šídák's multiple comparisons test; Tukey's multiple comparisons test.

# Results and Discussion

## 3.1 WHY2 function on mtDNA

### 3.1.1 Aberrant mtDNA products in mutant lines under genotoxic agent

Evidences from the literature show that WHIRLY proteins modulate DNA repair in chloroplasts and mitochondria (Cappadocia et al., 2013; Cai et al., 2015). WHY2 in fact is a ss-mtDNA binding protein that plays a role in mtDNA repair by avoiding the accumulation of microhomology-mediated DNA rearrangements (Cappadocia et al., 2010), given that WHY2 avoids non-homologue recombination during mitochondrial DNA replication. To confirm the evidence that WHIRLY2 is important for the accurate repair of mitochondrial DNA lesions, functional characterization of mutant lines was performed treating the plants with ciprofloxacin, a genotoxic agent that selectively inhibits mitochondrial DNA topoisomerase and DNA-gyrase, inducing double-strand mtDNA breaks. These damages activate the DNA repair system, which, in absence of WHY2, leads to the accumulation of aberrant mtDNA recombinant products. Performing a PCR with opposite direction primers it is possible to amplify the aberrant mtDNA products, that accumulate in a dose-dependent way based on ciprofloxacin concentration (Cappadocia et al., 2010; figure 3.1).

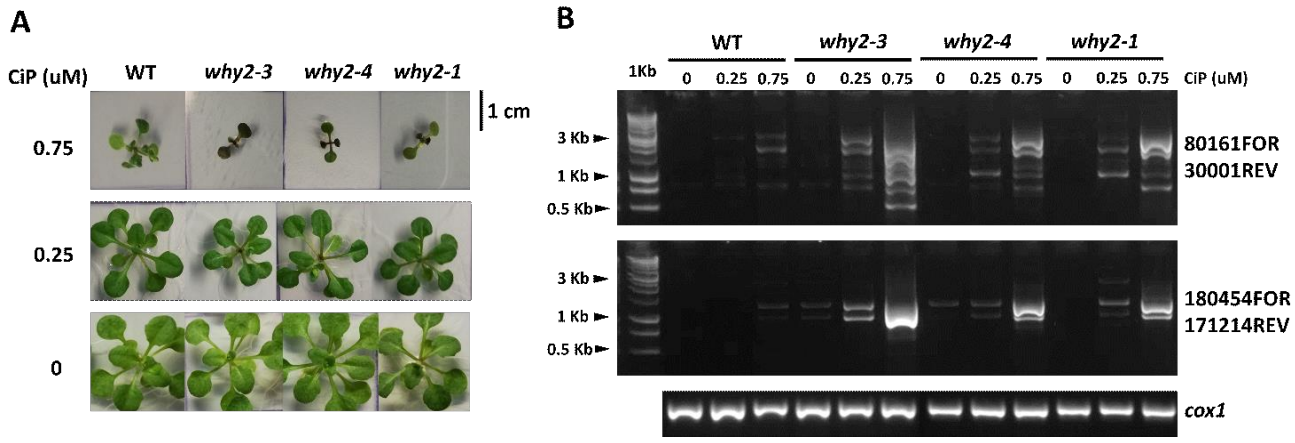


**Figure 3.1: (A)** Growth of WT and knock-out lines (*why2-3, why2-4* and *why2-1*) under different concentrations of ciprofloxacin (0, 0.25 and 0.75 µM). Plants were grown for 23 Days After Sowing (DAS) in solid medium (2.2.3) **(B)** Electrophoretic analysis of representative PCR performed with 2 inward-facing mitochondria genome-directed primers. Low cycle amplification of the *cox1* mitochondrial gene were used as loading controls. The oligonucleotides used for each PCR are indicated on the side.

DNA rearrangements accumulate in WT line only under the highest ciprofloxacin concentration (0.75 µM), while in mutant lines they increase proportionally with the concentration of the genotoxic agent and are even lightly detectable after growth in solid medium without ciprofloxacin. These results suggest that *why2-3* and *why2-4* as well as *why2-1* lack the repair protein WHY2.

### 3.1.2 Mitochondrial morphology of *why2-1* and *why2-3* knock-out lines

The absence of WHY2 is associated with aberrant mitochondrial morphology in cultured cells and seedlings in *why2-1* line (Golin, Negroni et al., 2020). To further confirm that the elongated mitochondrial phenotype was due to the lack of WHY2, we analysed mitochondrial morphology in the *why2-3* mutant using the potentiometric dye TMRM (see M&M). Mitochondria morphology was evaluated by confocal microscope analysis in WT and *why2-3* line by staining 5-day-old seedlings and analysing the root tissues, in concomitance with the area where the root hairs arise.

During plant's life cycle, mitochondria have different morphology, for example during seeds germination mitochondria in the embryo are clustered around the nucleus and elongated (Paszkiewicz et al., 2017), while during seedlings growth the mitochondrial morphology is rather homogeneous in tissues, small and circular. To quantify the irregularities, we performed a quantification of mitochondrial area and mitochondrial shape. Thanks to this analysis we observed that *why2-1* as well as *why2-3* seedlings contain elongated mitochondria in the root tissues, compared with WT mitochondria that appear smaller and circular (figure 3.2). We observed that the area of each mitochondrion in mutant line is about 3 times with respect to WT; the circularity value is instead lower than 1, with 1 corresponding to a perfect circularity and <1 implying elongated mitochondria (figure 3.2).

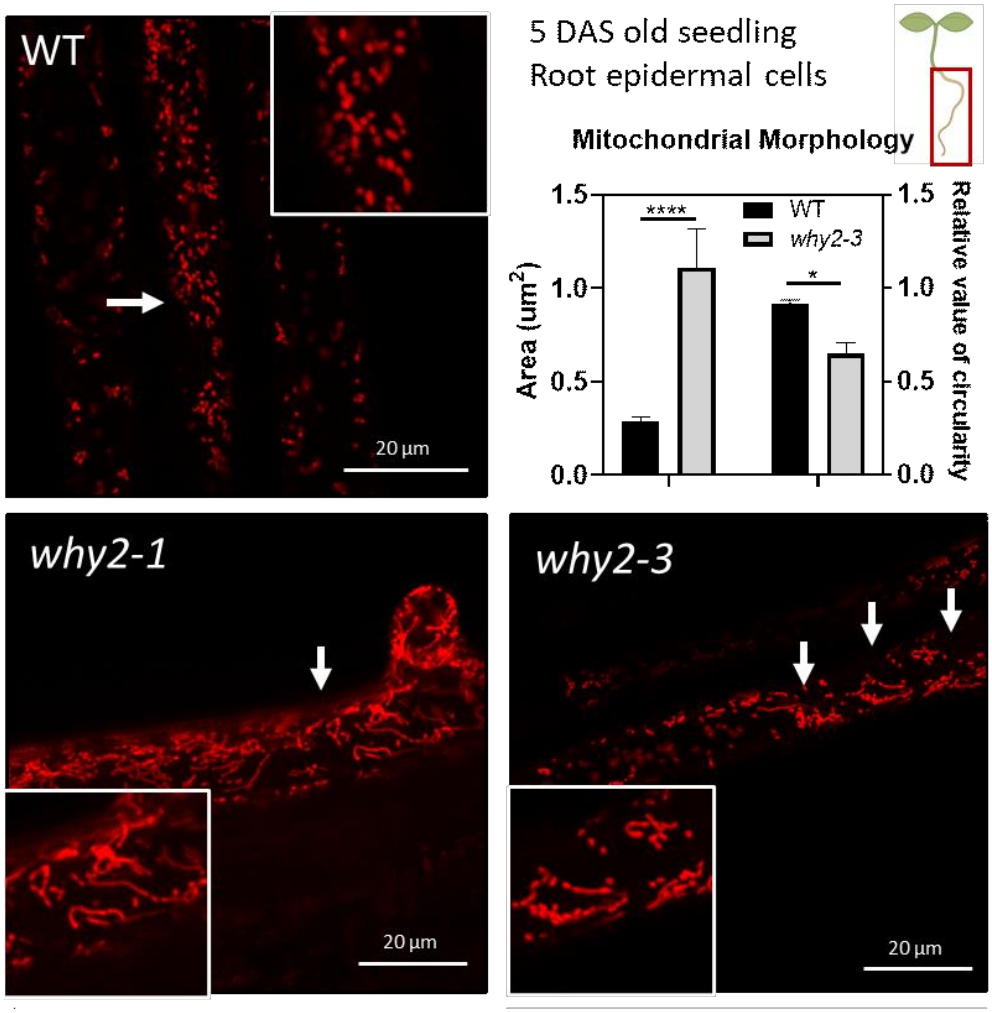

**Figure 3.2: (A)** Representative images of mitochondrial morphology analyses performed on root tissue cells of 5 DAS old *A. thaliana* seedlings stained with 200 nM TMRM and photographed by CLSM. Scale bar: 20 µm. The graph reports mitochondrial area on the right and mitochondrial circularity value on the left (1: circular; <1: elongated). Error bars: SD. White arrows indicate stained mitochondria. Asterisks describe the level of significance: * = $p < 0.05$; **** = $p < 0.0001$. Statistic: Student's t-test method.

### 3.1.3 Mitochondrial morphology of *why2-1* knock-out lines during the primary root growth

To further confirm the mitochondrial morphology in root tissues, we expressed the mitochondrial marker mt-YFP in the *why2-1* background and performed a side-by-side comparison of mitochondria morphology during root development. Elongated mitochondria were confirmed in root cells (red arrows indicate root hair, figure 3.3). Given this observation, we decided to look at different stages of development of the primary root. In the region where root hairs develop, an elongated morphology was observed only during the first days after germination. As figure 3.3 shows, in *why2-1* mt-YFP plants, mitochondria maintain an elongated profile up to 7 Days After Sowing (DAS), while from 9 DAS onwards, such shape was no longer observable.

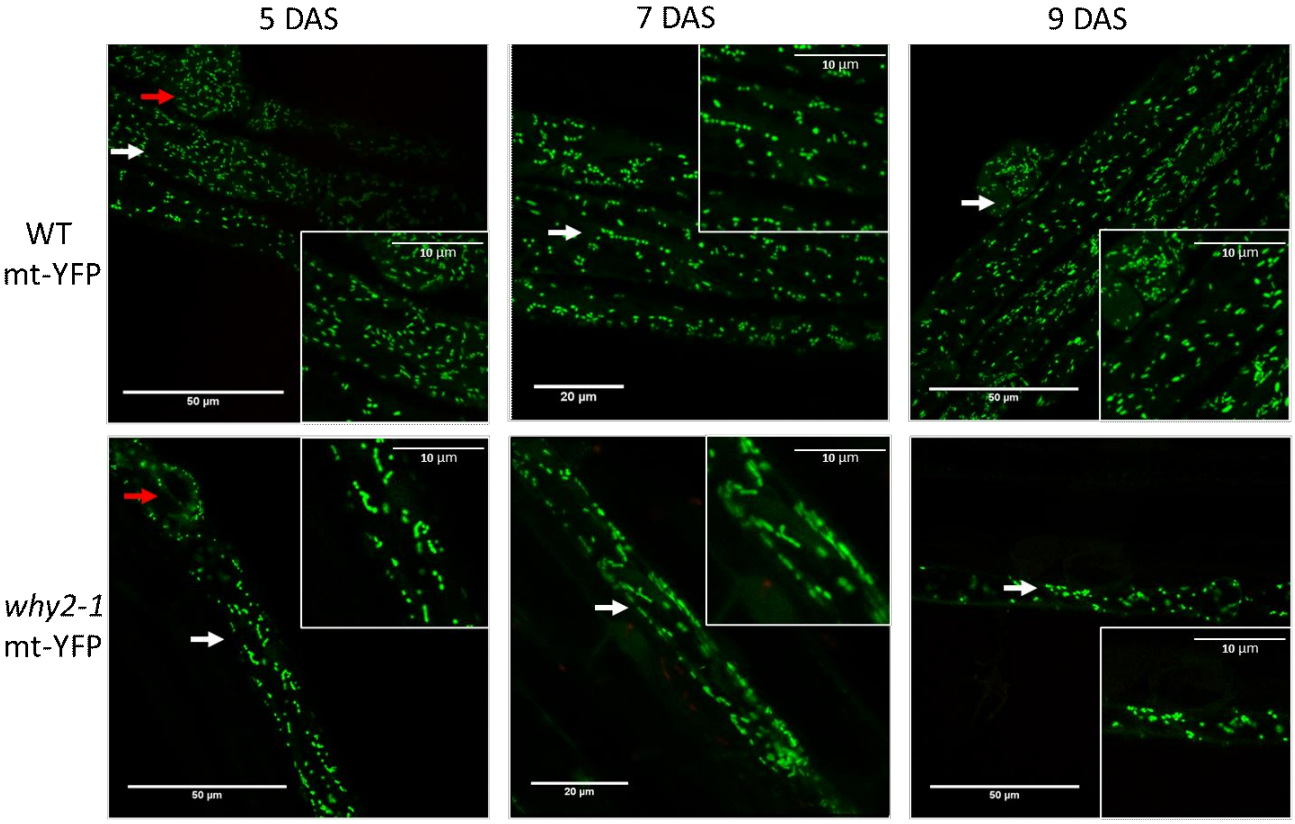


**Figure 3.3:** Representative images of mitochondrial morphology analyses performed on root tissue cells of 5, 7 and 9 DAS old *A. thaliana* seedlings from mt-YFP WT and *why2-1*. Pictures were taken by CLSM. Scale bar: 50 µm for 5 and 9 DAS; 20 µm for 7 DAS. Inserts scale bar: 10 µm. White arrows indicate stained and fluorescent mitochondria, and red arrows represent the point where a root hair is born confirming the root epidermal tissue.

A possible explanation of this observable morphology until the seventh day of development, could be that the absence of WHY2 causes a clear phenotype on cells owning a higher metabolic activity. The root epidermal tissue is in fact subject to metabolic changes due to the growth of root hairs during early development (Brechenmacher et al., 2009).

The previous mt-YFP knock-out lines were also characterized by reduced mitochondrial dynamics when compared with those present in WT root cells (Golin, Negroni et al., 2020; Appendix III), linking an aberrant mitochondrial morphology to an impairment in the mitochondrial mobility in *WHY2* mutant lines. This result is supported by evidence from the literature that link together plant mitochondrial shape, function and dynamics. Mitochondrial dynamics is fundamental for different cellular processes and also for the transport of ATP and molecules throughout the cell. For example, the interactions between mitochondria and ER became a focus of research during the last decade in animals, fungi and plants, linking ER-mitochondria contacts additionally to mitochondrial dynamics and quality control (Kornmann, 2013; Lackner, 2014; Mueller and Reski, 2015).

### 3.1.4 Aberrant Nucleoids morphology in *WHY2* knock-out plants

In order to analyse in more details mitochondria of mutant plants we performed transmission electron microscopy analyses on leaves of 5 day old seedlings. Having already analysed the mitochondrial morphology at the root level on 5 days seedlings and in *Arabidopsis* suspension cell cultures (Golin, Negroni et al., 2020), we decided to complete the analysis by acquiring TEM images of 5 DAS cotyledons, given also the difficulties to properly stain this organ with TMRM.

Figure 3.4 shows that WT cell lines mitochondria were round or oval, contained several cristae and an electron-dense matrix, mitochondria in the *why2-1* line, instead, appeared to be swollen, with a reduced number of cristae and a low electron density matrix that might be index of low mitochondrial functionality linked to mitochondrial pleomorphy and low motility (Logan, 2006; Vigani et al., 2015). Approximately 30% of the mitochondria in leaves of the mutant line exhibited such altered morphology compared with the WT (Figure 3.4). Furthermore, as calculated from TEM images of 23 weeks-old leaf sections, the relative intracristae surface area decreased by about 40% ($p < 0.05$) in the *why2-1* mutant line when compared to the WT (Golin, Negroni et al., 2020). Interestingly, a large translucent area (figure 3.4 right panel) in the centre of the organelles is present, where fibrillar structures resembling unpacked DNA are evident (figure 3.4, insert at the top of the *why2-1* right panel). In these plants mtDNA is less compact (figure 3.4) suggesting that the absence of WHY2 might be involved in mitochondrial nucleoid organization, resembling the role of WHY1 in chloroplast (Krupinska et al., 2014).

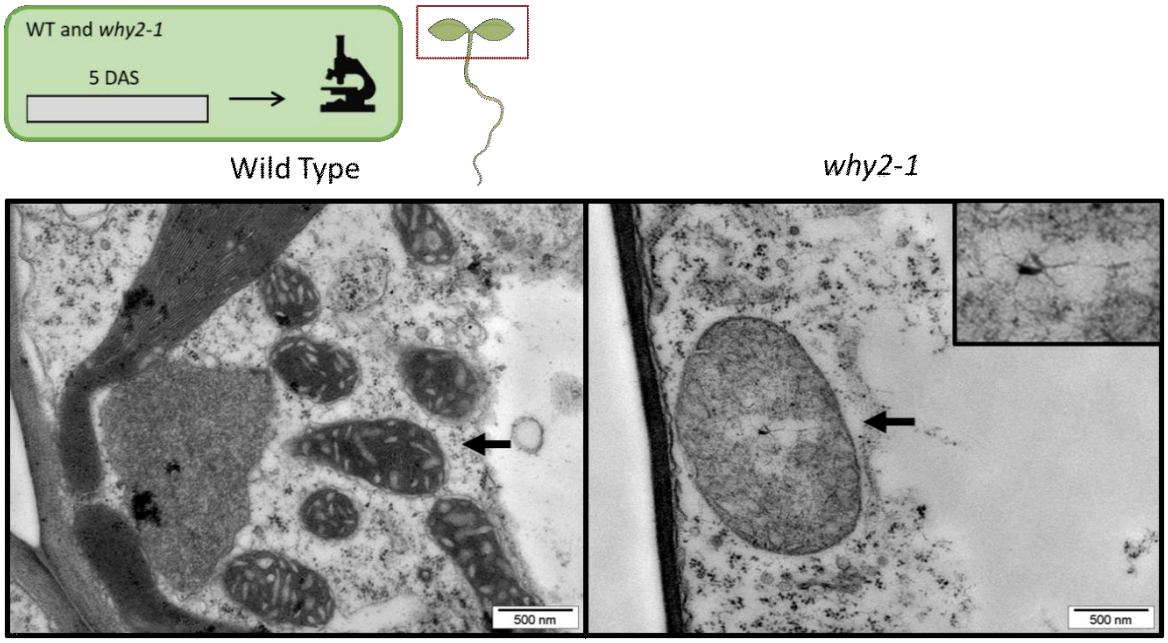


**Figure 3.4:** Mitochondria and nucleoids morphology in 5 DAS plant tissues. Transmission electron microscope images were taken of mitochondria from leaf of WT and mutant plants. Arrows in the WT panels indicate healthy mitochondria, and in the right panel arrows indicate a translucent area within mitochondria matrix in *why2-1* mutant line.

By staining 5 DAS old *Arabidopsis* roots seedlings mitochondria with TMRM together with picoGREEN staining the mtDNA in WT and mutant lines, we were able to evaluate the number of nucleoids per mitochondria. picoGREEN, is a dsDNA quantitation reagent that quickly enters mitochondria and marks mtDNA. Images were analysed setting a threshold for fluorescence signals, (only picoGREEN intensity values above 10 were considered) in order to take in account only strong picoGREEN signal that is associated to dense and packed mitochondrial nucleoids.

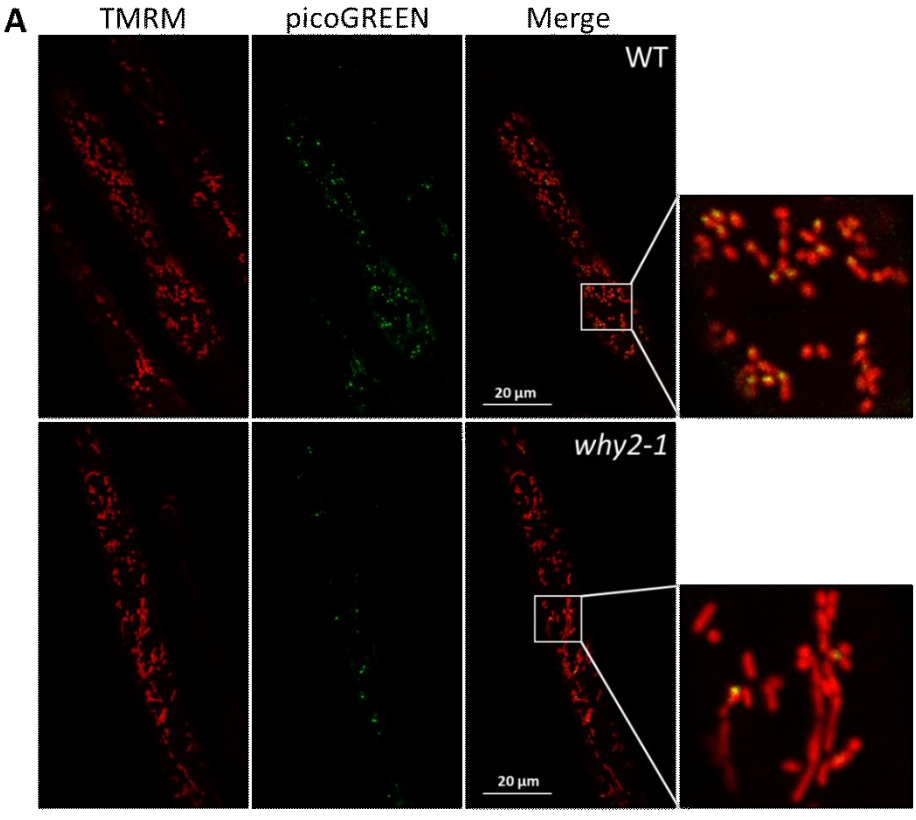

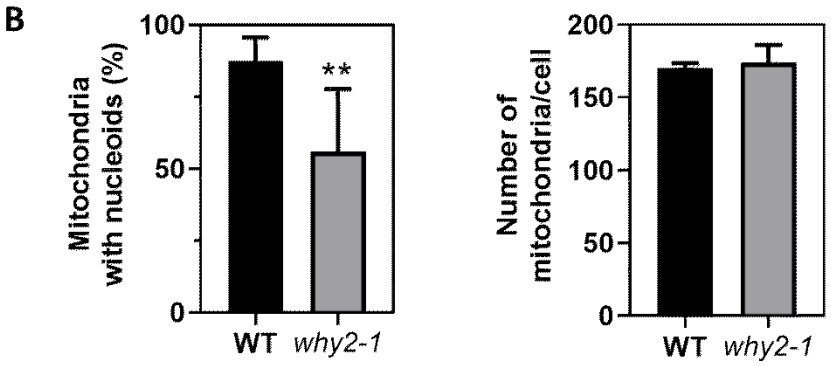


**Figure 3.5: (A)** Confocal images of 5 DAS old seedlings roots of WT and why 2-1 plants stained with TMRM and picoGREEN. The images represent the signal emitted by TMRM, picoGREEN and the merge of the two. **(B)** The first graph represents the detected percentage of mitochondria with at least one nucleoid per cell; the second graph shows the number of mitochondria per cell. The experiments have been performed at least 2 times with 3 biological replicates and at least 9/10 cells were analyzed for each line. Error bars: SD. Asterisks describe the level of significance: ** = $p < 0.005$. Statistic: Student's t-test method. The analysis has been performed with the Volocity software setting a fixed threshold for the fluorescent signals.

Summarizing the total amount of mitochondria per cell and the percentage of mitochondria with at least one nucleoid were evaluated. In mutant lines, where mitochondria are elongated as already described above, mitochondria do not always appear with a nucleoid (figure 3.5). In WT line around 88% of mitochondria have at least one nucleoid, while in *why2-1* mutant the fraction is only 55% of mitochondria stained with picoGREEN, while the other mitochondria do not exhibit any fluorescent signal. On the other hand, there is no statistical difference in the number of total mitochondria per cells.

The lowest number of nucleoids highlighted in the elongated mitochondria in mutant lines were interpreted as an impairment in nucleoids organization. We wondered whether this signal drop was due to a decrease in the net amount of mtDNA or to a disorganization of mtDNA (less nucleoids). Therefore, we measured the mtDNA copy number.

### 3.1.5 Mitochondrial DNA copy number

A mtDNA copy number analysis was performed through RT-PCR on mitochondrial genes (Morley and Nielsen, 2016) on whole 6 DAS seedlings and on leaves and roots of 23 DAS old plants. A broad spectrum of different tissues and developmental phases were chosen to investigate a possible impairment in the mtDNA copy number. As a "housekeeping gene" the single-copy nuclear gene *AtRpotp* (nuclear plastid-RNA polymerase; Morley and Nielsen, 2016) has been chosen. To study the variation of mtDNA copy number we selected two mitochondrial genes: *COX1* (mitochondrial cytochrome oxidase 1 subunit) and *orf170mito* (mitochondrial RNA-dependent DNA polymerase).

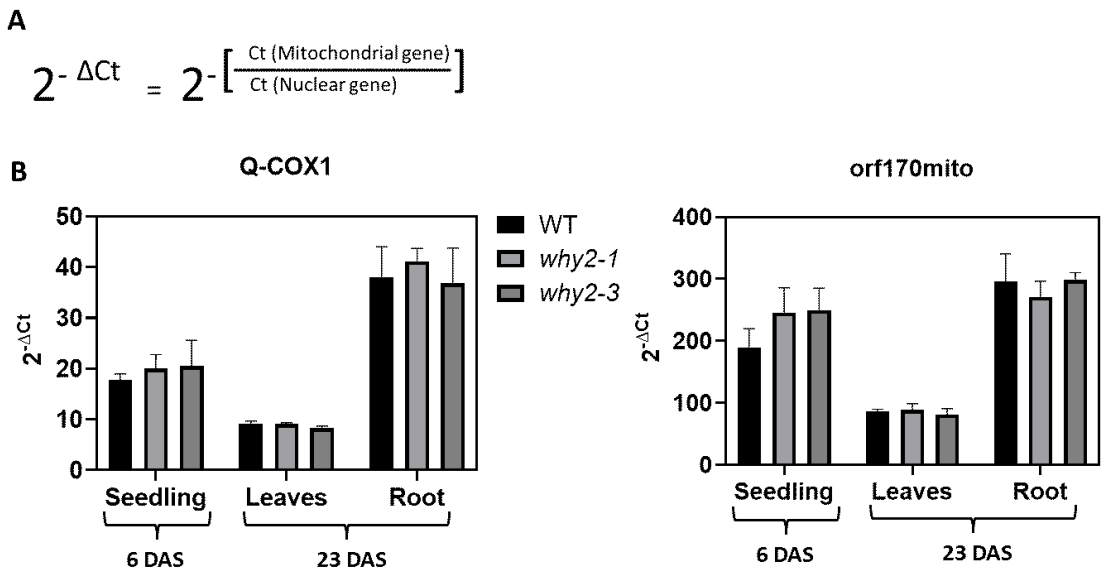


**Figure 3.6: (A)** The results were analysed with the technique of 2^(-ΔCt), the used formula is shown in the figure. **(B)** Real-Time PRC on 6 and 23 DAS WT and *why2-1* and *why2-3* lines. Mitochondrial analysed genes: *COX1* (mitochondrial cytochrome oxidase 1 subunit) and *orf170mito* (mitochondrial RNA-dependent DNA polymerase). As housekeeping gene has been used *AtRpotp* (nuclear plastid-RNA polymerase). Error bars: SD. Statistic: Two-way ANOVA.

mtDNA copy number does not vary in young seedlings neither in old leaves nor roots plants (figure 3.6). This means that the absence of WHY2 does not impact the amount of mtDNA, but that instead it causes a disorganization of the nucleoid structures reflected in the decrease of picoGREEN signal as previously reported.

To sum up the results obtained so far, we noticed that the absence of WHY2 impairs nucleoids structural integrity and results in aberrant mitochondrial morphology, meaning that there must be a tight link between mtDNA integrity and organization, and mitochondrial morphology and dynamics. We hypothesize that nucleoids might have a scaffold role, and that the lack of these structures could impact on both shape and movement of the whole organelle. Corroborating this hypothesis, it has been demonstrated that the integrity of mtDNA/nucleoids plays an important role in the remodelling of cristae structures in animal cells (Ban-Ishihara et al., 2013). In this context, the loss of a ssDNA-binding protein such as WHY2 leads to an unpacking of mtDNA and loss of nucleoids, luckily for an impaired recruitment of other scaffold proteins.

## 3.2 Role of WHIRLY2 in plant growth, germination and embryo development

### 3.2.1 Phenotyping of *why2-3* and *why2-4* CRISPR/Cas9 knock-out lines

In order to identify possible phenotypic variations in WHY2 knock-out lines during plant growth and development, we performed phenotyping analyses. For the phenotype characterization, primary root growth, rosette development and primary flower growth were evaluated in *why2-3* and *why2-4*. As figure 3.7.A shows it was observed that the absence of WHY2 had a statistically significant impact in the early root growth at 7 DAS in both mutant lines. In the other studied development

stages, instead, no significant differences were observed respect to wild type (figure 3.7). The absence of WHY2 does not have a strong impact during vegetative growth (figure 3.7.A; B and C), in fact after the 7 DAS no differences were noticed in the primary root growth between knock-out lines and WT, but also in any of the analysed stages during *rosetta* development and primary flower growth a difference was noted. These results confirmed previous observations on *why2-1* mutant line (Maréchal et al. (2008).

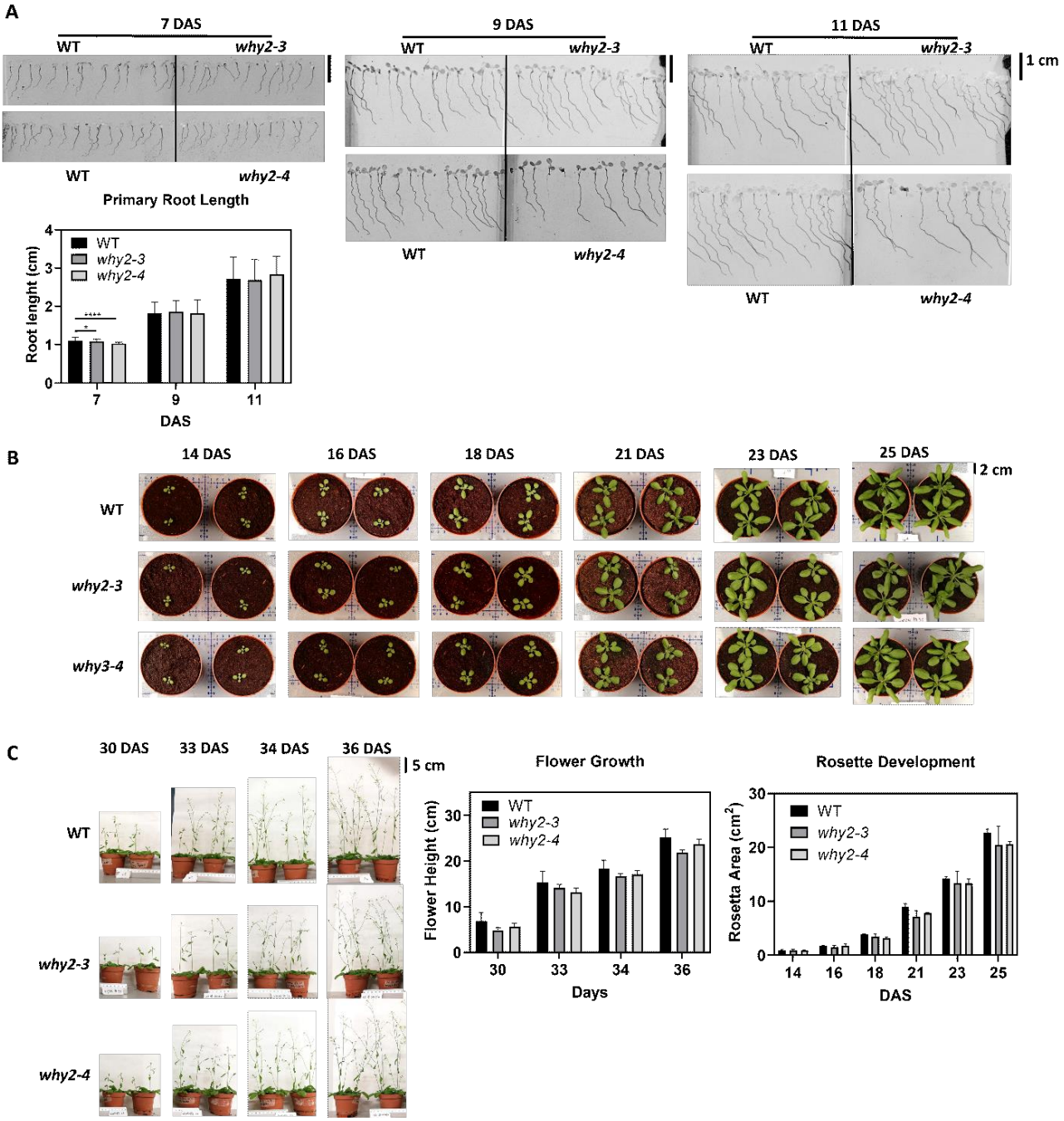


**Figure 3.7:** Phenotypic characterization of *why2-3* and *why2-4* mutant lines in comparison to the wild type control (Col-0, WT). **(A)** Primary root growth analysis: vertical root growth on standard solid medium (2.2.3). Scale bar: 1 cm. Tukey's multiple comparisons test has been performed, statistically significant differences between *why2KO* lines and WT were observed only after the first 7 DAS. The experiment was repeated 2 times with at least 20 plants per genotype. **(B)** Rosette development analysis were performed in pots containing soil. Scale bar: 2 cm. No statistical differences between *why2KO* lines and WT were noticed. The experiment was repeated 2 times with 4 plants per genotype. **(C)** Flower growth analyses were performed in pots containing soil. Scale bar: 5 cm. No statistically relevant differences between *why2KO* lines and WT. The experiment was repeated 2 times with 4 plants per genotype. Asterisks describe the level of significance: * = $p < 0.05$; **** = $p < 0.0001$. Statistic: Student's t-test method.

### 3.2.2 WHY2 in embryo development

Since mitochondria provide ATP to the cells, our studies were focused on cells with an active metabolism that have a high energy demand, such as those undergoing division, in which organelles functionality is particularly necessary. Functional mitochondria are indeed important during the first phases of embryo development. In fact, properly developed embryos and surrounding tissues are essential to obtain vital and vigorous seeds. For these reasons, we decided to investigate the impact of WHY2 during embryo development, pollen maturation and seed germination.

To do that we used transgenic plants harbouring the reporter gene GUS under the control of *WHY2* promoter (Cai et al., 2015). Four-week-old plants were manually pollinated to precisely monitor through GUS staining the *WHY2* promoter activity during every phase of embryo development (figure 3.8). After pollination, the formation of the zygote starts, and it is possible to follow the subsequent embryo development steps (figure 3.8).

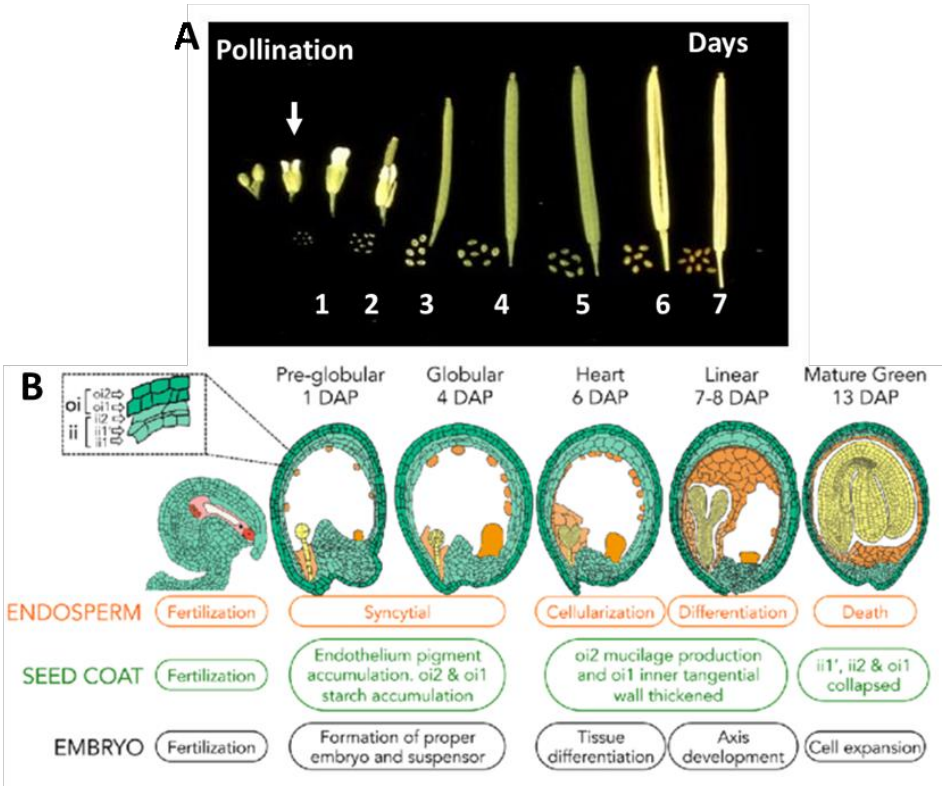


**Figure 3.8: (A)** Representation of different *A. thaliana* siliquae maturation phases, the white arrow represents the mature flower ready for pollination, numbers represent the days after pollination (DAP) at which siliquae development was monitored. **(B)** Schematic representation of seed development in *Arabidopsis*. Diagrams of an unfertilized ovule and the five stages of seed development from the pre globular (1 day after pollination-DAP) to mature green (13 DAP) stage. Embryo developmental stages were adapted from Le et al. (2010). Detail of the five seed coat layers according to Appelhagen et al. (2014). Seed coat developmental events are specified by Beeckman et al. (2000). Endosperm development is presented according to Lafon-Placette and Kohler (2014). Drawings are not to scale. Abbreviations and colour code: oi outer integument, ii inner integument, DAP days after pollination. Green seed coat, orange endosperm, yellow embryo.

Firstly, we monitored *WHY2* promoter activity, which can be used as a proxy of gene transcription before and after pollination: figure 3.9.A.1 shows that there isn't any detectable GUS staining before pollination; pollinated flowers, instead, have several blue stained embryos mirroring high level of *WHY2* promoter activity (figure 3.9.A.2 and 3). The GUS staining linked to the WHY2 promoter

activity can be appreciated more in detail at higher magnification in 3 days after pollination (DAP) (figure 3.9.B.2 and 3) in which we can confirm that there is no GUS staining before pollination (Figure 9.B.1) and that *WHY2* promoter have a high activity particularly in the endosperm and chalazal endosperm cells (Figure 9.B.2 black arrows), in globular embryo (Figure 9.B.3 white circle) and embryo surrounding region (Figure 9.B.3 black arrows).

Figures 3.9.C represents the GUS staining in embryos at 1, 2, 3 and 4 DAP: in the first 3 DAP the embryos and the surrounding regions show an intense blue staining while at 4 DAP the signal is lost. This could be due to a low *WHY2* promoter activity, or a physical hindrance given by the hardening of the seed coat that does not allow the penetration of the substrate in the deep tissues.

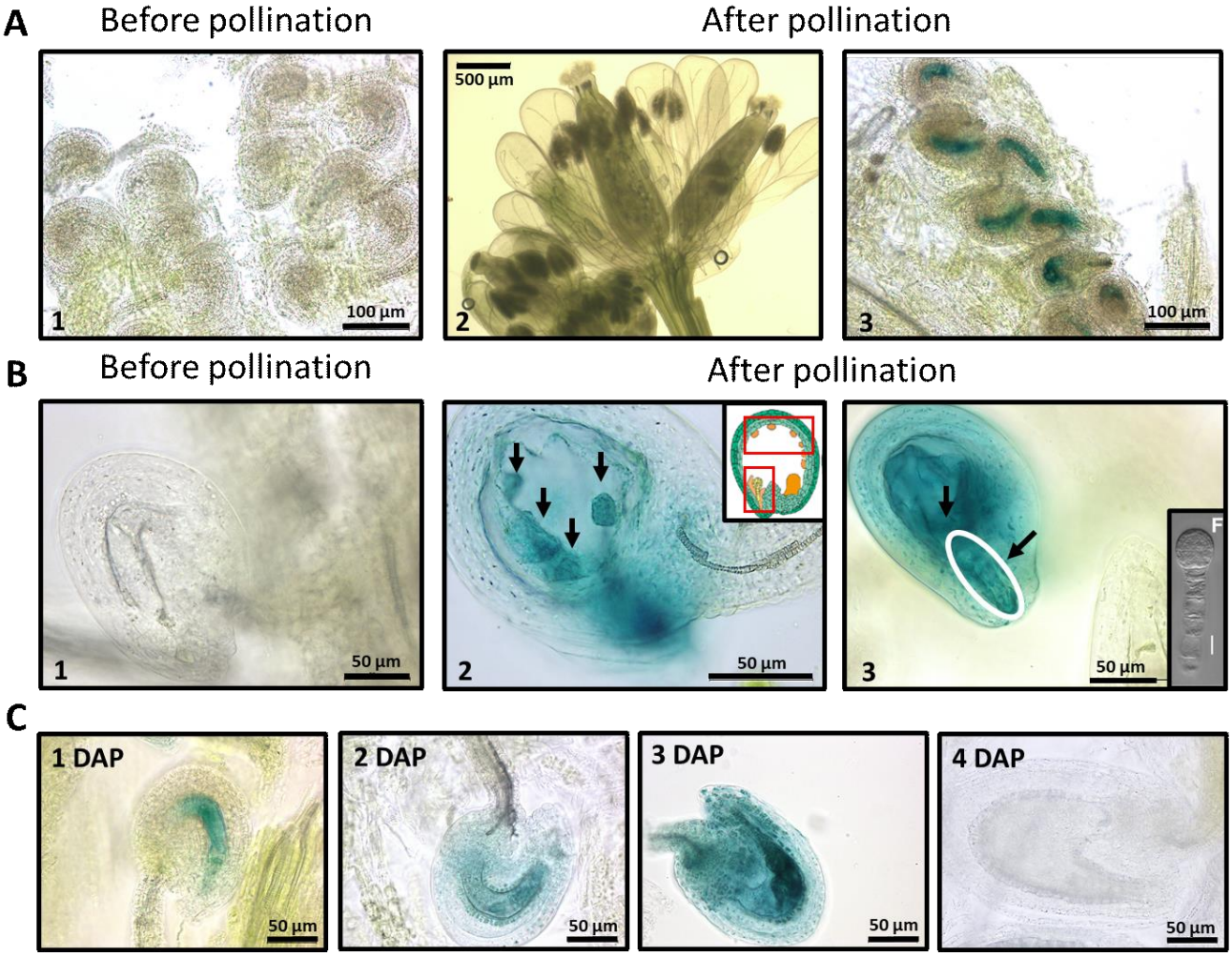


**Figure 3.9:** pWHY2:GUS line from Cai Q et al., 2015. The figures are representative the GUS assay performed. Plants were grown for 4 weeks in pot on soil and siliquae obtained by manually pollinated flowers were then analyzed. **(A) 1** Embryo sac before pollination, scale bar: 100 µm; **2** Image of 1 DAP flower, scale bar: 500 µm; **3** Image of 1 DAP zygotes formation, scale bar: 100 µm; **(B) 1** Embryo sac before pollination, scale bar: 50 µm; **2** and **3** represent 2/3 DAP embryos, the black arrows in **2** point the endosperm cells, in **3** the arrows point the chalazal endosperm cells, the globular embryo and embryo surrounding region, scale bar: 50 µm; **(C)** the images represent the GUS assay performed on 1,2,3 and 4 DAP, scale bar 50 µm.

In parallel, the gene expression analysis of *WHY2* was determined by RT-PCR at 2, 3, 4 and 5 DAP, as shown in Figure 3.10.

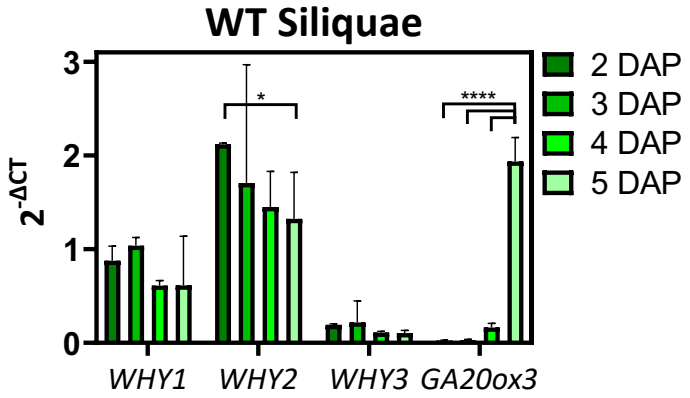


**Figure 3.10:** Real-Time PCR on 2, 3, 4 and 5 DAP WT siliquae. Analyzed genes: *WHY1, WHY2, WHY3 and GA20ox3 i.e.,* the 3 WHIRLY genes and a gene involved in the Gibberellin pathway. ACT2 has been used as housekeeping gene. The results were analyzed with the 2^(-ΔCt) technique. Error bars: SD. Asterisks describe the level of significance: * = $p < 0.05$; **** = $p < 0.0001$. Statistic: Tukey's multiple comparisons test.

Higher expression of *WHY2* is detected at 2 DAP, followed by a constant decrease. At 4 DAP there are still moderate levels of *WHY2* expression as in the following stages, this leads us to suggest that there is not an abrupt stop of *WHY2* expression as observed in the GUS assay, but a more gradual decrease. Probably the lack of GUS staining was due to the hardening of the seeds after the 4 DAP or could depend on the stability of the RNA.

In addition to *WHY2*, we also monitored the expression levels of *WHY1* and *WHY3* where no variation in expression was found. We investigated the expression levels of the various WHIRLY genes to understand their impact during this precise developmental stage, confirming a predominant role of *WHY2* compared to the other two WHY genes. GIBBERELLIN 20-OXIDASE 3 (*GA20ox3*) is involved in the gibberellin biosynthesis pathway, playing a key role during germination, and it is highly expressed in developing siliques (Rieu et al., 2007). Its induction is in line with the development process, confirming that the siliquae maturation is progressing normally.

An increase in the expression level of *GA20ox3* and a constant decrease of *WHY2* during the embryo development are in agreement with what was previously seen by Raju Datla Lab in *Arabidopsis*, through a genome-wide analysis during embryo development (Xiang et al., 2011). In conclusion, high promoter activity of *WHY2* in the early phases of embryo development was observed through the GUS staining assay and then confirmed with RT-PCR. This supports the hypothesis that WHY2 is necessary for those developmental phases characterized by high energy requirements and intense cell division. Indeed, during these stages mitochondria need to highly transcribe and replicate mtDNA, both processes require accurate DNA remodelling, helped by a functioning repair system and thus by WHY2.

Then, we decided to investigate whether the absence of *WHY2* could compromise these developmental stages, and generate an impairment in the formation of viable seeds in the knock-out siliquae.

Plants were sown in soil and, after 4 weeks, WT(m) x WT(f) and *why2-1*(m) x *why2-1*(f) plants were manually crossed and after 10 days after pollination (DAP) the number of viable seeds determined (see M&M). Only early flowers were taken to avoid variation in the results due to the variability of seed production during late flowering stage. It was observed that *why2-3* line produces around 26% less seeds than WT line and that this happens despite having the same siliquae length (figure 3.11.A). An increase in the number of aborted seeds was observed, in figure 3.11.B, the black arrows indicate aborted seeds in the mutant line.

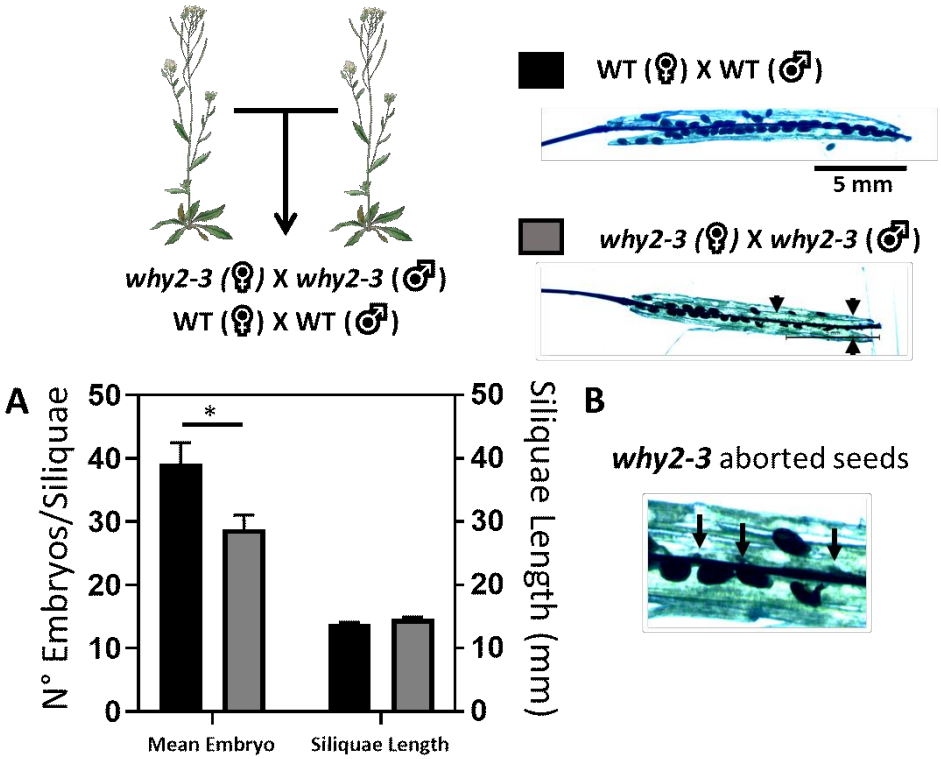


**Figure 3.11:** Analysis of embryo development in WT and *why2-3*. Wild-type and mutant plants were manually crossed simultaneously. 10/15 siliquae were analyzed. Around 10-15 crossed silique were analysed for each genotype. The experiments have been performed at least 3 times. Scale bar: 5 mm. **(A)** The graph represents on the left axis the number of developed seeds per siliques, instead the right axis reports the siliquae length (mm). Error bars: SD. Asterisks describe the level of significance: * = $p < 0.05$. Statistic: Student's t-test method. **(B)** The black arrows represent the aborted seeds in the *why2-3* line.

This preliminary result is encouraging, it indicates that plants lacking *WHY2* are partially impaired in seed production, suggesting that during this phase in which mitochondria replication and reorganization are needed to sustain cell division, the maintenance of mtDNA stability and organization is particularly crucial.

### 3.2.3 WHY2 and pollen development

Another important high energy demand developmental process is pollen development. Thanks to the pWHY2:GUS line we confirmed what was reported by Cai Q et al., 2015. *AtWHY2* promoter activity and gene expression decrease during pollen development, in parallel with the rapid degradation of mtDNA. Only in the first phases of pollen maturation, *WHY2* seems to play a key role,

we, in fact, observed an induction of *WHY2* during pollen maturation, precisely during the polarised microspore phase and not in early and mature pollen developmental phases (figure 3.12). Vegetative pollen cells begin development at the microspore stage (Eady et al., 1995). An early accumulation of *WHY2* in the vegetative cell can prevent mtDNA degradation. These results are therefore in line with WHY2 function: protection of mtDNA during high-energy demand developmental phases.

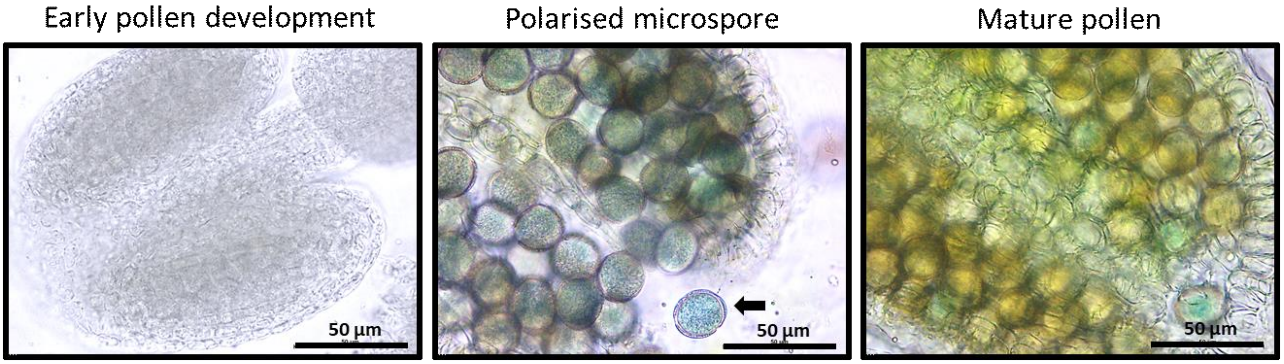


**Figure 3.12:** Analysis of pollen development in pWHY2:GUS line. Scale bar: 50 µm. The black arrow indicates the signal from a pollen grain.

### 3.2.4 WHY2 during seed germination

Germination is an energy-demanding process in which cell division and development processes occur. Reactivation of mitochondria to supply the required energy is thus a key process underpinning germination and seedling formation. Reactivation of mitochondrial bioenergetics, indeed, is followed by a drastic reorganization of the chondriome involving massive fusion to enable mixing of previously discrete mitochondrial DNA nucleoids (Paszkiewicz et al., 2017). To evaluate the impact of the absence of WHY2 on seed germination, we performed a germination test on all the three knock-out lines available. The rupture of the seed testa and primary root outflow were used as parameters to evaluate seed germination (Figure 3.13). As reported in fig. 3.13, in all the analysed mutant lines a significant reduction (25%) in the percentage of germination compared to the WT was observed. We analysed by RT-PCR the expression of *WHY2* in different developmental phases, from imbibed seeds to the flowering stage. The results showed a relatively high expression level in 24 h imbibed seeds (Golin, Negroni et al., 2020). Furthermore, The *Arabidopsis* eFP Browser from the AtGenExpress Consortium (Winter et al., 2007) shows that the predicted *WHY2* gene expression is higher in 24 h imbibed seeds and in organs with a high degree of cell division such as shoot apex (Appendix I). All these data taken together highlight the important role of WHY2 in a phase of plant life characterized by active mtDNA synthesis, such as seed germination.

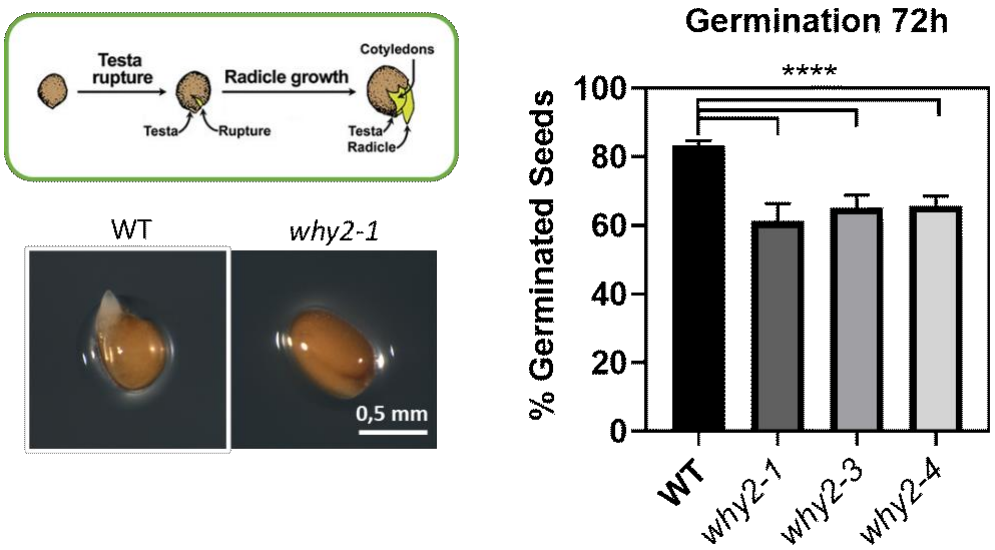


**Figure 3.13:** Analysis of seeds germination, WT, *why2-1, why2-3,* and *why2-4* lines were analyzed. Scale bar: 0.5 mm. Germination was performed in solid standard medium; images were acquired after 72 h from the sawing. The experiments have been performed at least 2 times. Error bars: SD. Asterisks describe the level of significance: **** = $p < 0.0001$. Statistic: Student's t-test method.

In conclusion, the absence of *WHY2* does not affect plant development in terms of primary root growth, rosette development and flowering. In contrast, a strong phenotype is observed during energy-demanding growth phases, such as germination and embryo development, heterotrophic growth phases in which functional mitochondria and high ATP levels are required.

## 3.3 The role of WHY2 in salt stress response

As reported above, WHY2 is fundamental for mtDNA and nucleoids stability, and its absence leads to aberrant mitochondrial morphology and impaired dynamics (figure 3.2; 3.4 and Appendix III). Mitochondria also play a relevant role in stress sensing, response and adaptation. Being first stress sensors, functional mitochondria are needed for plant response and survival in presence of stress (Van Aken 2021; Eckl et al., 2021). For all these reasons, we decided to characterize WHY2 knock-out lines under stress conditions.

### 3.3.1 Cis-regulatory elements of *WHIRLY2* gene

In order to get more in details on the role of WHY2 an *in-silico* analysis was performed. Transcription factor binding site (TFBS) for *AtWHY2* gene was performed on their 2000 bp upstream sequence, starting from the first intron. This region includes the 1 intron, 1 exon, 5'UTR and the upstream region. The cis-regulatory elements are DNA sequences that regulate the transcription of the gene to which they belong. The study of such regulatory elements provided information on gene function and the conditions under which its expression is modulated.

>First_introne_to_2kb_upstream_3'->5'

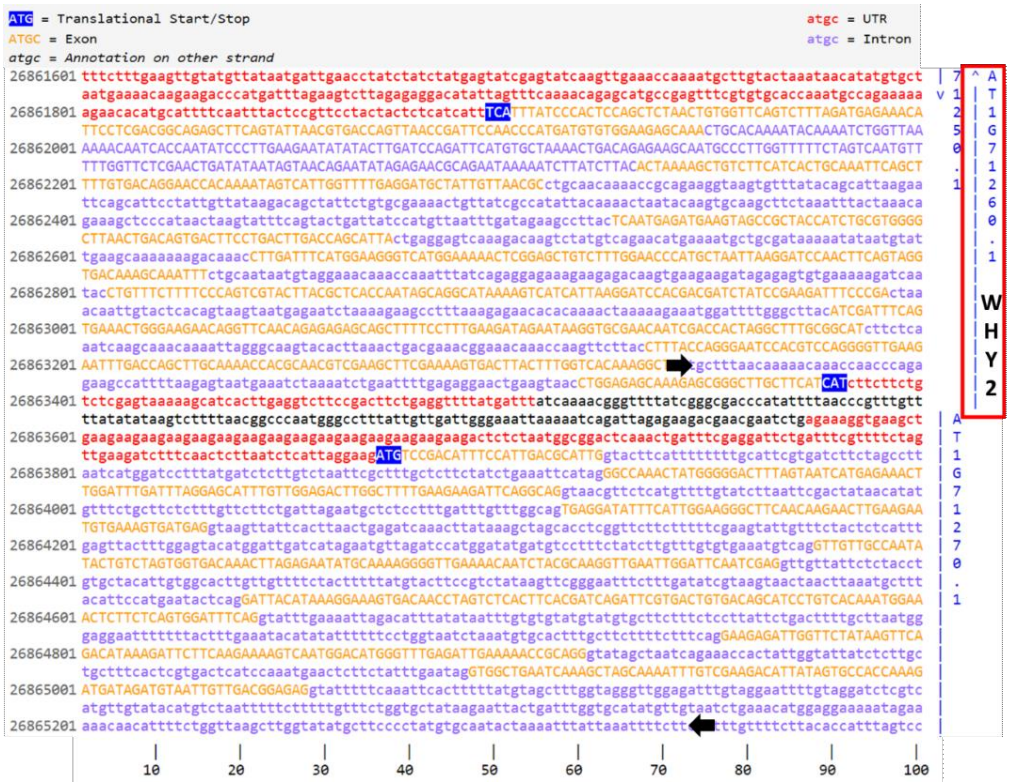


**Figure 3.14:** Sequence used for the promoter analysis, from the first intron to 2 kb upstream of the 3'->5'. The black arrows indicate the used sequence. The red square indicates *WHY2*. The legend is present above the image of the sequence. In grey: introns; in green: exons; in blue: putative promoter and in white the upstream region. Sequence obtained from SeqViewer Nucleotide View (Tair).

The more abundant cis-regulatory elements identified in the upstream region of *WHY2* are reported in Figure 3.15, in particular, we focussed on the sequences associated with response to abiotic stresses.

| Cis-acting element | Sequence | Description |
|---|---|---|
| SORLIP3AT | CTCAAGTGA | Light-Induced Promoters |
| EBOXBNNAPA | CANNTG | R response element |
| MYCCONSENSUSAT | CANNTG | dehydration-responsive gene |
| LTRECOREATCOR15 | CCGAC | cold- or drought- induced gene expression |
| GT1CONSENSUS | GRWAAW | light-regulated gene |
| IBOXCORE | GATAA | light-regulated |
| MYBCORE | CNGTTR | water stress |
| MYB2CONSENSUSAT | YAACKG | dehydration-responsive gene |
| ASF1MOTIFCAMV | TGACG | salicylic acid and light regulation |
| TCA1MOTIF | TCATCTTCTT | salicylic acid and stress |
| GT1GMSCAM4 | GAAAAA | pathogen and salt-induced gene |

**Figure 3.15:** Simplified *WHY2* promoter analysis, showing only cis-regulatory elements responding to biotic and abiotic stresses. The promoter analyses were performed with the use of New PLACE (A Database of Plant Cis-acting Regulatory DNA Elements). https://www.dna.affrc.go.jp/PLACE/?action=newplace.

The number of detected transcription factor binding sites (TFBSs) in the promoter sequences from the first intron to 2 kb upstream of the 3'->5' of *AtWHY2* gene were shown in figure 1.16. A total of 10 type TFs more abundant and related to abiotic stresses (TCA1MOTIF, SORLIP3AT, MYCCONSENSUSAT, LTRECOREATCOR15, GT1CONSENSUS, IBOXCORE, MYBCORE, GT1GMSCAM4, MYB2CONSENSUSAT and ASF1MOTIFCAMV) were detected in our analysis. The highest number of cis-regulatory elements was found as 18 for GT1CONSENSUS, followed by 16 for MYCCONSENSUSAT, 7 for GT1GMSCAM4 and 5 for MYBCORE. The consensus GT-1 binding site (GT1CONSENSUS) was found in many light-regulated genes (Terzaghi and Cashmore, 1995). MYCCONSENSUSAT is a MYC recognition site found in the promoters of the dehydration-responsive gene *rd22* and many other genes, and also a binding site of ICE1 (inducer of CBF expression 1) that regulates the transcription of CBF/DREB1 genes during cold in *Arabidopsis* (Abe et al., 2003). GT1GMSCAM4 is a "GT-1 motif" found in the promoter of soybean (*Glycine max*) CaM isoform (SCaM-4), it plays a role in pathogen- and salt-induced SCaM-4 gene expression (Buchel et al., 1999). Finally, MYBCORE is a binding site for two plant MYB proteins ATMYB1 and ATMYB2, ATMYB2 is involved in the regulation of genes that are responsive to water stress (Urao et al., 1993).

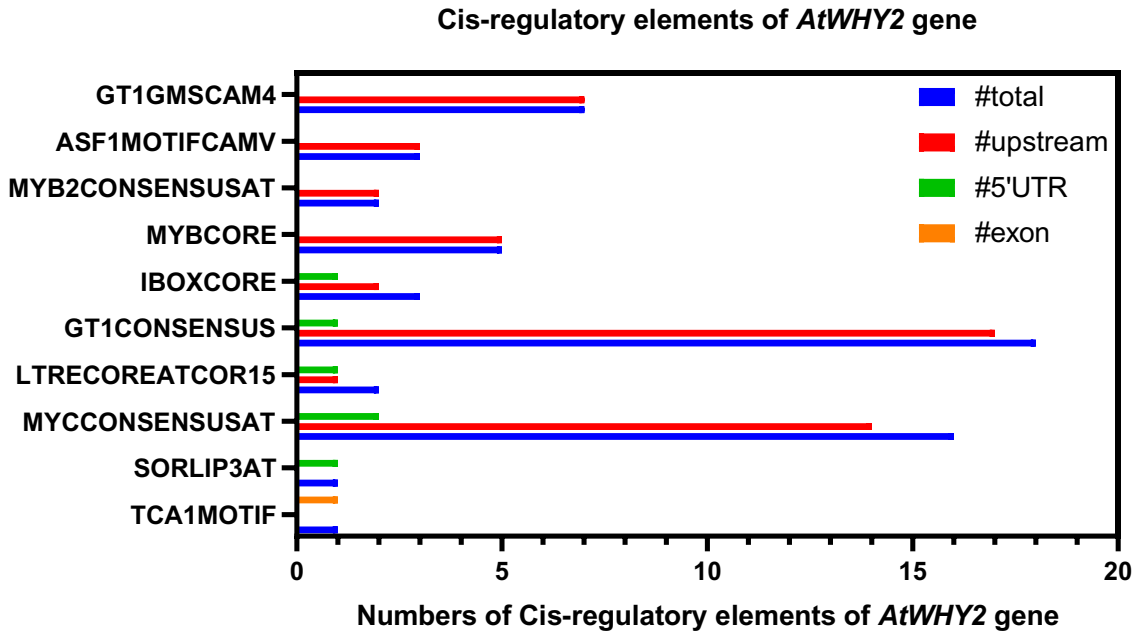


**Figure 3.16:** In the image is represented the abundance of putative TF binding sites in the 2000 bp promoter sequence for *AtWHY2* gene. In blue the numbers of Cis-regulatory elements in Total, in red in the upstream region, in green in the 5'UTR and in orange in the first exon.

The mitochondrial alteration, as we have seen, compromises plants response during high energy demand developmental stages. Our previous results on *WHY2* promoter analysis were supported by the Zhao et al. (2018) hypothesis of an involvement of WHIRLY2 under stress that is another physiological condition in which high energy is required. Knowing the relevance of organelles under stress, Zhao et al. (2018) tested the involvement of WHY2 in response to several stresses and discovered an induction of *WHY2* expression after exposing plants to salt in *Solanum lycopersicum*. In addition, lines over-expressing *SlWHY2* showed higher resistance to drought and pathogens (Zhao

et al., (2018). In Appendix II, the full promoter analysis is reported, showing all the found cis-regulatory elements in the upstream region of *AtWHY2*. These results together with the data reported by Zhao et al pushed us to better define the possible role of *AtWHY2* in abiotic stress responses. In particular, among abiotic stresses, some well-known response mechanisms are those to saline stress. Soil salinity between abiotic stresses is a major environmental constraint in agricultural productivity (Greenway and Munns, 1980; Rhoades and Loveday, 1990). Moreover, constantly changing environmental conditions, such as temperature and precipitation, as well as agricultural practices cause rapid modifications in levels of salinity. Salinity affects growth by challenging plants with both osmotic and ionic stress. The presence of high concentrations of salt lowers soil water potential, thus making it harder for roots to take up water, while the ionic stress is associated with the gradual accumulation of salts in plant tissues over time (Munns and Tester, 2008). In the long term, the ability to detect changes in ion levels and provide an appropriate response is a requisite for plant survival in saline environments.

### 3.3.2 Expression profile of *WHY2* during salt stress

To evaluate *WHY2* expression under salt stress in *A. thaliana*, WT plants were grown for 14 DAS in standard solid medium (see M&M) and subsequently exposed to salt (150 mM NaCl) for 8 h in liquid medium, while control samples were incubated in the same liquid medium without adding salt. Samples were then collected, and specific genes expression profile was determined by RT-PCR. The *WHIRLYs* family genes and *WRKY15* expression level were analysed under salt stress. It is evident from the gene expression analysis, reported in figure 3.17, that *WHY2* expression level is doubled after only 8 h of exposure to salt stress, as well as *WRKY15*, a typical salt stress marker gene. the ROS-inducible *A. thaliana* WRKY15 transcription factor (AtWRKY15) modulates plant growth and salt/osmotic stress responses. Salt- and oxidative-stress responsiveness of the *WRKY15* transcript was confirmed by quantitative RT-PCR analysis (Vanderauwera et al., 2012).

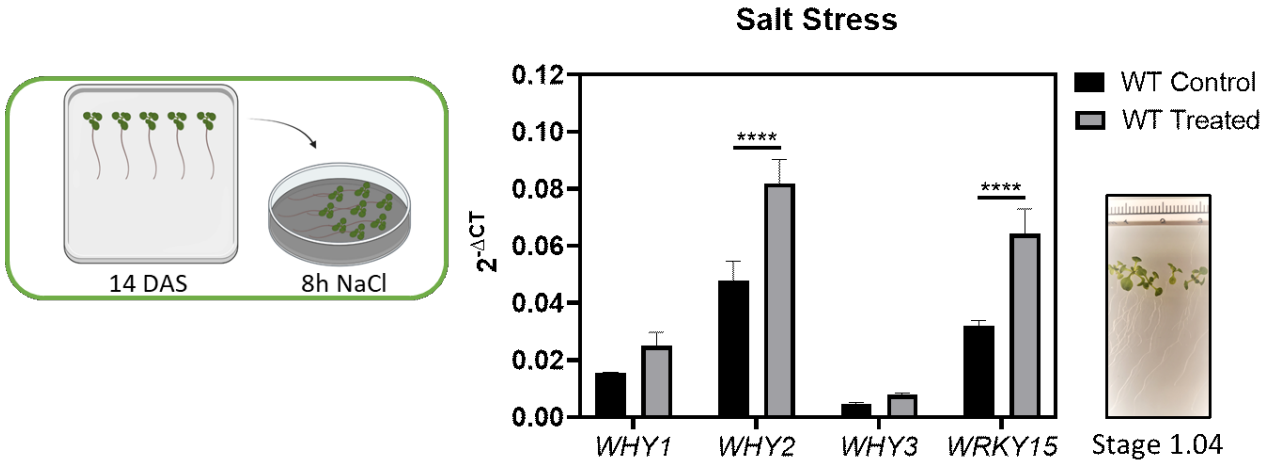


**Figure 3.17:** Real-Time PCR on 14 DAS old seedlings treated for 8h with 150 mM NaCl. Analysed genes: *WHY1, WHY2, WHY3* and *WRKY15;* 3 WHIRLYs genes and a gene involved in salt stress response. ACT2 has been used as housekeeping gene. The results were analysed with the 2^(-ΔCt) technique. Error bars: SE. Asterisks describe the level of significance: **** = $p < 0.0001$. Statistic: Tukey's multiple comparisons test.

It is worth noting that only *WHY2* increases in presence of salt stress while the other two WHIRLY genes (*WHY1* and *WHY3*) did not show any significant change.

### 3.3.3 Mitochondrial DNA damages under salt stress and recovery

WT seedlings harbouring YFP in the mitochondrial matrix (WT mtYFP) were grown for 7 days on standard solid medium, exposed to liquid medium with 50 mM NaCl and analysed by confocal microscopy, to observe the mitochondrial behaviour during the first phases of salt stress. In preliminary results it was observed that salt treatment induced clustering and mitochondrial elongation as early as 4 h (figure 3.18) in the WT line, this pattern was also observed after 6 h (data not shown).

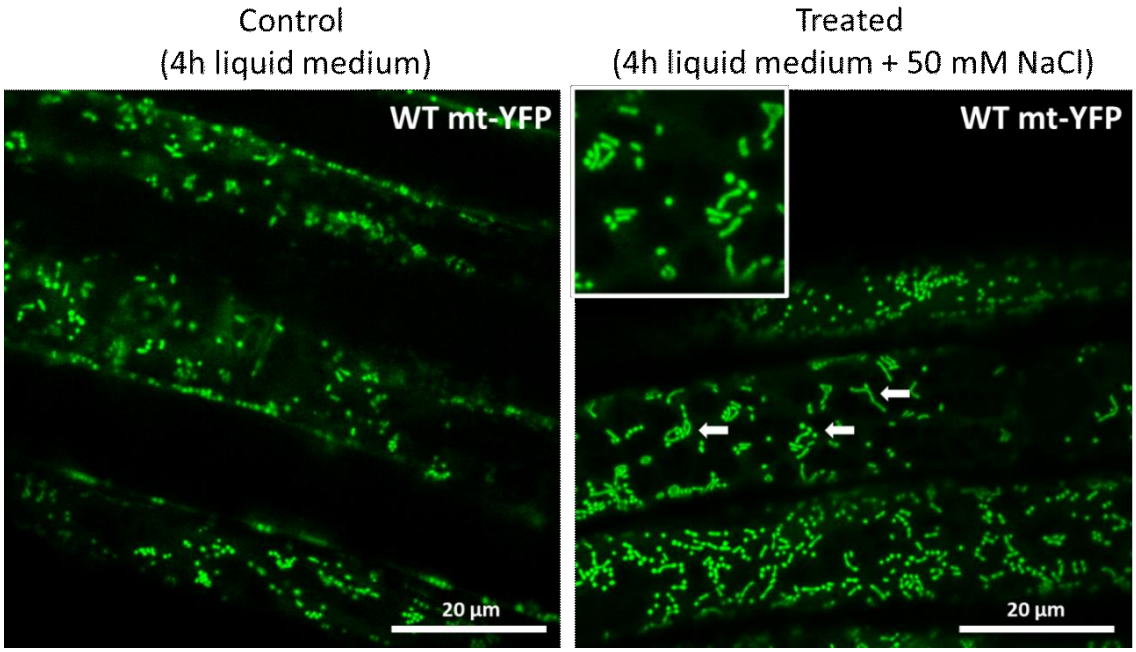


**Figure 3.18:** Representative images of mitochondria from root tissue cells of 7 DAS old WT *Arabidopsis* seedlings harbouring the mt-YFP. Seedlings were grown on standard solid medium and then exposed for 4 h on salt stress (liquid standard medium with 50 mM NaCl) images were taken by CLSM. Scale bar: 20 µm. The white arrows indicate elongated and clustered mitochondria.

Clustering helps mitochondrial fusion and their spatial reorganization allows the cell to adequately respond to the stress, allocating resources (ATP and metabolites) where needed (Arimura et al., 2018). It is well known that mitochondrial fusion is important for the maintenance of respiratory capacity, for allowing mitochondrial DNA exchanges, for recombination as well as for the exchange of metabolic compounds (Logan 2010, Scholz and Westerman, 2013). Usually, a massive mitochondria fusion occurs during high cell replication developmental processes, with the effect of aiding mtDNA replication, repartition and organization in mitochondria (Ray et al., 2021; Logan 2017). A similar mechanism might be induced during stress response, in fact, Steiner et al. in 2018 observed mitochondrial fusion after exposure to ionic stress in *Micrasterias denticulata*.

Since we observed a clustering of mitochondria after salt stress, we decided to evaluate if such process could impact on mtDNA replication and reorganization. In addition, we analysed if the absence of *WHY2* could impair the mtDNA replication during salt stress. Thus, we performed an experiment to evaluate the accumulation of aberrant mtDNA products exposing plants to different concentrations of salt. Plants were grown for 23 DAS on standard solid medium containing 0, 100 or 150 mM NaCl. PCR analyses were performed on collected material using opposite direction primers as previously described. WT plants show very little amount of aberrant mtDNA products even after exposure to the highest salt concentration. On the opposite, *WHY2* mutants contain such products in increasing amounts depending on the severity of the stress (figure 3.19).

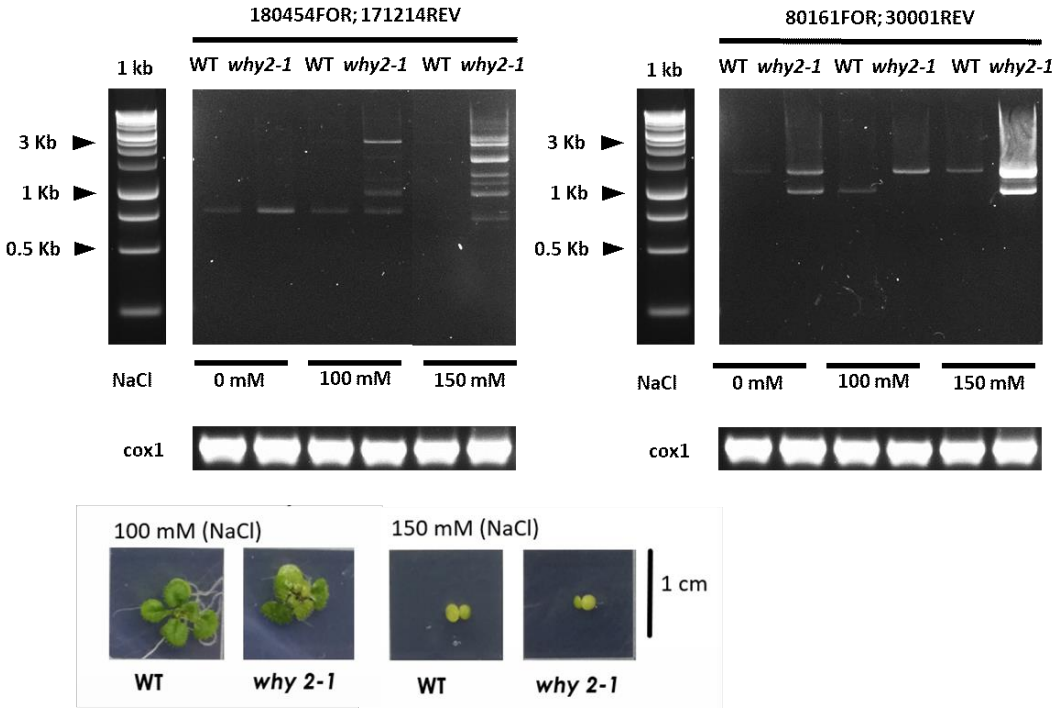


**Figure 3.19:** Electrophoretic analysis of representative PCR performed with 2 inward-facing mitochondria genome-directed primers. The *cox1* mitochondrial gene were used as loading controls. The oligonucleotides used for each PCR are indicated. Plants were growth for 23 DAS in normal solid medium under different concentration of salt (0, 100 or 150 mM NaCl). DNA rearrangements accumulate primarily in the mitochondria of plants lacking *WHY2*. The experiment was repeated 3 times for different concentration of salt stress, around 36 plants per biological replicate.

This observation suggests that a high rate of mitochondrial DNA replication and rearrangement occurs during salt stress, and also that the mtDNA repair is in progress during the stress, a process in which WHY2 seems to have a key role. When the absence of WHY2 occurs the organization of nucleoids, that allows spatial proximity of DNA with replication and repair systems, lose compactness and the recruitment of proteins into complexes might be deregulated leading to improper replication and to non-homologous recombination events, functions where WHY2 seems to play a fundamental role in mitochondria.

Hypothesising that WHY2 has a scaffold role and knowing that its absence induces compromised mitochondrial dynamics, we thought that an impairment in these processes, fundamental for mtDNA exchange, would not allow a recovery on aberrant mtDNA products. We decided to perform a recovery assay, moving the plants treated with salt to a standard solid medium for 10 days to

observe if damaged mtDNA would decrease or be absent. Figure 3.20.A shows that the mtDNA aberrant products are still present after recovery time, underlining the fact that WHY2 is deeply involved in mtDNA maintenance and repair during prolonged salt stress. This result supports a fundamental role of WHY2 in the repair mechanism to avoid mtDNA damages during and following the stress, which could affect organelle functionality and plants' survival and recovery.

Through RT-PCR analyses (figure 3.20.B) we observed that *WHY2* transcription is induced in 14 DAS seedlings after 8 h of pulse salt stress treatment (150 mM NaCl), while the same behaviour is not observed for other genes known to be involved in mtDNA repairs like *ODB1, MSH1, OSB1* and *SSB1*.

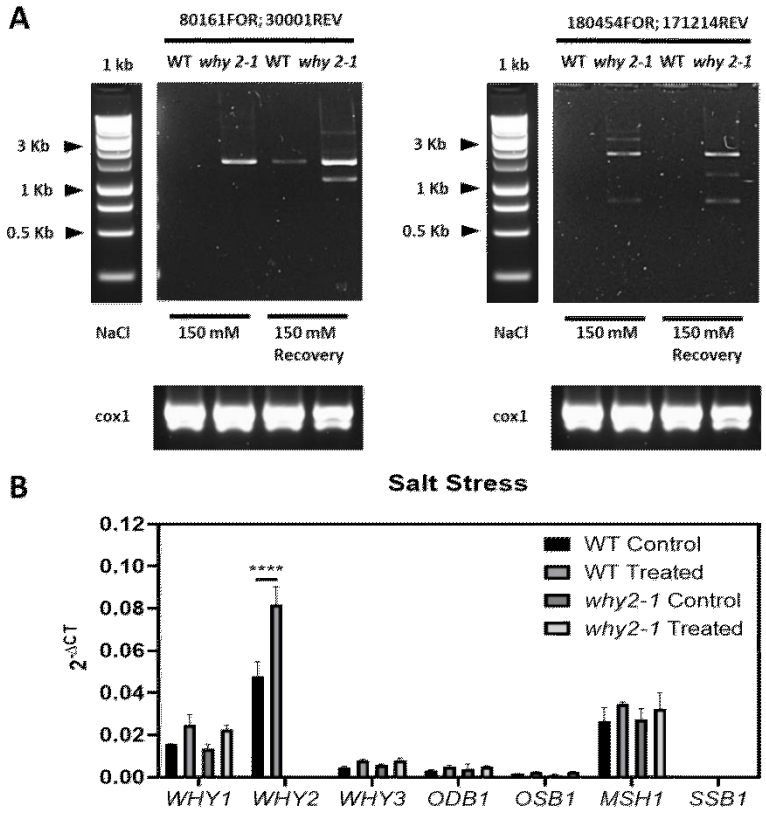


**Figure 3.20: (A)** Electrophoretic analysis of representative PCR performed with 2 inward-facing mitochondria genome-directed primers. The *cox1* mitochondrial gene were used as loading controls. The oligonucleotides used for each PCR are indicated. Plants were grown for 23 DAS in standard solid medium under salt stres (150 mM NaCl) and recovered for 10 days on standard solid medium. DNA rearrangements accumulate primarily in the mitochondria of plants lacking *WHY2*. The experiment has been repeated 3 times for different concentrations of salt stress, around 36 plants per biological replicate. **(B)** Real-Time PCR on 14 DAS old seedlings treated for 8 h in liquid medium with 150 mM NaCl. Analyzed genes: *WHY1, WHY2, WHY3, ODB1, OSB1, MSH1* and *SSB1*; the 3 WHIRLY genes and other mitochondrial genes involved in the mtDNA repair. As housekeeping gene has been used *ACT2*. The results were analyzed with the technique of 2^(-ΔCt). Error bars: SE. Asterisks describe the level of significance: **** = p < 0.0001. Statistic: Tukey's multiple comparisons test.

In conclusion, WHY2 seems to play an essential role in the maintenance of mtDNA stability during salt stress, and its role seems not to be redundant. In fact, none of the other genes involved in mtDNA repair were seen to be expressed following salt stress in the RT-PCR, confirming that the observed aberrant recombinant products in mtDNA were caused by the absence of WHY2. This result points for the first time the attention to the role of WHY2 to avoid non-homologue recombinant products during prolonged salt stress, linking his function on mtDNA repair and salt stress.

### 3.3.4 The absence of WHY2 affects root mitochondrial morphology under salt stress

In order to evaluate the impact of salt stress on mitochondrial morphology, we performed a TEM analysis comparing WT and mutant lines, as shown in figure 3.21. Plants were grown for 23 days in standard solid medium with 0 and 100 mM NaCl.

Roots are the first plant organs exposed to salt in the medium and, for this reason, we decided to focus our analyses on roots. In control conditions, the presence of 30% of swollen mitochondria and the decrease of the number of cristae were confirmed along with a translucent central area showing disorganization in the nucleoids on 23 days root plant in *why2-1* mutant (figure 3.21), as already observed in cotyledons of 6 DAS seedlings. Figure 3.21 also shows in detail mitochondria of knock-out lines after 23 DAS salt stress with a wide central area empty of cristae with fibrillar structures resembling unpacked DNA in around 60% of mitochondria (double compared to control condition). Under salt stress, the translucent area is wider than in standard conditions and the unpacked DNA is present in most of the analysed images.

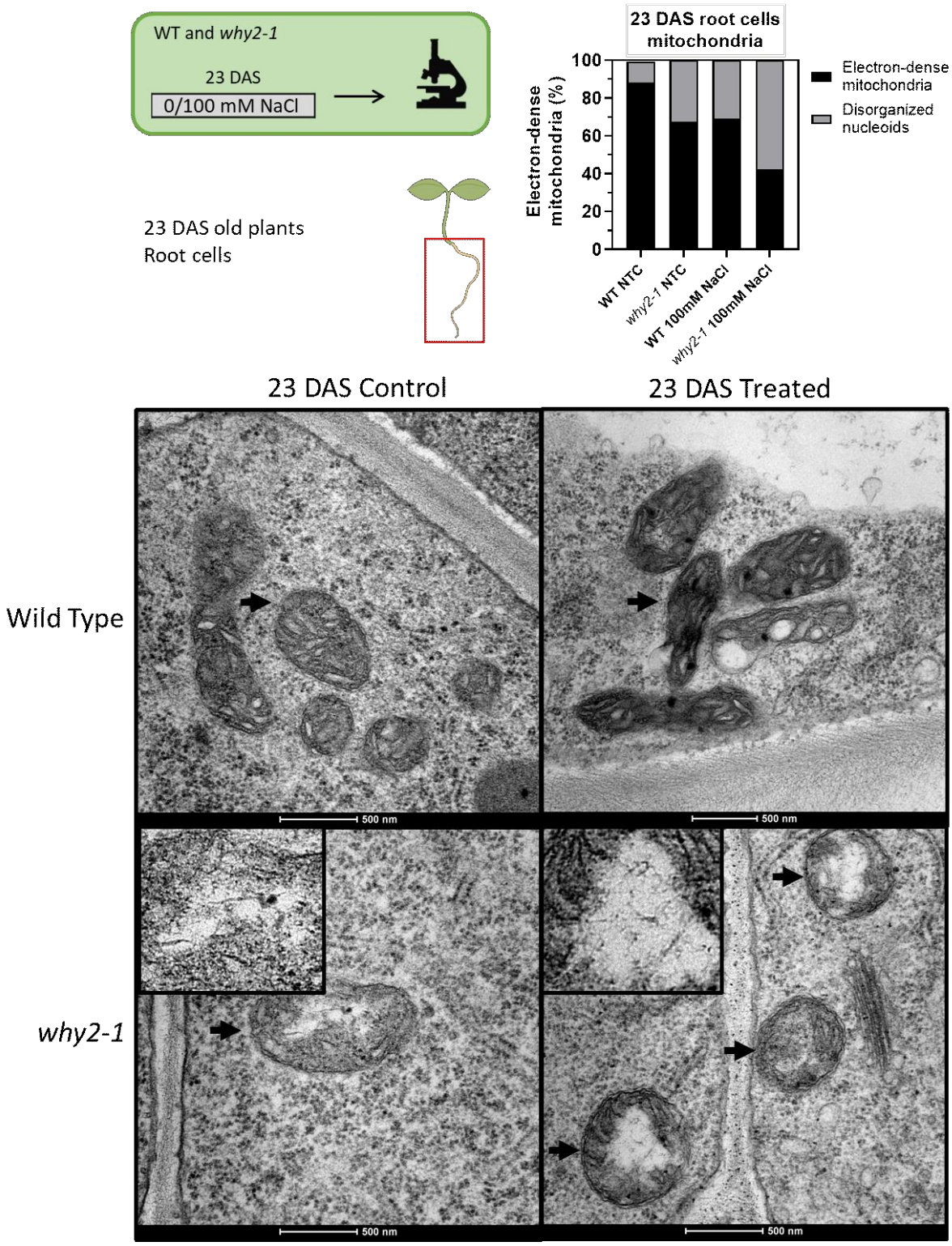


**Figure 3.21:** Mitochondria and nucleoids' morphology in 23 DAS plant root tissues, in control condition and directly grown on 100 mM NaCl medium. Transmission electron microscope images of mitochondria from root section in WT and *why2-1* mutant plants. Arrow indicates in the WT panels electron dense mitochondria, and in the bottom panel arrows indicate mitochondria with a translucent area within mitochondria matrix in *why2-1* mutant line. Scale bar: 500 µm.

### 3.3.5 Mitochondrial DNA copy number under salt stress

We investigated if the absence of *WHY2* could also alter the mtDNA content as a consequence of an aberrant replication in disorganized nucleoid structures under salt stress. For this purpose, we evaluate mtDNA copy number, performing a PCR experiment on mitochondrial genes (*Q-COX1* and *orf170mito*) and a nuclear gene (*AtRpoTp*; Morley et al., 2016). Plants were grown for 23 DAS on standard solid medium with 0 and 150 mM NaCl, followed by a recovery for 10 days on standard solid medium. An increase in the relative amount of mtDNA was observed in *why2-1* and WT plants after 23 days of growth on solid medium with 150 mM NaCl, but in the mutant line the increase was statistically significant higher compared to the WT (figure 3.22). Instead in control condition and after 10 days of recovery we did not notice any difference in the mtDNA copy number between WT and the mutant line.

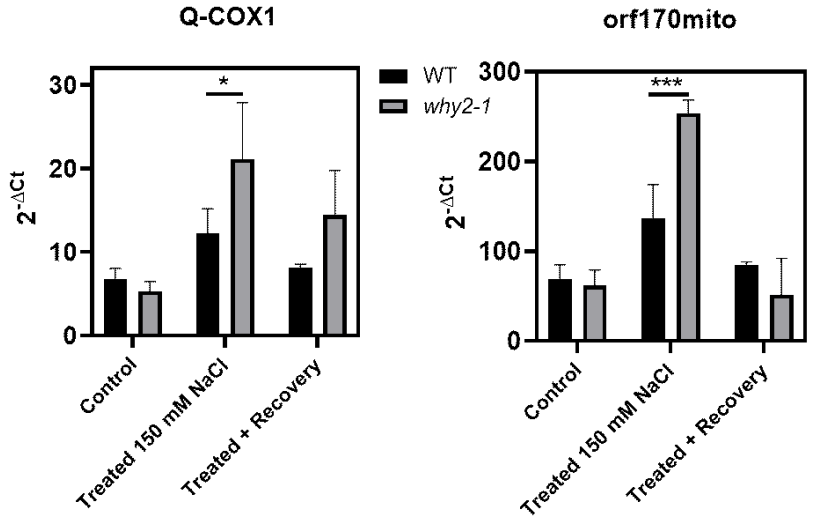


**Figure 3.22:** Real-Time PCR on 23 DAS WT and *why2-1* lines. Samples were either untreated (control), treated with 150 mM NaCl for 23 DAS and also recovered for 10 days. Mitochondrial analyzed genes: *COX1* (mitochondrial cytochrome oxidase 1 subunit) and *orf170mito* (mitochondrial RNA-dependent DNA polymerase). *AtRpotp* (nuclear plastid-RNA polymerase) has been used as housekeeping gene. The results were analyzed with the 2^(-ΔCt) technique. Error bars: SD. Asterisks describe the level of significance: * = $p < 0.05$; *** = $p < 0.001$. Statistic: Two-way ANOVA.

The increase in the mtDNA copy number after 23 DAS of salt stress suggests that, when *WHY2* mutant plants are exposed to salt stress, mtDNA undergoes aberrant replication causing a rise in mtDNA amount as well as an increase in non-homologous recombination events.

To confirm the observed increase in the mtDNA copy number we checked the expression level of *WHY2* and a mitochondrial polymerase I B (*POLIB*; At3g20540) after 23 DAS salt stress (100 mM NaCl). It was decided to perform the experiment under 100 mM NaCl given the difficulty in extracting RNA with optimal quantity and quality from plants grown for 23 days under 150 mM salt stress. Figure 3.29 confirms a high transcription level of *WHY2*, but also an induction of *POLIB* in both WT and *why2-1* lines. This gene encodes an organellar DNA polymerase I that is also involved in double-strand breaks repair on organellar DNA via homologous and non-homologous mechanisms to reform a continuous DNA helix (Ayala-García et al., 2018; Wu et al., 2020; figure

3.23). A high level of *POLIB* expression supports the results obtained on an increase in the mtDNA copy number and an induced replication of the mtDNA after prolonged salt stress.

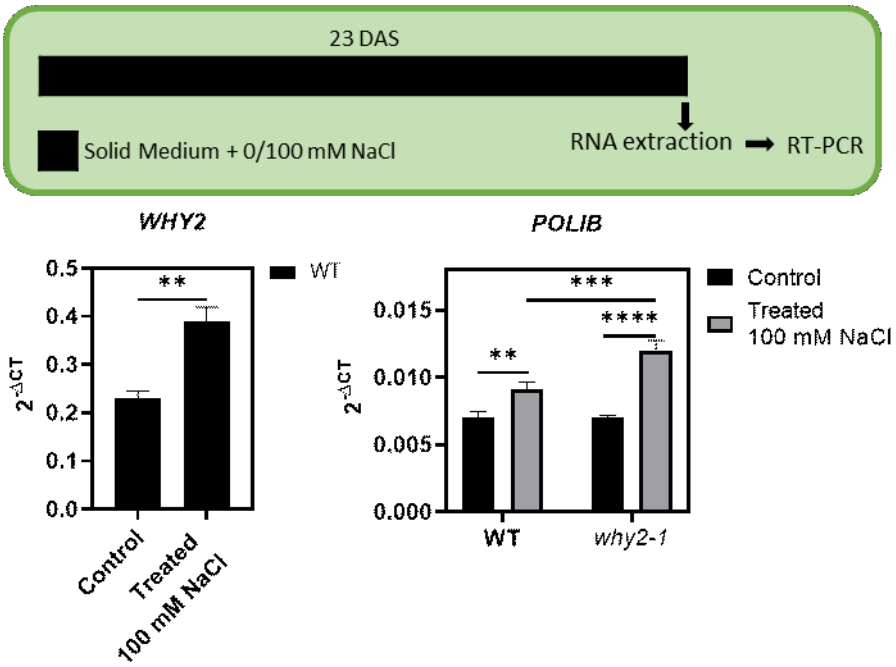


**Figure 3.23:** Real-Time PCR on 23 DAS old plants directly grown on solid standard medium with 100 mM NaCl. Analyzed genes: *WHY2* and *POLIB,* a POLYMERASE 1 B involved in mtDNA replication. *ACT2* has been used as housekeeping gene. The results were analyzed with the 2^(-ΔCt) technique. Error bars: SD. Asterisks describe the level of significance: ** = $p < 0.005$; *** = $p < 0.001$; **** = $p < 0.0001$. Statistic: Student's t-test method and Tukey's multiple comparisons test.

Interestingly, the knock-out line shows a higher expression level of *POLIB,* which is linked to mtDNA replication and repair rescue mechanism on aberrant mtDNA products. That is the proof of an increase in mtDNA synthesis and therefore of a higher mtDNA copy number in the *why2-1* line.

Excessive replication could be a mechanism through which the cell tries to restore mitochondrial functionality that is hindered by the accumulated of mtDNA damages due to the absence of WHY2. An excess of produced mtDNA could be an intracellular signal to the nucleus for communicating the presence of mitochondrial damages caused by a high stress.

Wu et al. in 2019 discovered that, in mammalian cells, a reduced expression of the mtDNA-binding protein TFAM causes elongation of mitochondria, enlargement of nucleoids and an increase in the release of mtDNA into the cytoplasm. This release acts as a signal to the nucleus for priming an antiviral response. Thus, as suggested by this work, a variation of the mtDNA copy number could imply the involvement of a retrograde signalling mechanism.

To sum up, the high level of replication during salt stress is associated to a high recombination rate that, in absence of WHY2 lead to the accumulation of aberrant fragments. The WT line also exhibits a high level of *WHY2* expression after 23 DAS of stress, suggesting a role of this gene also after prolonged salt stress exposure.

### 3.3.6 The absence of WHY2 affects plants growth under salt stress

In order to determine the salt sensitivity of *WHY2* knock-out mutants, we performed a germination test. WT and mutant seeds were sown on solid medium with 0 and 100 mM NaCl and germination rate was assessed after 96 hours. Data reported in figure 3.24 show that in the presence of salt, germination is compromised both in WT and mutant lines. However, the germination rate in salt medium in *why2-3* plants was 40%, while in WT was 70% (Figure 3.24), indicating a higher salt stress sensitivity in knock-out mutants.

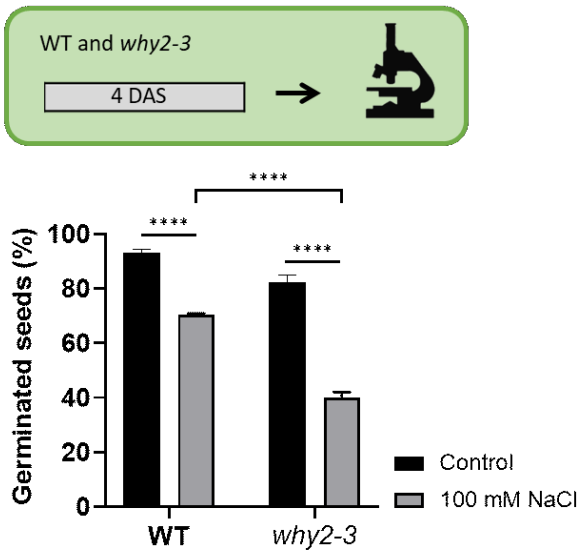


**Figure 3.24:** Analysis of seeds germination, WT and *why2-3* lines were analyzed. Germination was performed in solid standard medium with 0 and 100 mM NaCl, images were acquired after 96h from the sawing. The experiments have been performed on 3 biological replicates per sample, each biological replicates were around 25 seeds. Error bars: SD. Asterisks describe the level of significance: **** = $p < 0.0001$. Statistic: Student's t-test method.

On the basis of these results, we hypothesize that WHY2 could play a role in the response to such stress. This is expected considering that stress response is a highly energy-consuming process and adequate mitochondrial activity and motility are required (Liberatore et al., 2016).

We also investigated other developmental phases as primary root growth and *rosetta* development under prolonged salt stress. For the primary root growth measurements, seedlings were directly sawn in solid medium with 0 or 100 mM NaCl in which primary root length was continuously monitored. Interestingly, in standard conditions there are no differences in the primary root length between WT and mutant lines, instead in presence of salt stress it is possible to notice a slowdown in root extension in the mutant lines from 12 DAS onwards (figure 3.25). During salt stress a decrease in root growth is observed also in WT plants, but the impact of the stress is stronger on plants lacking WHY2, and this effect is visible after some days. This result showed an impairment in the primary root growth under prolonged salt stress caused by the absence of *WHY2*, suggesting an important function of this gene during stresses.

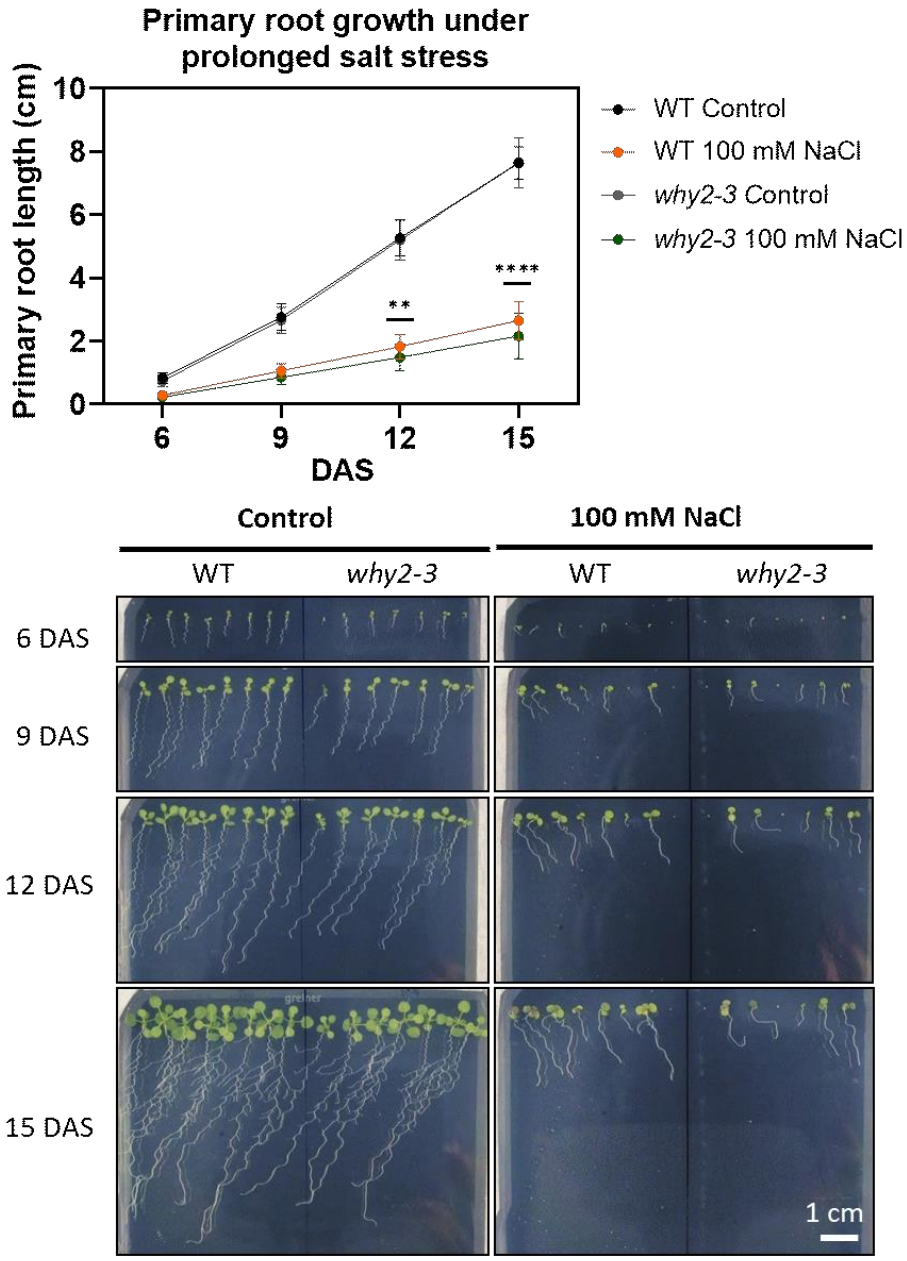


**Figure 3.25:** Primary root growth of WT and *why2-3* lines under prolonged salt stress. Vertical root growth on standard solid medium with 0 and 100 mM NaCl. Scale bar: 1 cm. The experiment was repeated 2 times with around 40 plants per type. Asterisks describe the level of significance compared to the WT: ** = $p < 0.005$; **** = $p < 0.0001$. Statistic: Šídák's multiple comparisons test.

To determine the salt stress sensitivity of WT and mutant lines, plants of both genotypes were grown in salt-containing medium for 23 days. In preliminary data, plants survival was evaluated, 54±4% of WT plants compared to 30±8% of mutants survived in long stress treatment. *why2-1* mutants showed a reduced development of the aerial parts along with the presence of yellow leaves, both signs of senescence and death, meaning that plants lacking WHY2 are more sensitive to salt stress. It was also observed a delay in growth rate in mutant plants compared to WT when exposed to salt stress.

### 3.3.7 The absence of WHY2 affects root cell integrity during salt stress

Performing a TEM analysis of root cells we could observe that in general the epidermal tissues of *why2-1* line are highly affected by the presence of salt compared to WT. Root cells of WT plants under salt stress present enlarged vacuoles occupying most of the cell, only a thin layer of cytoplasm can be seen (figure 3.26). Instead in mutant plants, root tissues are severely damaged: some cells are detached from the cell wall with some showing clear signs of breakage of the plasma membrane and cell death (figure 3.26).

The severity of root damages is more evident in those conditions in which mitochondrial morphology is more compromised and nucleoids are less packed (figure 3.21), suggesting a link between root cell survival under salt stress and WHY2. Root integrity is severely compromised in *why2-1* line in presence of prolonged salt stress, possibly explaining the lower rate of survival obtained in preliminary results.

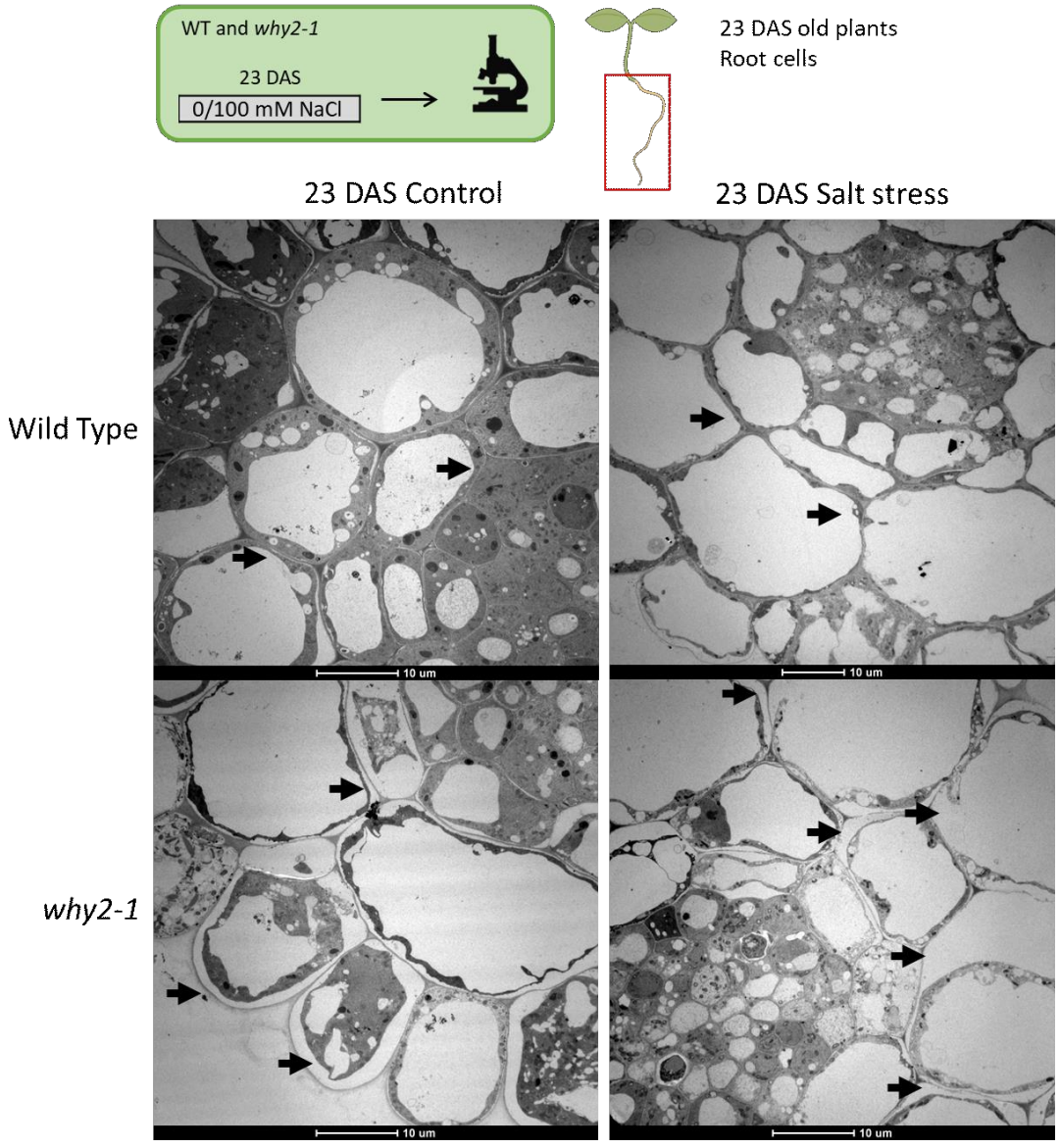


**Figure 3.26:** 23 DAS plant epidermal root tissues, cross-section, in control condition and directly grown on 100 mM NaCl. Transmission electron microscope images of WT and *why2-1* mutant plants. Arrow indicates epidermal root tissues, in the WT panels root tissues are normal, in the bottom

panel arrows indicate *why2-1* mutant line with epidermal damaged root tissues in control and treated conditions (the plasma membrane is divided from the cell wall and in some cells it is also broken). Scale bar: 10 µm.

Taken together, all these results point to the fact that knock-out plants respond differently to salt stress with respect to WT. In conclusion, it seems that the absence of WHY2, inducing all the above reported mitochondrial changes (paragraphs 3.3.3 and 3.3.4), could affect the plant ability to tolerate high salt concentration.

### 3.3.8 ATP homeostasis during salt stress

During salt stress, the intracellular homeostasis state changes and many signals and responses are induced to face the stress. After the stress perception, cells undergo a metabolic reorganization with a change in the expression of many genes, together with the mobilization of different molecules. Salinity stress interferes with energy metabolism: plants must draw a wide fraction of the available ATP to restore the equilibrium and subsequently they must deal with the energy loss. Mitochondria functionality is particularly needed to sustain stress-related energy requirements (Zhu et al., 2012).

To study ATP homeostasis during salt stress, plants harbouring the genetically encoded biosensor ATeam which is targeted to the cytosol and allows the in *vivo* analyses of $MgATP^{2-}$ levels were used. To analyse ATP intracellular level in control condition and after salt stress, we treated 8 DAS old seedlings for 24 h in standard liquid medium with 0 and 150 mM NaCl. The seedlings were kept in the dark for 30 min before image acquisition to avoid potential effects of active photosynthesis (De Col et al., 2017).

In untreated samples there were no significant changes in $MgATP^{2-}$ content in mutant plants, $MgATP^{2-}$ supply in all the examined tissues is not impaired (figure 3.27). After salt stress, WT plants show a decrease in $MgATP^{2-}$ intracellular level in the root tip and cotyledons suggesting an increase in its consumption to adapt and cope with the stress. On the other hand, in *why2-1* line no changes were detected after 24 h of salt exposure (figure 3.27).

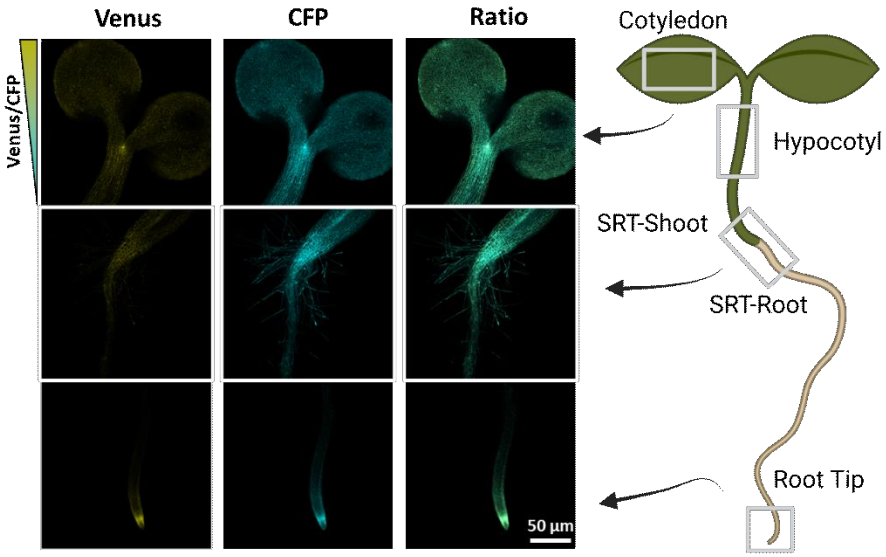

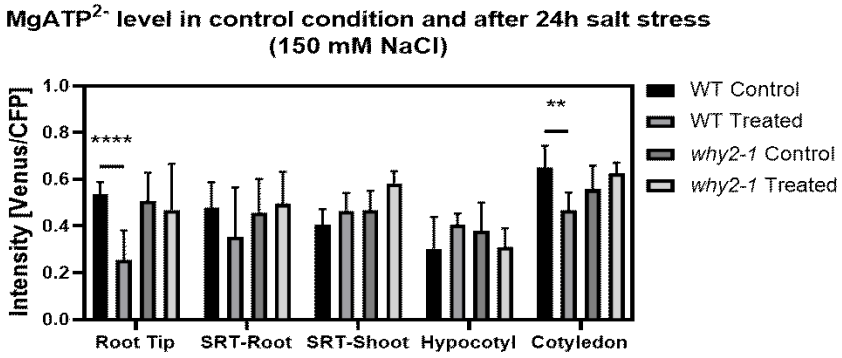


**Figure 3.27:** Generic $MgATP^{2-}$ map of *A. thaliana* seedlings. WT and *why2-1* seedlings expressing cytosolic ATeam were grown in solid medium for 5 DAS and then treated in liquid medium with 0 mM NaCl or 150 mM NaCl, plants were analyzed by CLSM. Fluorescence of Venus and CFP was recorded; the merge image shows both fluorescence channels projected on the respective dark field image. In ATeam WT and *why2-1* seedlings 4 regions of interest (ROIs) were defined to calculate the Venus/CFP ratio: cotyledon, hypocotyl, SRT-shoot, SRT-root and root-tip. The ratio corresponds to $MgATP^{2-}$ levels. Scale bar = 50 µm. Error bars: SE. Asterisks describe the level of significance: ** = $p < 0.005$; **** = $p < 0.0001$. Statistic: Two-way ANOVA, Multiple comparisons.

The observation that $MgATP^{2-}$ amount does not decrease in *why2-1* mutant supports the hypothesis of an impairment in the salt stress perception in this mutant line, and a failure in activating those pathways that help the cell buffering the damage and recover from the stress. For this reason, we decided to investigate in which step the absence of WHY2 compromises the stress perception.

### 3.3.9 Salt-induced $Ca^{2+}$ dynamics

Calcium ions ($Ca^{2+}$) play an important role in stimulus-response as a second messenger during stresses. Under standard conditions, cells maintain a low cytoplasmic $Ca^{2+}$ concentration and mobilize it in response to a given stimulus. The cytosolic $Ca^{2+}$ increase can be dependent by the influx of $Ca^{2+}$ from the apoplast or from intracellular $Ca^{2+}$ stores. The intracellular free $Ca^{2+}$ concentration changes in response to different stimuli determining specific "$Ca^{2+}$ signatures". In order to evaluate the salt-induce cytosolic $Ca^{2+}$ increase in WT and *why2-1* seedlings, the *in vivo* changes in $[Ca^{2+}]$cyt were measured in roots seedlings of transgenic plants harbouring the genetically encoded biosensor Yellow Cameleon 3.6 (YC 3.6). The cpVenus/CFP ratio which reflect a change in $Ca^{2+}$ concentration was determined over Regions Of Interests (ROIs) corresponding to large root tip areas (ROI 1, ROI 2, ROI 3; see figure 3.28.C) in 7 DAS seedlings.

Roots were placed in a small chamber and bathed with an imaging buffer in perfusion, then a 150 mM NaCl solution (in the same buffer imaging; see M&M) was applied through a continuous perfusion system. Salt-addition elicited a rapid $Ca^{2+}$ transient both in WT and *why2-1* roots. The salt-removal also induced a second $Ca^{2+}$ transient in both WT and *why2-1* roots (figure 3.28.A and B). In figure 3.28.D, it is reported the value of the maximum ΔR/R0 ratio upon NaCl addition (IN) and removal (OUT) for all the three analysed ROIs. The two time points of the two peaks are related to two different responses, salt addition and salt removal. The value of maximum ratio ΔR/R0 showed no significant differences in both peaks in WT and *why2-1* seedlings (figure 3.28).

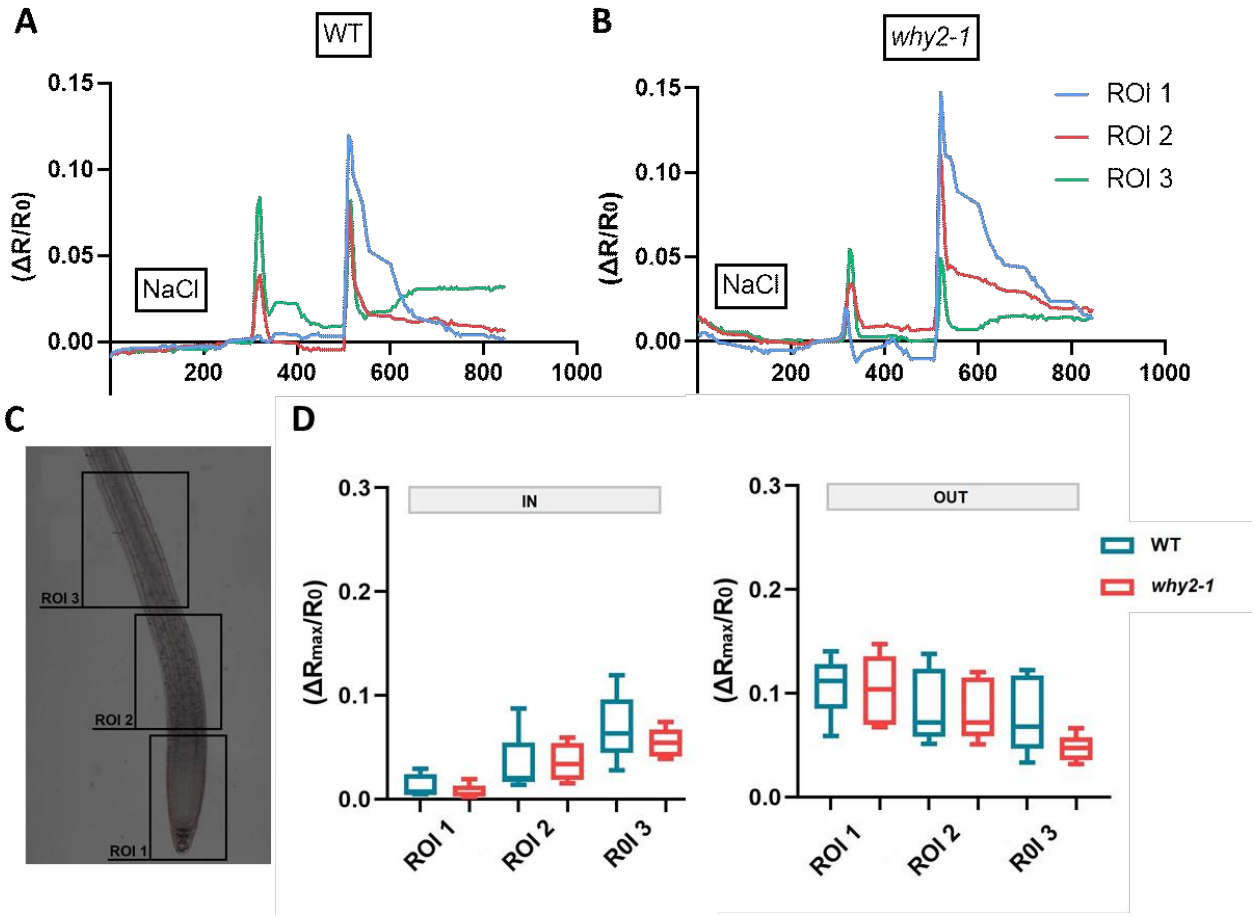


**Figure 3.28:** A representative image of NaCl-induced $Ca^{2+}$ dynamics in WT **(A)** and *why2-1* **(B)** 7 DAS *Arabidopsis thaliana* seedlings. Samples were treated with 100 mM NaCl for 2 minutes. A representative experiment of $Ca^{2+}$ transient induced by salt is provided. The FRET ratio is normalized as ΔR/R0, and plotted over time. **(C)** Confocal image of representative *Arabidopsis thaliana* root at 7 day-after-sowing. Root is divided into three different ROIs (ROI 1; 2 and 3). **(D)** Statistical analyses of the value of ΔR/R0 maximum increase or decrease during NaCl-addition (IN) or removal (OUT). Data were pooled for a statistical analysis with a one-way ANOVA followed by the Tukey test. N=5; error bars=SD.

No differences were noticed in the maximum ΔR/R0 ratio upon NaCl addition (IN) and removal (OUT) comparing WT and knock-out line for every ROIs. These results show similar salt-induced $Ca^{2+}$ dynamics in the WT and *why2-1* seedlings, a proper $Ca^{2+}$ signatures in the knock-out line as in WT line are represented in figure 3.28.A and B. We therefore concluded that the $Ca^{2+}$ dynamics in absence of WHY2 was not compromised.

### 3.3.10 Is WHY2 involved in retrograde signalling?

In the last few years, the relevance of plant organelles and their role in stress sensing and response is being unveiled more and more. The three different WHIRLY proteins in *A. thaliana* are localized in different subcellular compartments (mitochondria and plastids). Recently, it has been demonstrated that WHIRLY1 can translocate from the plastids to the nucleus making the WHIRLY family proteins ideal candidates as retrograde signalling molecules (Isemer et al., 2012; Foyer et al., 2014).

Mitochondria are crucial for intracellular stress perception, and it is known that salt stress induces a mitochondrial retrograde signalling response (Van Aken et al., 2009). Hence, we decided to evaluate in plants exposed to salt stress the transcription levels of some genes known to be involved in this process, together with WHIRLY genes.

As already mentioned above, *WHY2* transcription is induced in seedlings by salt stress. A RT-PCR experiment was performed on 14 DAS WT seedlings after 8 h of exposure to 150 mM NaCl. The transcription profile of *WHY2* together with other nuclear-encoded genes related to retrograde signalling and ROS detoxification were analysed. The chosen genes related to retrograde signalling are the following: *AOX1a* and *mtHSC70-1*. *AOX1a* codes for an alternative oxidase of plant mitochondria that transfers electrons from the ubiquinone pool to oxygen without energy conservations and it is considered a common mitochondrial retrograde signalling marker (Ng et al., 2013). *mtHSC70-1* codes for a heat shock protein involved in the mitochondrial unfolded protein response (UPR$^{mt}$; Wei et al., 2019).

Upon salt treatment, *AOX1a* and *mtHSC70-1* were significantly induced in WT line, together with *WHY2* (figure 3.29). These results were expected given that salt stress, inducing a hydrogen peroxide burst (ROS increase) triggers mitochondrial stress linked to the unfolded protein response (UPR$^{mt}$; *mtHSC70-1*) and retrograde response as highlight by *AOX1a* induction. *AOX1a* is an ANAC017-regulated gene during retrograde signalling response (Van Aken et al., 2016).

In knock-out line under the same conditions, we observed an induction of both *mtHSC70-1* and *AOX1a* upon saline stress (figure 3.29). Although starting from the same basal level of expression of these two genes in WT and knock-out, in knock-out line the mitochondrial stress marker is significantly higher (*mtHSC70-1*) then in WT. On the other hand, the alternative oxidase, despite being induced, is considerably lower than in WT (figure 3.29).

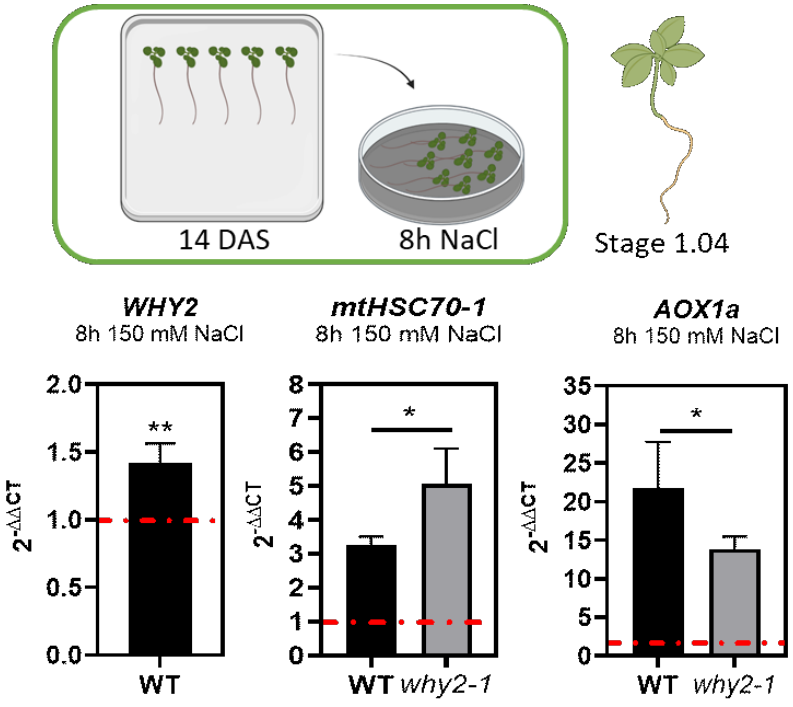

**Figure 3.29:** Real-Time PCR on 14 DAS old seedlings treated for 8h with 150 mM NaCl. Analyzed genes: *WHY2, mtHSC70-1* and *AOX1a;* genes involved in the retrograde signalling. *ACT2* has been used as housekeeping gene. The results were analyzed with the 2^(-ΔΔCt) technique. Error bars: SD. Asterisks describe the level of significance: * = $p < 0.05$; ** = $p < 0.005$. Statistic: Student's t-test method.

It has been recently reported that, in plants treated with doxycycline or antimycin A, $UPR^{mt}$ is largely overlapping with mitochondrial retrograde signalling, mediated by ANAC017 (Kacprzak et al., 2020). In the present work, we observed that in *WHY2* mutants salt stress is associated with an impaired retrograde response and a potentiated $UPR^{mt}$ response. These data seem to suggest that a different regulation occurs in RS and $UPR^{mt}$ when the trigger is salt stress in the absence of WHY2. The absence of WHY2 may have somehow compromised the retrograde response which controls the expression of *AOX1a*, while proteotoxic stress seems to be exacerbated.

In conclusion, in the knock-out line, salt stress induced the expression of *AOX1a*, but to a lower extent than in WT. The lower expression level of this gene in the mutant line and the induction of *WHY2* in WT line under salt stress might suggests that WHY2 is involved in retrograde signalling response. However, further studies will be necessary to better understand the molecular mechanism underlying the salt stress response and the possible involvement of WHY2.

### 3.3.11 ROS scavenging system during salt stress

During exposure to high NaCl concentrations, one of the main challenges for the cells is to face the intracellular increase of ROS, caused by the entry of $Na^+$ ion in cells. High cytosolic $Na^+$ causes a depolarization of membranes and induces the formation of ROS (Che-Othman et al., 2017). High levels of this ion cause osmotic stress and high levels of cell toxicity, affecting TCA cycle, several metabolic pathways and proteins functionality (Che-Othman et al., 2017).

In response to such stimuli plants induce a precise response to re-equilibrate the intracellular redox state, trying to preserve metabolic activity and to protect lipids, proteins and nucleic acids from the action of ROS. Several molecules and enzymes play a role in ROS detoxification: some of the main actors in this process are catalase and ascorbate peroxidase, two enzymes that react with $H_2O_2$ reducing it to less toxic products.

Trying to further characterize the oxidative response triggered by salt stress in WT and knock-out lines, we performed an enzymatic and non-enzymatic antioxidants assay (in collaboration with De Pinto's lab - University of Bari). 14 DAS seedlings were treated for 8 h in liquid medium with 150 mM NaCl as the previous experiment reported in paragraph 3.3.10.

Figure 3.30, clearly shows an increase in the activity of catalase and ascorbate peroxidase in WT line confirming an appropriate perception of salt stress and intracellular response, likely associated with an increase in ROS production. Instead, knock-out lines (*why2-1* and *why2-3*) catalase activity is not induced by salt stress while the ascorbate peroxidase activity is only slightly increased. Since the basal enzymatic activity in control samples is comparable between WT and knock-out lines, these

results suggest that in *why2-1* and *why2-3* plants there is an impairment in the ROS detoxification response. This effect might be due to a lack of ROS-related signals, to a failure in the activation of stress responsive genes, or to a dysfunctional enzymatic activity (figure 3.30).

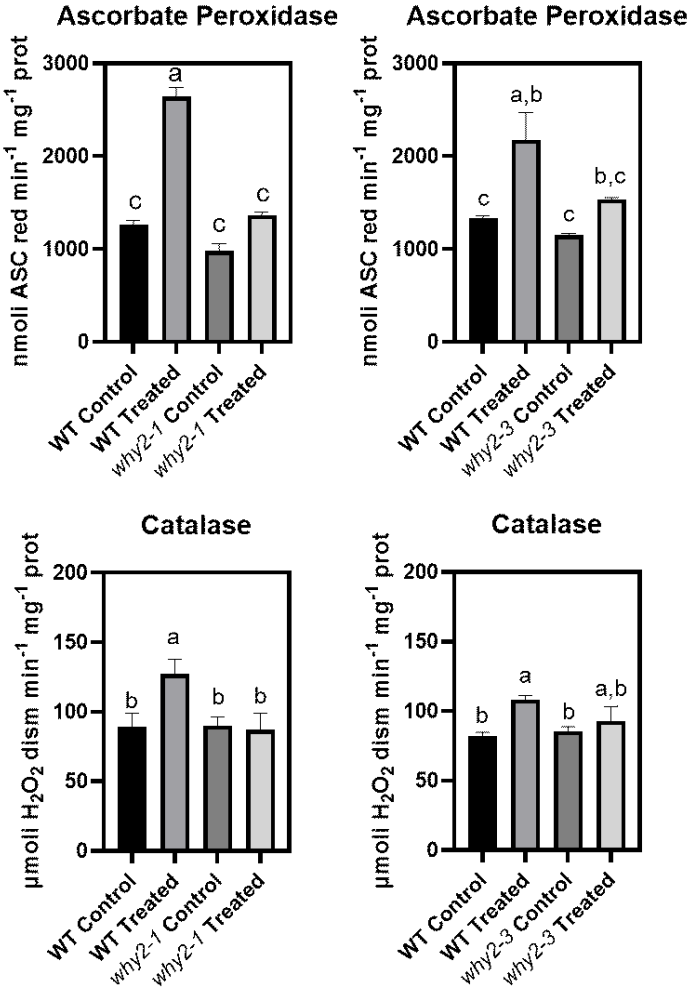


**Figure 3.30:** Enzymatic activity in 14 DAS old seedlings (WT, *why2-1* and *why2-3* lines) treated for 8h with 0 and 150 mM NaCl. Analysed enzymes: Ascorbate peroxidase and catalase. Error bars: SE. Letters describe the level of significance between samples. Statistic: Two-way ANOVA.

Furthermore, we studied the levels of non-enzymatic antioxidants related to ROS detoxification: ascorbic acid (ASA) and glutathione (GSH). The pool of these two antioxidant molecules does not change in WT line, possibly due to a high turnover in stress conditions. Interestingly, in the mutant lines AsA levels are already higher in control conditions and decrease after the stress. The higher level of ascorbic acid matches with the lower level of lipid peroxidation observed in untreated knock-out samples: high AsA better protects lipids from ROS-mediated oxidation in mitochondria. After the treatment, there is a reduction in the total ascorbate level, meaning that it is consumed. Regarding the total glutathione amount we saw no significant changes in both WT and knock-out lines (figure 3.31). Since GSH pool does not change, our results suggest that the absence of *WHY2* specifically involves AsA and is directly linked to its increase.

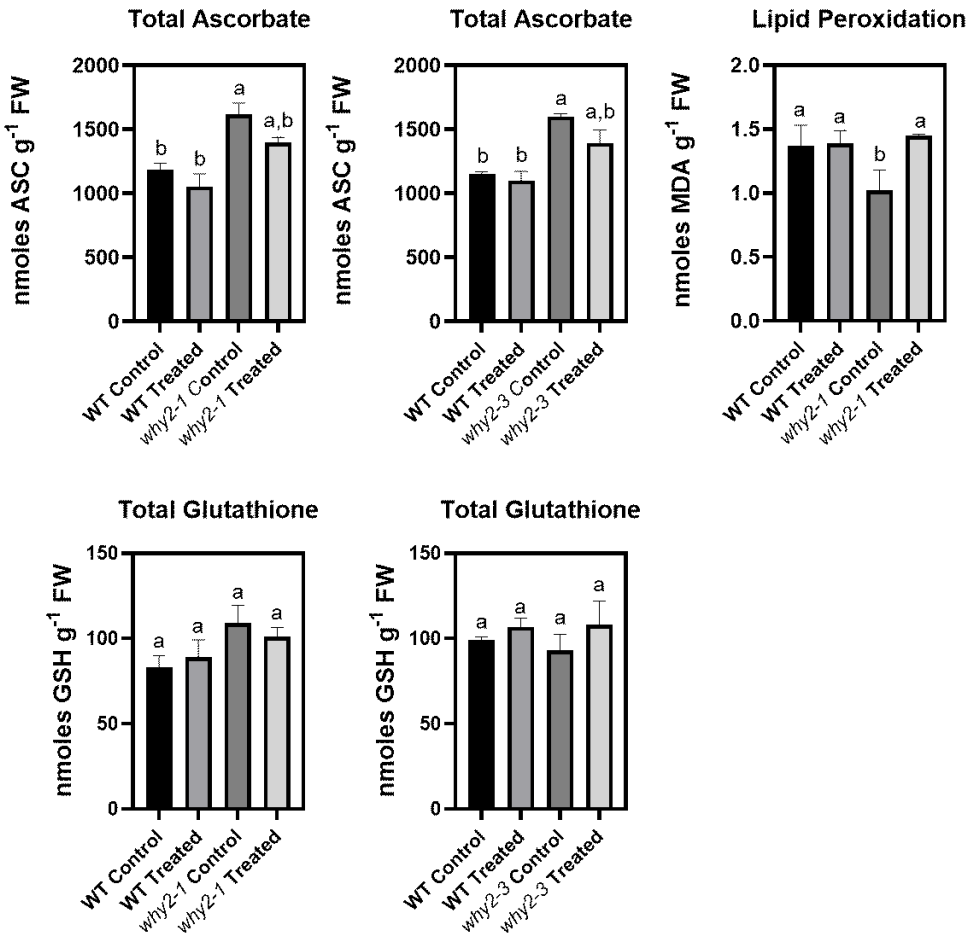


**Figure 3.31:** Non-enzymatic antioxidants in 14 DAS old seedlings (WT, *why2-1* and *why2-3* lines) treated for 8h with 150 mM NaCl. Analyzed compounds: Total ascorbic acid and total glutathione. Also included, lipid peroxidation in WT and *why2-1* lines. Error bars: SE. Letter describe the level of significance between samples. Statistic: Two-way ANOVA.

To sum up, it was observed that after salt stress in the knock-out line there is a lower expression of the retrograde marker gene *AOX1a* and a higher induction of *mtHSC70-1* that is related to the ROS intracellular level. These results suggest a lack in the ROS detoxification response associated to the missed induction of ascorbate peroxidase and catalase enzymatic activities, linked to the absence of WHY2. Ascorbic acid levels in control conditions are higher than in WT, we thus hypothesized that the higher basal level of this antioxidant molecule might scavenge the ROS in mitochondria and cause an impairment in retrograde signalling response triggered by exposure to salt. This miscommunication between mitochondria and the nucleus might explain the failed increase in antioxidant activity.

In conclusion, a reduced signalling of the stress in knock-out lines has been confirmed also by the enzymatic and non-enzymatic antioxidants assays, in agreement with the result obtained through RT-PCR on *AOX1a*. Taken together, our results may highlight an impairment in the retrograde signalling pathway that involves AOX1a, and a consequent failure in the activation of an appropriate scavenging system, one of the first processes induced in response to salt.

# Conclusions

Human population is constantly increasing worldwide. This has an impact on every aspect of society from an economic, scientific, social and health point of view. As a direct consequence of this forecast, one of the most important challenges is the increase of global food production. Therefore, an improvement in agricultural productivity is of fundamental relevance. Moreover, climate changes further undermine crop yield improvement by making the environment more hostile for plant growth and by triggering stress mechanisms with a significant impact on food quantity and quality. In this context, the increase in soil salinity is one of the most impacting abiotic stresses, responsible of a serious reduction in crop quality and in productivity of arable lands.

In the last few years, the role of plant mitochondria is deeply investigated, undercovering the fundamental role they take in high-energy demanding growth phases and in stress response. Recently, it has been discovered that proper replication of mitochondrial DNA is fundamental for organellar division and activity: a correct genetic inheritance is essential to ensure the functioning of the many metabolic steps housed in the mitochondrion.

In *Arabidopsis thaliana*, mitochondria are mainly transmitted by the egg cell, while sperm cells or generative cells reveal a 50-fold degradation of mtDNA during pollen development. This gives a fundamental role to the genetic inheritance of mtDNA transmitted by the female part of the plant. Mutations on mitochondrial genes were found to cause also male sterility in different plant species (Wang et al., 2010).

Other than mtDNA, proteins expressed or active in mitochondria are of particular interest, being important in different metabolic pathways and intracellular responses. Many proteins are now known to have multiple intracellular localisation and activity, even simultaneously. This allows fast travelling of information and stimuli through the cell from organelles to the nucleus in a phenomenon called retrograde signalling.

Foreseeing a possible application to crop plants improvement, we decide to focus on the multifaceted role of plant mitochondria from investigating their replication, morphology and dynamics till to analysing stress response and complex signalling induced by it. We especially studied the nuclear-encoded mtDNA-binding protein WHIRLY2. This protein is known to be involved in the mtDNA repair by avoiding non-homologue recombination during mtDNA replication, but its intracellular role under developmental and stress conditions is still to be fully understood.

## 4.1 The role of WHIRLY2 during different developmental processes

At the beginning of this project thesis, we generated two new knock-out WHRLY2 lines: *why2-3* with an insertional mutation in the first exon of the gene, and *why2-4* in the second one. We also used

in our experiments another mutant *why2-1,* containing a T-DNA insertion in the last intron, already available. The phenotyping of the two new lines confirmed previous results from Maréchal et al. in 2008, in *why2-1*: no evident phenotype observed during vegetative growth, but a stronger accumulation of aberrant mtDNA products in plants exposed to the genotoxic agent ciprofloxacin (Cappadocia et al., 2010). This was explained by the known role of WHY2 in the homologue recombination repair system that helps mtDNA replication (Cappadocia et al., 2010).

We began by checking *WHY2* expression levels at different developmental stages, and the result was that it is particularly induced during pollen development, in 24 hour imbibed seeds and during embryo development. When our experiments were focused on such high-energy demanding processes, some peculiar characteristics were noticed: all knock-out lines showed a partial failure in seed germination (25%) along with an increase in seeds abortion associated to the absence of WHY2. These results suggest that mtDNA integrity (and accordingly mitochondria functionality) is fundamental when ATP and metabolites are highly required. On the other hand, the absence of WHY2 does not impair plant growth during vegetative growth. Germination is mainly supported by mitochondrial activity, these organelles are in fact the only energy producers in the first phases after sawing, that are particularly relying on heterotrophic metabolism. Pre-existing mitochondria are activated in seeds during germination while new mitochondria are produced to sustain the energy requirements of the process. This justifies the mitochondrial related transcript abundancy, including TCA cycle and respiratory chain related proteins (Howell et al., 2006). In the context of an induction of mitochondrial replication, WHY2 might be particularly important for its role in mtDNA repair that can ensure a proper mtDNA replication and the organelle functionality.

Similarly, the first phases of embryo development are supported by heterotrophic metabolism, and this may explain why we observed a reduction of about 25% of developed embryos in the siliquae in the absence of *WHY2*. During high cell division phases, cells require large amounts of ATP to ensure a correct plant development. Moreover, organellar functioning is fundamental for the activity of different tissues and organellar biogenesis, therefore accurate mtDNA replication is crucial to support all these functions. In conclusion, the activity of WHY2 seems to play a key role to ensure a correct mtDNA replication and functionality of mitochondria, needed during specific plant growth phases.

## 4.2 WHY2 function on mtDNA and nucleoids organization

It was recently demonstrated that the absence of WHY2 is associated with a compromised nucleoids organization (Golin, Negroni et al., 2020). Nucleoids are DNA-nucleoproteins complexes where mtDNA is packed and organized, and their structural disruption in *WHY2* mutants could suggest a scaffold role of this protein at nucleoid level. However, such loss of compactness could also be

ascribed to the effect of intense mtDNA replication. This possibility was excluded by checking mtDNA copy number in WT and mutant lines that showed no differences.

An incorrect organization of the nucleoid is also linked to an impairment in mitochondrial morphology and dynamics. In plants lacking WHY2, aberrant mitochondrial morphology and dynamics were observed in specific tissues and developmental phases (Golin, Negroni et al., 2020). In *WHY2* mutants, mitochondria are elongated with few cristae and reduced motility, while WT mitochondria are circular and full of cristae. We confirmed those results performing further analyses on mitochondrial morphology both *in vivo* and *in vitro*. Taken together, these observations suggest a relationship between WHY2, disorganized nucleoids, and elongated mitochondria, possibly implying a novel function of WHY2 as scaffold of proteins involved in mitochondria structure maintenance, and surely confirming its part in avoiding non-homologue recombination during mtDNA replication. In mammals, it has already been proved that the organization of cristae strongly depends on the integrity of mtDNA/nucleoids (Ban-Ishihara et al., 2013). We suggested that the accumulation of mtDNA rearrangements and the absence of WHY2 could be responsible for nucleoid disorder and consequently for the elongation of mitochondria and their reduced motility. An important experimental approach would be the identification of proteins interacting with WHY2, based on the hypothesis that WHY2 can work as a scaffold protein of mtDNA nucleoids.

## 4.3 WHY2 function on mtDNA repair, copy number and nucleoids organization under salt stress

Mitochondria play a relevant role in stress sensing, response and adaptation. Since previous results show that WHY2 is fundamental for mtDNA and nucleoids' stability and that its absence leads to reduced mitochondrial functionality, we decided to characterize WHY2 knock-out lines response under stress conditions. When exposed to stress, plant cells require high levels of ATP to firstly reduce the intracellular damage, secondly to remove the source of stress and, finally, to restore basal functions and to recover. Functional mitochondria and their active repositioning throughout the cell are particularly necessary in these conditions.

We opted for one of the most relevant detrimental stimuli when considering crop plants: salt stress. As already said, when plants are exposed to salt stress, cell requirement for ATP and other molecules coming from mitochondria vastly increases. Mitochondria are needed to restore ion balance, reduce ROS formation and buffer the damages induced by free radicals. Hence, immediately after exposure to salt stress, WT mitochondria reorganize themselves clustering and inducing mitochondrial fission and fusion. During this process, an increase in mtDNA amount has been observed (figure 3.22), possibly due to an induction of its replication. Therefore, an accurate regulation of replication and an active mtDNA repair system are particularly required. We hypothesized that these could be the perfect conditions for studying the function of WHY2 and the effects given by its lack, since WHY2

is involved in the repair system and could also act as nucleoid scaffold protein ensuring appropriate mitochondrial cristae structure and the mitochondria overall morphology and dynamics.

For the first time it has been observed a clear phenotype in *WHY2* mutants: after a prolonged exposure to salt, mtDNA was much more damaged than in WT. We also observed a stronger increase in the total amount of mtDNA, confirming a high mtDNA replication rate and a fundamental repair activity under salt stress. Our results show that WHY2 is not a marginal protein in the mtDNA repair process, in fact, it seems to be the only mtDNA repair protein induced by salt stress. Moreover, in an experiment performed on plants exposed to salt stress and then left for 10 days without salt, no recovery from mtDNA damage in mutant lines was observed.

The absence of WHY2, in combination with prolonged exposure to salt stress, seems to cause problems at different developmental stages such as during germination, primary root growth and plant survival. This shows that an impairment in the mtDNA repair system leads to serious developmental problems under certain conditions. In conclusion, it has been discovered that during salt stress *WHY2* mutant lines show an abnormal mtDNA replication, proved by the increase in mtDNA copy number. At the same time, a rise in non-homologous recombination events was observed, that could be the cause of reduction in salt tolerance.

## 4.4 A possible connection between WHY2 and retrograde signalling

In the last years, a fundamental mitochondrial function as stress sensor has been highlighted, also considering the retrograde signalling pathway induced by stresses. The obtained results on the *AOX1a* expression level on the pulse salt stress show a different induction of the retrograde signalling in WT compared to knock-out lines, suggesting an impairment in the retrograde signalling response. Instead, a higher induction of *mtHSC70-1*, suggests higher mitochondrial stress after treatment. These findings are also supported by the results obtained under prolonged and pulsed salt stress treatments on the antioxidant activity and the ATP homeostasis assays: the activity of different ROS-scavenging enzymes (catalase and ascorbate peroxidase) is not induced in mutant lines, and the $MgATP^{2-}$ cytosolic amount does not decrease as much as in WT. Also, a higher level of ascorbate could suggest an impairment in the stress perception caused by a lower ROS level in control conditions in mutant lines. All these results in fact support the hypothesis of an impairment in the salt stress perception. Furthermore, a recent work reporting multiple intracellular localization of WHY2 protein (Huang et al., 2020), suggests an involvement of this protein in the intracellular retrograde signalling mechanism as well already suggested for WHIRLY1 in retrograde signalling from the chloroplast (Foyer et al., 2014)

It would be interesting in further experiments to expose WT and *WHY2* mutants to different stresses (for example high light and drought stress) and investigate whether WHY2 has a broader role in stress perception or if its loss is only detrimental during salt stress.

The results presented in this thesis are opening a new conception of mitochondria as key players during stresses. Future programs to enhance plant production will have to take into account not only the improvement of plant genetics but also to ensure mitochondrial well-being and their optimal response to stress conditions.

# Appendix

## Appendix I

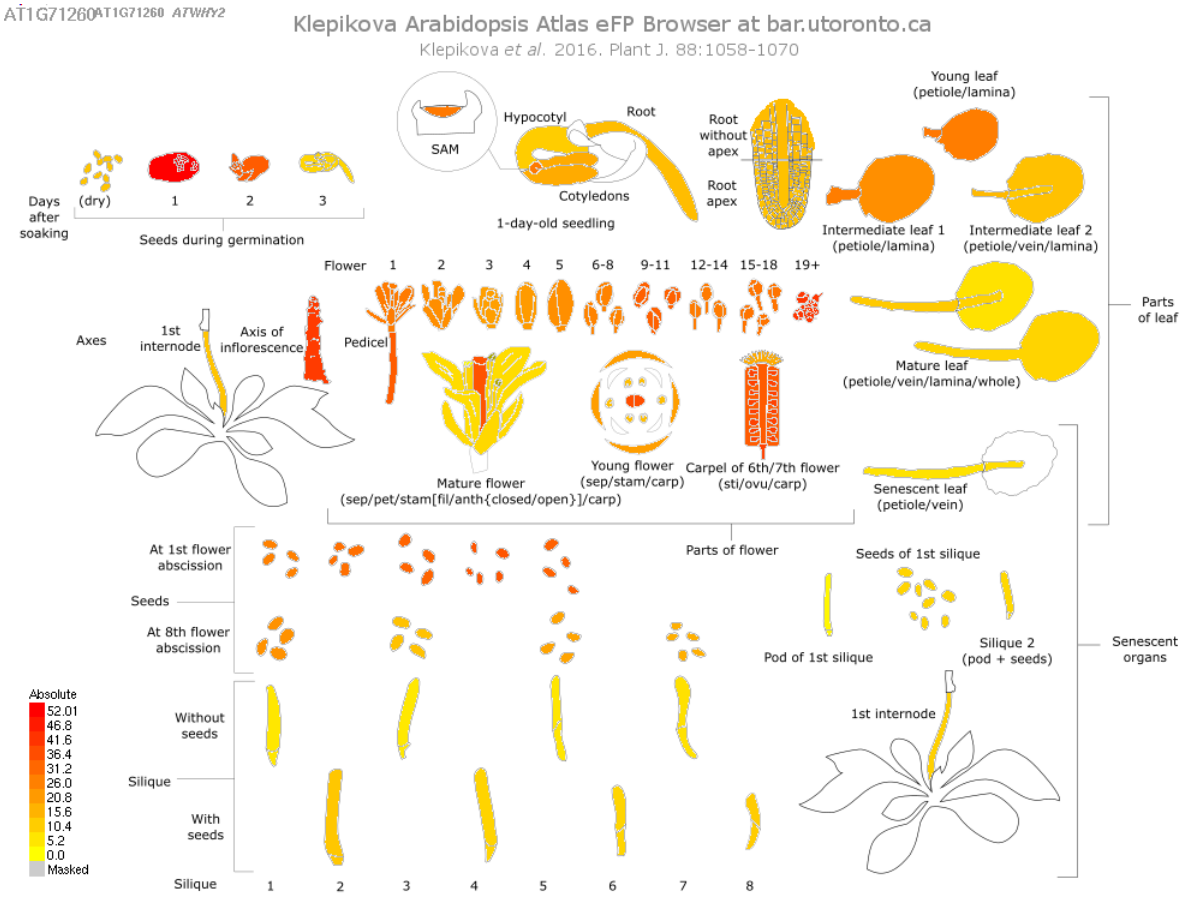


Data from A high resolution map of the Arabidopsis thaliana developmental transcriptome based on RNA-seq profiling: Klepikova et al., 2016, Plant J. 88:1058-1070. Total RNA was extracted with RNeasy Plant Kit and Illumina cDNA libraries were generated using the respective manufacturer's protocols. cDNA was then sequenced using Illumina HiSeq2000 with a 50bp read length. The read data are publicly available in NCBI's Sequence Read Archive under the BioProject ID 314076 (accession: PRJNA314076). Reads were aligned to the reference TAIR10 genome (Lamesch et al., 2012) using TopHat (Trapnell et al., 2009). Default TopHat settings and job resource parameters were used, with read groups unspecified. Reads per gene were counted with an in-house Python script using functions from the HTSeq package (Anders et al., 2015). Reads were filtered so that only uninterrupted reads corresponding to a region within exactly one gene were used for RPKM calculation. If a gene's expression level is not displayed, this indicates the reads for this gene did not pass the filtering criteria. RPKM values were compiled using an in-house R script.

**Appendix I:** Expression of *AtWHY2* in different tissues and developmental stages of *Arabidopsis* from the eFP Browser microarray database. Expression pattern of *AtWHY2* in the developmental series generated by Arabidopsis eFP Browser.

| Cis-acting element | Sequence | | Keywords | Position | #total | #upstream | #5'UTR | #exon | #intron |
|---|---|---|---|---|---|---|---|---|---|
| TCA1MOTIF | TCATCTTCTT | DE TCA-1 (tobacco nuclear protein 1) binding site; Related to DE salicylic acid-inducible expression of many genes; Found in DE barley beta-1,3-glucanase and over 30 different plant genes which DE are known to be induced by one or more forms of stress; A similar DE sequence (TCATTTCTT) was found in tobacco Tnt1 retrotransposon DE promoter (Mhiri et al., 1997); | SA; salicylic acid; stress; | 116 | 1 | | | 1 | |
| ARFAT | TGTCTC | DE ARF (auxin response factor) binding site found in the promoters DE of primary/early auxin response genes of Arabidopsis thaliana DE (A.t.); AuxRE; See S000337; Binding site of Arabidopsis ARF1 DE (Auxin response factor1); Sequence found in NDE element in DE Soybean (G.m.) SAUR (Small Auxin-Up RNA) 15A gene promoter; See DE S000359, S000360; Found in D1 or D4 element in Soybean (G.m.) GH3 DE promoter; This element was enriched in the 5'-flanking region of DE genes up-regulated by both IAA and BL (Goda et al., 2004); | auxin; AuxRE; ARF; ARF1; Au | 127 | 1 | | 1 | | |
| SORLIP3AT | CTCAAGTGA | one of "Sequences Over-Represented in Light-Induced Promoters DE (SORLIPs) in Arabidopsis; Computationally identified phyA-induced DE motifs; See also S000482, S000483, S000485, S000486 (all DE SORLIPs), and also S000487, S000488, S000489, S000490 (all DE SORLREPs) | phyA; phytochrome; light | 145 | 1 | | 1 | | |
| MYCCONSENSUSAT | CANNTG | MYC recognition site found in the promoters of the DE dehydration-responsive gene rd22 and many other genes in DE Arabidopsis; Binding site of ATMYC2 (previously known as DE rd22BP1); see S000144 (E-box; CANNTG), S000174 (MYCATRD22); DE N=A/T/G/C; MYC recognition sequence in CBF3 promoter; Binding DE site of ICE1 (inducer of CBF expression 1) that regulates the DE transcription of CBF/DREB1 genes in the cold in Arabidopsis; ICE1 DE (Chinnusamy et al., 2004);) This sequence is also known as RRE (R DE response element)(Hartmann et al., 2005) | MYC; rd22BP1; ABA; leaf; se | 146;646;724,924,1143,1320,1650,1892,(x2) | 16 | 14 | 2 | | |
| LTRECOREATCOR15 | CCGAC | Core of low temperature responsive element (LTRE) of cor15a gene DE in Arabidopsis (A.t.); A portion of repeat-C (C-repeat), DE TGGCCGAC, which is repeated twice in cor15a promoter (Baker et DE al., 1994); ABA responsiveness; Involved in cold induction of DE BN115 gene from winter Brassica napus; LTRE; See S000157, DE S000152; Light signaling mediated by phytochrome is necessary for DE cold- or drought- induced gene expression through the C/DRE in DE Arabidopsis | low temperature; cold; LTRE | 159-468 | 2 | 1 | 1 | | |
| ARR1AT | NGATT | "ARR1-binding element" found in Arabidopsis; ARR1 is a response DE regulator; N=G/A/C/T; AGATT is found in the promoter of rice DE non-symbiotic haemoglobin-2 (NSHB) gene (Ross et al., 2004) | ARR1; Response regulator | 51,58,177,,270,286,290,309,398,407,413,449,529,615,630,635,674,752,771,948,1099,1105,1247,1291,1341,1471,1509,1536,1470,1597,1689,1799,1882,1902 | 34 | 31 | 1 | | 2 |
| GT1CONSENSUS | GRWAAW | Consensus GT-1 binding site in many light-regulated genes, e.g., DE RBCS from many species, PHYA from oat and rice, spinach RCA and DE PETA, and bean CHS15; R=A/G; W=A/T; For a compilation of related DE GT elements and factors, see Villain et al. (1996); GT-1 can DE stabilize the TFIIA-TBP-DNA (TATA box) complex; The activation DE mechanism of GT-1 may be achieved through direct interaction DE between TFIIA and GT-1; Binding of GT-1-like factors to the PR-1a DE promoter influences the level of SA-inducible gene expression | GT-1; light; TATA; TFIIA; T | 180,195,276,473,899,1356,,1460,1461,1468,1576,1617,1759,1848,1917,1918,1926,1936,1993 | 18 | 17 | 1 | | |
| IBOXCORE | GATAA | "I box"; "I-box"; Conserved sequence upstream of light-regulated DE genes; Conserved sequence upstream of light-regulated genes of DE both monocots and dicots | I-box; rbcS; light regulati | 1.811.961.618 | 3 | 2 | 1 | | |
| MYBCORE | CNGTTR | Binding site for all animal MYB and at least two plant MYB DE proteins ATMYB1 and ATMYB2, both isolated from Arabidopsis; DE ATMYB2 is involved in regulation of genes that are responsive to DE water stress in Arabidopsis; A petunia MYB protein (MYB.Ph3) is DE involved in regulation of flavonoid biosynthesis (Solano et al. DE EMBO J 14:1773 (1995) | MYB; myb; dehydration; wate | 188.220.245.246.858 | 5 | 5 | | | |
| MYB2CONSENSUSAT | YAACKG | MYB recognition site found in the promoters of the DE dehydration-responsive gene rd22 and many other genes in DE Arabidopsis; Y=C/T; K=G/T; See S000177 (MYB2), S000175 DE (MYBATRD22) | MYB; rd22BP1; ABA; leaf; se | 245-858 | 2 | 2 | | | |
| SORLIP2AT | GGGCC | one of "Sequences Over-Represented in Light-Induced Promoters DE (SORLIPs) in Arabidopsis; Computationally identified phyA-induced DE motifs; See also S000482, S000484, S000485, S000486 (all DE SORLIPs), and also S000487, S000488, S000489, S000490 (all DE SORLREPs) | phyA; phytochrome; light | 249-257-590 | 3 | 3 | | | |
| CCAATBOX1 | CCAAT | Common sequence found in the 5'-non-coding regions of eukaryotic DE genes; "CCAAT box" found in the promoter of heat shock protein DE genes; Located immediately upstream from the most distal HSE of DE the promoter; "CCAAT box" act cooperatively with HSEs to increase DE the hs promoter activity | HSE (Heat shock element); C | 252;272;487;798;1023;1098;1511;1611 | 8 | 8 | | | |
| CAREOSREP1 | CAACTC | "CAREs (CAACTC regulatory elements)" found in the promoter region DE of a cystein proteinase (REP-1) gene in rice | aleurone; GARE; gibberellin | 441 | 1 | 1 | | | |
| ASF1MOTIFCAMV | TGACG | "ASF-1 binding site" in CaMV 35S promoter; ASF-1 binds to two DE TGACG motifs; See S000023 (AS1); Found in HBP-1 binding site of DE wheat histone H3 gene; TGACG motifs are found in many promoters DE and are involved in transcriptional activation of several genes DE by auxin and/or salicylic acid; May be relevant to light DE regulation; Binding site of tobacco TGA1a; TGA1a and b show DE homology to CREB; TGA6 is a new member of the TGA family; Abiotic DE and biotic stress differentially stimulate "as-1 element" DE activity | TGACG; root; leaf; CaMV; 35 | 481;1746,1799 | 3 | 3 | | | |
| WRKY71OS | TGAC | "A core of TGAC-containing W-box" of, e.g., Amy32b promoter; DE Binding site of rice WRKY71, a transcriptional repressor of the DE gibberellin signaling pathway; Parsley WRKY proteins bind DE specifically to TGAC-containing W box elements within the DE Pathogenesis-Related Class10 (PR-10) genes (Eulgem et al., 1999); DE See S000390 (TTGAC), S000442 (TGACT) | WRKY; GA; MYB; W box; TGAC; | 481-1011-1042-1265-1298-1304-1316-1412-1552-1641-1746-1826 | 12 | 12 | | | |
| INRNTPSADB | YTCANTYY | "Inr (initiator)" elements found in the tobacco psaDb gene DE promoter without TATA boxes; Light-responsive transcription of DE psaDb depends on Inr, but not TATA box | initiater; light-responsive | 75-495-1277 | 3 | 2 | | | 1 |
| NTBBF1ARROLB | ACTTTA | NtBBF1(Dof protein from tobacco) binding site in Agrobacterium DE rhizogenes (A.r.) rolB gene; Found in regulatory domain B (-341 DE to -306); Required for tissue-specific expression and auxin DE induction | rolB; Dof; auxin; domain B; | 608 | 1 | 1 | | | |
| CIACADIANLELHC | CAANNNNATC | Region necessary for circadian expression of tomato (L.e.) Lhc DE gene | circadian; light; Lhc; leaf | 773-1736 | 2 | 2 | | | |

| Cis-acting element | Sequence | | Keywords | Position | #total | #upstream | #5'UTR | #exon | #intron |
|---|---|---|---|---|---|---|---|---|---|
| CATATGGMSAUR | CATATG | Sequence found in NDE element in soybean (G.m.) SAUR (Small DE Auxin-Up RNA) 15A gene promoter; Involved in auxin DE responsiveness | SAUR; NDE; auxin | 725-1893 (x2) | 4 | 4 | | | |
| MYB2AT | TAACTG | Binding site for ATMYB2, an Arabidopsis MYB homolog; ATMYB2 DE binds oligonucleotides that contained a consensus MYB recognition DE sequence (TAACTG), such as is in the SV40 enhancer and the maize DE bronze-1 promoter (Urao et al., Plant Cell 5:1529 (1993)); ATMYB2 DE is involved in regulation of genes that are responsive to water DE stress in Arabidopsis | MYB; myb; SV40; enhancer; b859 | | 1 | 1 | | | |
| TBOXATGAPB | ACTTTG | "Tbox" found in the Arabidopsis thaliana (A.T.) GAPB gene DE promoter; Located between -94 and -89 (T1) and also between -84 DE and -79 (T2); Mutations in the "Tbox" resulted in reductions of DE light-activated gene transcription; GAPB encodes the B subunit of DE chloroplast glyceraldehyde-3-phosphate dehydrogenase(GADPH) of DE A.T. | GAPB; glyceraldehyde-3-phos | 935-1442:1485 | 3 | 3 | | | |
| TATCCAOSAMY | TATCCA | "TATCCA" element found in alpha-amylase promoters of rice (O.s.) DE at positions ca.90 to 150bp upstream of the transcription start DE sites; Binding sites of OsMYBS1, OsMYBS2 and OsMYBS3 which DE mediate sugar and hormone regulation of alpha-amylase gene DE expression; See also S000021 (AMYBOX2); S000256 (TATCCAY motif) | alpha-amylase; MYB proteins | 975 | 1 | 1 | | | |
| WRKY71OS | TGAC | "A core of TGAC-containing W-box" of, e.g., Amy32b promoter; DE Binding site of rice WRKY71, a transcriptional repressor of the DE gibberellin signaling pathway; Parsley WRKY proteins bind DE specifically to TGAC-containing W box elements within the DE Pathogenesis-Related Class10 (PR-10) genes (Eulgem et al., 1999); DE See S000390 (TTGAC), S000442 (TGACT) | WRKY; GA; MYB; W box; TGAC; | 482-1012-1043-1266-1299-1305-1317-1413-1553-1642-1747-1827 | 12 | 12 | | | |
| 10PEMVPSBD | TATTCT | "-10 promoter element" found in the barley (H.v.) chloroplast DE psbD gene promoter; Involved in the expression of the plastid DE gene psbD which encodes a photosystem II reaction center DE chlorophyll-binding protein that is activated by blue, white or DE UV-A light | psbD; chloroplast gene expr | 1055-1118-1408 | 3 | 3 | | | |
| P1BS | GNATATNC | PHR1-binding sequence found in the upstream regions of phosphate DE starvation responsive genes from several plant species; phr1 DE (phosphate starvation response 1) gene codes for PHR1 protein DE related to PSR1 gene in C. reinhardtii | phosphate; starvation; MYB | 1056-1955 (x2) | 4 | 4 | | | |
| SORLIP1AT | GCCAC | one of "Sequences Over-Represented in Light-Induced Promoters DE (SORLIPs) in Arabidopsis; Computationally identified phyA-induced DE motifs; SORLIP 1 is most over-represented, and most statistically DE singnificant; See also S000483, S000484, S000485, S000486 (all DE SORLIPs), and also S000487, S000488, S000489, S000490 (all DE SORLREPs); Over-represented in light-induced cotyledon and root DE common genes and root-specific genes (Jiao et al. 2005; see DE S000486) | phyA; phytochrome; light | 1140-1676-1720 | 3 | 3 | | | |
| TATAPVTRNALEU | TTTATATA | "TATA-like motif"; A TATA-like sequence found in Phaseolus DE vulgaris tRNALeu gene promoter; Frequently observed upstream of DE plant tRNA genes; Found in maize glycolytic DE glyceraldehyde-3-phospate dehydrogenase 4 (GapC4) gene promoter; DE Binding site of TATA binding protein (TBP) | TATA; tRNA; re-initiation; | 229-1369 | 2 | 2 | | | |
| WBOXNTERF3 | TGACY | "W box" found in the promoter region of a transcriptional DE repressor ERF3 gene in tobacco; May be involved in activation of DE ERF3 gene by wounding;(Nishiuchi et al., 2004) Y=C/T | W box; ERF3; wounding; | 1299-1413-1552-1642 | 4 | 4 | | | |
| ERELEE4 | AWTTCAAA | "ERE (ethylene responsive element)" of tomato (L.e.) E4 and DE carnation GST1 genes; GST1 is related to senescence; Found in the DE 5'-LTR region of TLC1.1 retrotransposon family in Lycopersicon DE chilense (Tapia et al.); ERE motifs mediate ethylene-induced DE activation of the U3 promoter region | Ethylene; E4; GST1; senesce | 1445 | 1 | 1 | | | |
| PYRIMIDINEBOXHVEPB1 | TTTTTTCC | "Pyrimidine box" found in the barley (H.v.) EPB-1 (cysteine DE proteinase) gene promoter; Located between -120 to -113; Required DE for GA induction | EPB; cysteine proteinase; | G1460 | 1 | 1 | | | |
| GT1GMSCAM4 | GAAAAA | "GT-1 motif" found in the promoter of soybean (Glycine max) CaM DE isoform, SCaM-4; Plays a role in pathogen- and salt-induced DE SCaM-4 gene expression; See also S000198 (GT-1 consensus) | GT-1 box | 900-1461-1577-1760-1849-1919-1927 | 7 | 7 | | | |
| MYB1AT | WAACCA | MYB recognition site found in the promoters of the DE dehydration-responsive gene rd22 and many other genes in DE Arabidopsis; W=A/T | MYB; rd22BP1; ABA; leaf; | se17-1604-1943 | 3 | 2 | | | 1 |
| MYBGAHV | TAACAAA | Central element of gibberellin (GA) response complex (GARC) in high-pI alpha-amylase gene in barley (H.v.); Similar to c-myb and v-myb consensus binding site; GAmyb binds specifically to the TAACAAA box in vitro; GAmyb is the sole GA-regulated transcriptional factor required for transcriptional activation of the high-pI alpha-amylase; GARC consist of the pyrimidine, TAACAAA and TATCCAC boxes; GARE in RAmy1A gene; GARE and pyrimidine box in RAmy1A are partially involved in sugar repression; | myb; Myb; GAmyb; GA; gibber | 7 | 1 | | | | 1 |
| GAREAT | TAACAAR | GARE (GA-responsive element); Occurence of GARE in GA-inducible, DE GA-responsible, and GA-nonresponsive genes found in Arabidopsis DE seed germination was 20, 18, and 12%, respectively; see S000181; | GARE; GA | 7 | 1 | | | | 1 |
| MYB1AT | WAACCA | DE MYB recognition site found in the promoters of the DE dehydration-responsive gene rd22 and many other genes in DE Arabidopsis; W=A/T; | MYB; rd22BP1; ABA; leaf; | se17-1604-1943 | 3 | 2 | | | 1 |
| INRNTPSADB | YTCANTYY | DE "Inr (initiator)" elements found in the tobacco psaDb gene DE promoter without TATA boxes; Light-responsive transcription of DE psaDb depends on Inr, but not TATA box; | initiater; light-responsive | 76-496-1278-1572-1760 | 5 | 4 | | | 1 |

**Appendix II:** Full promoter analysis of *AtWHY2* from the first intron to 2kb upstream of the 3'->5'. The promoter analyses were performed with the use of New PLACE (A Database of Plant Cis-acting Regulatory DNA Elements). https://www.dna.affrc.go.jp/PLACE/?action=newplace. In yellow are represented the most abundant sequences.

## Appendix III

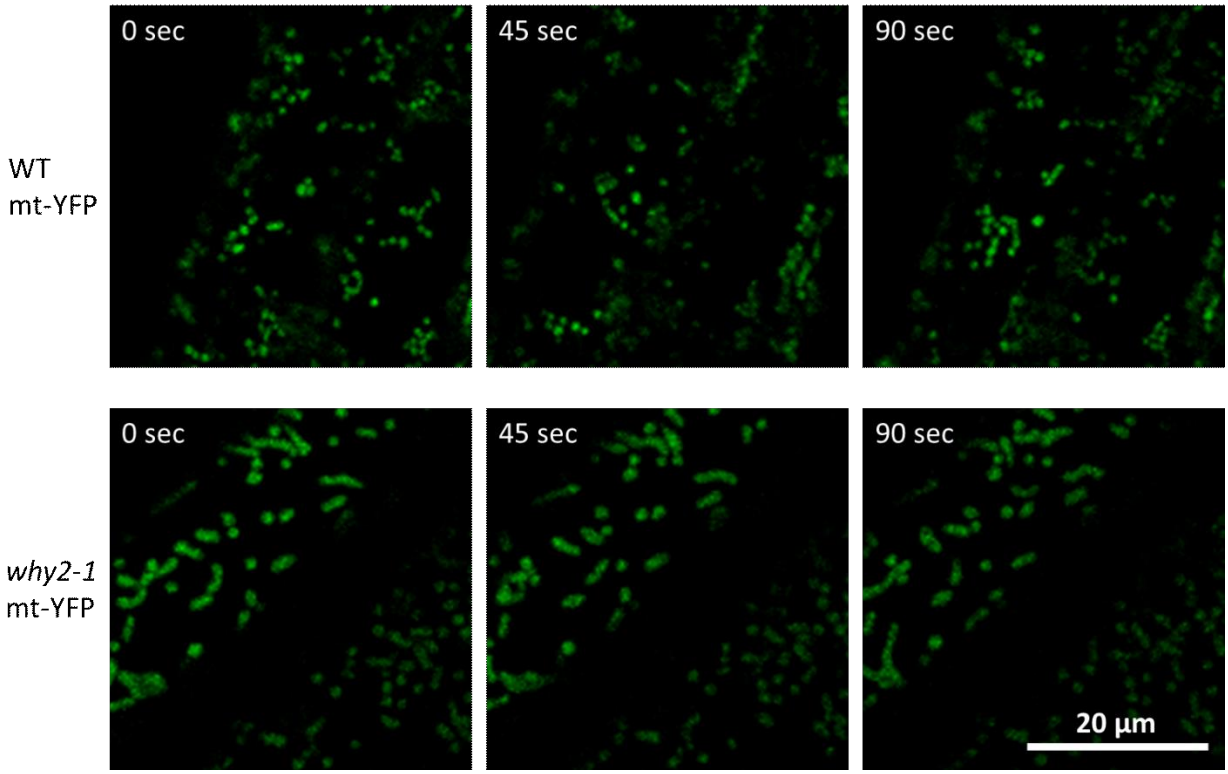


**Appendix III:** Representative images of mitochondrial dynamics analyses performed on root tissue cells of 5 DAS *A. thaliana* seedlings from mt-YFP WT and *why2-1*. Images show 3 frames (0, 45 and 90 seconds). Pictures were taken by CLSM. Scale bar: 20 µm.

# References

**Abe H, Urao T, Ito T, Seki M, Shinozaki K and Yamaguchi-Shinozaki K** (2003). *Arabidopsis* AtMYC2 (bHLH) and AtMYB2 (MYB) function as transcriptional activators in abscisic acid signalling. Plant Cell. 15(1):63-78. doi: 10.1105/tpc.006130.

**Adam Z** (2007). Protein stability and degradation in plastids. In: BockR (ed) Cell and molecular biology of plastids. Springer, Heidelberg, pp 315–338. DOI: 10.1007/978-1-62703-995-6_5.

**Akbudak MA and Filiz E** (2019). Whirly (Why) transcription factors in tomato (*Solanum lycopersicum L.*): genome-wide identification and transcriptional profiling under drought and salt stresses. Molecular Biology Reports, 46(4), 4139–4150. https://doi.org/10.1007/s1103 3-019-04863-y.

**Apel K and Hirt H** (2004). REACTIVE OXYGEN SPECIES: Metabolism, Oxidative Stress, and Signal Transduction. Annual Review of Plant Biology 55:1, 373-399. https://doi.org/10.1146/annurev.arplant.55.031903 .141701.

**Appelhagen I, Thiedig K, Nordholt N, Schmidt N, Huep G, Sagasser M and Weisshaar B** (2014). Update on transparent testa mutants from *Arabidopsis thaliana*: characterisation of new alleles from an isogenic collection. Planta240:955–970. doi:10.1007/s00425-014-2088-0.

**Arimura S** (2018). Fission and fusion of plant mitochondria, and genome maintenance. Plant Physiology, 176(1), 152–161. https://doi. Org/10.1104/pp.17.01025.

**Ayala-García VM, Baruch-Torres N, García-Medel PL and Brieba LG** (2018). Plant organellar DNA polymerases paralogs exhibit dissimilar nucleotide incorporation fidelity. FEBS J. 285, 4005–4018. https://doi.org/10.1111/febs.14645.

**Backert S, Dorfel P, Lurz R and Borner T** (1996). Rolling-circle replication of mitochondrial DNA in the higher plant *Chenopodium album* (L.). Molecular and Cellular Biology 16: 6285–6294. doi: 10.1128/mcb.16.11.6285.

**Backert S, Nielsen BL and Borner T** (1997). The mystery of the rings: structure and replication of mitochondrial genomes from higher plants. Trends in Plant Science 2: 477–483. https:// doi.org/10.1016/S1360-1385(97)01148-5.

**Backert S and Borner T** (2000). Phage T4-like intermediates of DNA replication and recombination in the mitochondria of the higher plant *Chenopodium album (L.).* Current Genetics, 37(5), 304-314 (2000) DOI: 10.1007/s002940050532.

**Ban-Ishihara R, Ishihara T, Sasaki N, Mihara K and Ishihara N** (2013). Dynamics of nucleoid structure regulated by mitochondrial fission contributes to cristae reformation and release of cytochrome c. Proceedings of the National Academy of Sciences of the United States of America, 110(29), 11863–11868. https://doi.org/10.1073/ pnas.13019 51110.

**Bartoli CG, Pastori G and Foyer CH** (2000). Ascorbate Biosynthesis in Mitochondria Is Linked to the Electron Transport Chain between Complexes III and IV. Plant Physiology, Volume 123, Issue 1, Pages 335–344, https://doi.org/10.1104/pp.123.1.335.

**Beeckman T, De Rycke R, Viane R and Inze D** (2000). Histological study of seed coat development in *Arabidopsis thaliana*. Journal of Plant Research. 113:139–148. doi:10.1007/PL00013924.

**Bendich AJ** (1996). Structural analysis of mitochondrial DNA molecules from fungi and plants using moving pictures and pulsed-field gel electrophoresis. Journal of Molecular Biology 255: 564–588. doi: 10.1006/jmbi.1996.0048.

**Boyes DC, Zayed AM, Ascenzi R, McCaskill AJ, Hoffman NE, Davis KR and Görlach J** (2001) Growth stage-based phenotypic analysis of *Arabidopsis*: a model for high throughput functional genomics in plants. Plant Cell. 13(7):1499-510. DOI: 10.1105/tpc.010011.

**Bradford MM** (1976). A rapid and sensitive method for the quantitation of microgram quantities of protein utilizing the principle of protein-dye binding. Analytical Biochemistry. 72. doi: 10.1006/abio.1976.9999.

**Brechenmacher L, Lee J, Sachdev S, Song Z, Nguyen TH, Joshi T, Oehrle N, Libault M, Mooney B, Xu D, Cooper B and Stacey G** (2009). Establishment of a protein reference map for soybean root hair cells. Plant physiology, 149(2), 670–682. https://doi.org/10.1104/pp.108.131649.

**Buchel AS, Brederode FT, Bol JF and Huub JM** (1999). Mutation of GT-1 binding sites in the Pr-1A promoter influences the level of inducible gene expression in vivo. Plant Molecular Biology 40, 387–396 (1999). DOI: https://doi.org/10.1023/A:1006144505121.

**Cai Q, Guo L, Shen ZR, Wang DY, Zhang Q and Sodmergen** (2015). Elevation of pollen mitochondrial DNA copy number by WHIRLY2: altered respiration and pollen tube growth in Arabidopsis. Plant Physiology, Vol. 169: 660–673. doi: 10.1104/pp.15.00437.

**Cappadocia L, Maréchal A, Parent JS, Lepage E, Sygusch J and Brisson N** (2010). Crystal Structures of DNA-Whirly Complexes and Their Role in Arabidopsis Organelle Genome Repair. The Plant Cell, Vol. 22: 1849-1867. doi: 10.1105/tpc.109.071399.

**Cappadocia L, Parent JS, Sygusch J and Brisson N** (2013). A family portrait: structural comparison of the Whirly proteins from *Arabidopsis thaliana* and *Solanum tuberosum*. Structural Biology and Crystallization Communications, ISSN 1744-3091. doi: 10.1107/S1744309113028698.

**Chen L and Liu YG** (2014). Male Sterility and Fertility Restoration in Crops. Annual Review of Plant Biology. Vol. 65:579-606. https://doi.org/10.1146/annurev-arplant-050213-040119.

**Cheng N, Lo YS, Ansari MI, Ho KC, Jeng ST, Lin NS and Dai H** (2017). Correlation between mtDNA complexity and mtDNA replication mode in developing cotyledon mitochondria during mung bean seed germination. New Phytologist, 213(2), 751–763. https://doi.org/10.1111/nph.14158.

**Che-Othman MH, Millar AH and Taylor NL** (2017). Connecting salt stress signalling pathways with salinity-induced changes in mitochondrial metabolic processes in C3 plants. Plant Cell Environ. 40: 2875– 2905. https://doi.org/10.1111/pce.13034.

**Chi W, Ma J and Zhang L** (2012). Regulatory factors for the assembly of thylakoid membrane protein complexes. Philosophical Transactions of the Royal Society B. 367:3420–3429. doi: 10.1098/rstb.2012.0065.

**Chustecki JM, Gibbs DJ, Bassel GW and Johnston IG** (2021). Network analysis of *Arabidopsis* mitochondrial dynamics reveals a resolved trade-off between physical distribution and social connectivity. Cell Systems, Volume 12, Issue 5, Pages 419-431.e4, ISSN 2405-4712, https://doi.org/10.1016/j.cels.2021.04.006.

**Crawford T, Lehotai N and Strand A** (2017). The role of retrograde signals during plant stress responses. Journal of Experimental Botany. doi:10.1093/jxb/erx481.

**Crawford T, Lehotai N and Strand A** (2018). The role of retrograde signals during plant stress responses. Journal of Experimental Botany, Volume 69, Issue 11, Pages 2783–2795. https://doi.org/10.1093/jxb/erx481.

**Cupp JD and Nielsen BL** (2014). Minireview: DNA replication in plant mitochondria. Mitochondrion 19: 231–237. doi: 10.1016/j.mito.2014.03.008.

**De Col V, Fuchs P, Nietzel T, Elsässer M, Voon CP, Candeo A, Seeliger I, Fricker MD, Grefen C, Møller IM, Bassi A, Lim BL, Zancani M, Meyer AJ, Costa A, Wagner S and Schwarzländer M** (2017). ATP sensing in living plant cells reveals tissue gradients and stress dynamics of energy physiology. eLife. https://doi.org/10.7554/eLife.26770.

**De Pinto MC, Francis D and De Gara L** (1999). The redox state of the ascorbate-dehydroascorbate pair as a specific sensor of cell division in tobacco BY-2 cells. Protoplasma 209. doi: 10.1007/BF01415704.

**De Pinto MC, Tommasi F and De Gara L** (2000). Enzymes of the ascorbate biosynthesis and ascorbate glutathione cycle in cultured cells of *tobacco* Bright Yellow 2. Plant Physiology and Biochemistry. 38. DOI:10.1016/S0981-9428(00)00773-7.

**Derevyanchuk M, Litvinovskaya R, Khripach V, Martinec J and Kravets V** (2015). Effect of 24-epibrassinolide on *Arabidopsis thaliana* alternative respiratory pathway under salt stress. Acta Physiologiae Plantarum. 37:215. DOI 10.1007/s11738-015-1967-8.

**De Souza A, Wang JZ and Dehesh K** (2017). Retrograde Signals: Integrators of Intraorganellar Communication and Orchestrators of Plant Development. The Annual Review of Plant Biology. 28;68:85-108. DOI:10.1146/annurev-arplant-042916-041007.

**Desveaux D, Allard J, Brisson N abd Jurgen S** (2002). A new family of plant transcription factors displays a novel ssDNA-binding surface. Nature Structural & Molecular Biology 9, 512–517. https:// doi.org/10.1038/nsb814.

**Desveaux D, Subramaniam R, Després C, Mess JN, Lévesque C, Fobert PR, Dangl JL and Brisson N** (2004). A "Whirly" Transcription Factor Is Required for Salicylic Acid-Dependent Disease Resistance in *Arabidopsis*. Developmental Cell, Vol. 6, 229–240. DOI:https://doi.org/10.1016/S1534-5807(04)00028-0.

**Desveaux D, Maréchal A and Brisson N** (2005). Whirly transcription factors: defence gene regulation and beyond. TRENDS in Plant Science, Vol. 10 No.2. DOI: 10.1016/j.tplants.2004.12.008.

**Do H, Kim IS, Jeon BW, Lee CW, Park AK, Wi AR, Shin SC, Park H, Kim YS, Yoon HS, Kim AW and Lee JH** (2016). Structural understanding of the recycling of oxidized ascorbate by dehydroascorbate reductase (OsDHAR) from *Oryza sativa L. japonica*. Sci Rep. https://doi.org/10.1038/srep19498.

**Dodd AN, Kudla J and Sanders D** (2010). The language of calcium signaling. The Annual Review of Plant Biology. 61, 593–620. doi: 10.1146/annurev-arplant-070109-104628.

**Doimo M, Pfeiffer A, Wanrooij PH and Wanrooij S** (2020). Chapter 1 - mtDNA replication, maintenance, and nucleoid organization. The Human Mitochondrial Genome, Academic Press, Pages 3-33, ISBN 9780128196564, https://doi.org/10.1016/B978-0-12-819656-4.00001-2.

**Eady C, Lindsey K and Twell D** (1995). The significance of microspore division and division symmetry for vegetative cell-specific transcription and generative cell differentiation. Plant Cell 7:65–74. https://doi.org/10.1105/tpc.7. 1.65.

**Eckl EM, Ziegemann O, Krumwiede L, Fessler E and Jae LT** (2021). Sensing, signaling and surviving mitochondrial stress. Cellular and Molecular Life Sciences. 78, 5925–5951. https://doi.org/10.1007/s00018-021-03887-7.

**Fauron C, Casper M, Gao Y and Moore B** (1995). The maize mitochondrial genome: dynamic, yet functional. Trends in Genetics, Volume 11, Issue 6, Pages 228-235, ISSN 0168-9525, https://doi.org/10.1016/S0168-9525(00)89056-3.

**Fernando VCD and Schroeder DF** (2016). Role of ABA in *Arabidopsis* Salt, Drought, and Desiccation Tolerance. Intech, open science. DOI: 10.5772/61957.

**Finkelstein RR, Wang ML, Lynch TJ, Rao S, Howard M and Goodman HM** (1998). The *Arabidopsis* Abscisic Acid Response Locus ABI4 Encodes an APETALA2 Domain Protein. The Plant Cell, Volume 10, Issue 6, Pages 1043–1054. https://doi.org/10.1105/tpc.10.6.1043.

**Frey T and Mannella CA** (2000). The internal structure of mitochondria. Trends in Biochemical Sciences 25(7):319-24. DOI:10.1016/S0968-0004(00)01609-1.

**Foyer CH, Karpinska B and Krupinska K** (2014). The functions of WHIRLY1 and REDOX-RESPONSIVE TRANSCRIPTION FACTOR 1 in cross tolerance responses in plants: a hypothesis. Biological sciences. doi: 10.1098/rstb.2013.0226.

**Fuchs P, Rugen N, Carrie C, Elsasser M, Finkemeier I, Giese J, Hildebrandt TM, Kuhn K, Maurino VG, Ruberti C, Schallenberg-Rudinger M, Steinbeck J, Braun H, Eubel H, Meyer EH, Muller-Schussele SJ and Schwarzländer M** (2020). Single organelle function and organization as estimated from *Arabidopsis* mitochondrial proteomics. The Plant Journal 101, 420–441. doi: 10.1111/tpj.14534.

**García-Medel PL, Baruch-Torres N, Peralta-Castro A, Trasviña-Arenas CH, Torres-Larios A and Brieba LG** (2019). Plant organellar DNA polymerases repair double-stranded breaks by microhomology-mediated end-joining. Nucleic acids research, 47(6), 3028–3044. https://doi.org/10.1093/nar/gkz039.

**Gao C, Xing D, Li L and Zhang L** (2008). Implication of reactive oxygen species and mitochondrial dysfunction in the early stages of plant programmed cell death induced by ultraviolet-C overexposure. Planta 227:755–767. doi: 10.3389/fpls.2015.00783.

**Giraud E, Van Aken O, Ho LH and Whelan J** (2009). The transcription factor ABI4 is a regulator of mitochondrial retrograde expression of ALTERNATIVE OXIDASE1a. Plant physiology, 150(3), 1286-1296. https://doi.org/10.1104/pp.109.139782.

**Golin S, Negroni YL, Bennewitz B, Klösgen RB, Mulisch M, La Rocca N, Cantele F, Vigani G, Lo Schiavo F, Krupinska K and Zottini M** (2020). WHIRLY2 plays a key role in mitochondria morphology, dynamics, and functionality in *Arabidopsis thaliana*. Plant Direct. https://doi.org/10.1002/pld3.229.

**Greenway H and Munns R** (1980). Mechanisms of salt tolerance in non halophytes. Annual Review of Plant Biology, pp. 149-190. https://doi.org/10.1146/annurev.pp.31.060180.001053.

**Gualberto JM, Mileshina D, Wallet C, Niazi AK, Weber-Lotfi F and Dietrich A** (2014). The plant mitochondrial genome: Dynamics and maintenance. Biochimie, Vol. 100, pp. 107–120. https://doi.org/10.1016/j.biochi.2013.09.016.

**Gualberto JM and Kühn K** (2014). DNA-binding proteins in plant mitochondria: Implications for transcription. Mitochondrion, 19, 323–328. https://doi.org/10.1016/j.

**Harrison SJ, Mott EK, Parsley K, Aspinall S, Gray JC and Cottage A** (2006). A rapid and robust method of identifying transformed *Arabidopsis thaliana* seedlings following floral dip transformation. Plant Methods 2, 19. https://doi.org/10.1186/1746-4811-2-19.

**Hasegawa PM** (2013). Sodium ($Na^+$) homeostasis and salt tolerance of plants. Environmental and Experimental Botany, 92, 19–31. DOI: 10.1016/j.envexpbot.2013.03.001.

**Ho LHM, Giraud E, Uggalla V, Lister R, Glen A, Thirkettle-Watts D, Van Aken O and Whelan J** (2008). Identification of regulatory pathways controlling gene expression of stress responsive mitochondrial components in *Arabidopsis*. Plant Physiology, 147: 1858–1873. doi: 10.1104/pp.108.121384.

**Hoppins S** (2014). The regulation of mitochondrial dynamics. Current Opinion in Cell Biology. Volume 29, Pages 46-52. https://doi.org/10.1016/j.ceb.2014.03.005.

**Howell KA, Millar AH and Whelan J** (2006). Ordered assembly of mitochondria during rice germination begins with pro-mitochondrial structures rich in components of the protein import apparatus. Plant Molecular Biology. 60(2):201-23. doi: 10.1007/s11103-005-3688-7.

**Huang C, Yu J, Cai Q, Chen Y, Li Y, Ren Y and Miao Y** (2020)., Triple-localized WHIRLY2 Influences Leaf Senescence and Silique Development via Carbon Allocation. Plant Physiology, Volume 184, Issue 3, Pages 1348–1362, https://doi.org/10.1104/pp.20.00832.

**Isemer R, Mulisch M, Schäfer A, Kirchner S, Koop HU and Krupinska K** (2012). Recombinant Whirly1 translocates from transplantomic chloroplasts to the nucleus. FEBS Letters 586, 85-88. https://doi.org/10.1016/j.febslet.2011.11.029.

**Isemer, R, Krause K, Grabe N, Kitahata N, Asami T and Krupinska K** (2012). Plastid located WHIRLY1 enhances the responsiveness of *Arabidopsis* seedlings toward abscisic acid. Frontiers in Plant Science, d https://doi.org/10.3389/fpls.2012.00283.

**Ismail A, Takeda S and Nick P** (2014). Life and death under salt stress: Same players, different timing. Journal of Experimental Botany. 65, 2963–2979. https://doi.org/10.1093/jxb/eru159.

**Jaipargas EA, Barton KA, Mathur N and Mathur J** (2015). Mitochondrial pleomorphy in plant cells is driven by contiguous ER dynamics. Frontiers in Plant Science, 6, 1–14. https://doi.org/10.3389/ fpls.2015.00783.

**Johnston IG** (2019). Tension and Resolution: Dynamic, Evolving Populations of Organelle Genomes within Plant Cells. Molecular Plant, Volume 12, Issue 6, Pages 764-783, ISSN 1674-2052, https://doi.org/10.1016/j.molp.2018.11.002.

**Jones DP** (1986). Intracellular diffusion gradients of O2 and ATP. American Journal of Physiology-Cell Physiology. 250, pp. C663-C675. doi: 10.1152/ajpcell.1986.250.5.C663.

**Kacprzak SM, Dahlqvist A and Van Aken O** (2020). The transcription factor ANAC017 is a key regulator of mitochondrial proteotoxic stress responses in plants. Philosophical Transactions of the Royal Society B. 22;375(1801):20190411. doi: 10.1098/rstb.2019.0411.

**Klepikova AV, Kasianov AS, Gerasimov ES, Logacheva MD and Penin AA** (2016). A high resolution map of the *Arabidopsis thaliana* developmental transcriptome based on RNA-seq profiling. The plant Journal. https://doi.org/10.1111/tpj.13312.

**Kornmann B** (2013). The molecular hug between the ER and the mitochondria. Current Opinion in Cell Biology. 25, 443–448. doi: 10.1016/j.ceb.2013.02.010.

**Krause K, Kilbienski I, Mulisch M, Rödiger A, Schäfer A and Krupinsk K** (2005). DNA-binding proteins of the Whirly family in *Arabidopsis thaliana* are targeted to the organelles. Fers Letters 579, 3707-3712. https://doi.org/10.1016/j.febslet.2005.05.059.

**Krebs M, Held K, Binder A, Hashimoto K, Den Herder G, Parniske M, Kudla J and Schumacher K** (2012). FRET-based genetically encoded sensors allow high-resolution live cell imaging of $Ca^{2+}$ dynamics. The plant journal. Volume 69, Issue1. https://doi.org/10.1111/j.1365-313X.2011.04780.x.

**Krupinska K, Oetke S, Desel C, Mulisch M, Schäfer A, Hollmann J, Kumlehn J and Hensel G** (2014). WHIRLY1 is a major organizer of chloroplast nucleoids. Frontiers in Plant Science. https://doi.org/10.3389/fpls.2014.00432.

**Kubo T and Newton KJ** (2008). Angiosperm mitochondrial genomes and mutations. Mitochondrion, pp. 5-14. Volume 8, Issue 1, Pages 5-14, ISSN 1567-7249, https://doi.org/10.1016/j.mito.2007.10.006.

**Kudla L, Becker D, Grill E, Hedrich R, Hippler M, Kummer U, Parniske M, Romeis T and Schumacher K** (2018). Advances and current challenges in calcium signalling. New Phytologist. 218, 414–431. https://doi.org/10.1111/nph.14966.

**Lackner LL** (2014). Shaping the dynamic mitochondrial network. BMC Biol. 12:35. doi: 10.1186/1741-7007-12-35.

**Lafon-Placette C and Kohler C** (2014). Embryo and endosperm, partners in seed development. Current Opinion in Cell Biology. 17:64–69. doi:10.1016/j.pbi.2013.11.008.

**Le BH, Cheng C, Bui AQ, Javier A, Wagmaister JA, Kelli F, Henry KF, Pelletier J, Kwong L, Belmonte M, Kirkbride R, Horvath S, Drews GN, Fischer RL, Okamuro JK, Harada JJ and Goldberg RB** (2010). Global analysis of gene activity during *Arabidopsis* seed development and identification of seed-specific transcription factors. PNAS 107:8063–8070. doi:10.1073/pnas.1003530107.

**Lee SR and Han J** (2017). Mitochondrial Nucleoid: Shield and Switch of the Mitochondrial Genome. Oxidative medicine and cellular longevity, 8060949. https://doi.org/10.1155/2017/8060949.

**Leister D** (2005). Genomics-based dissection of the cross-talk of chloroplasts with the nucleus and mitochondria in *Arabidopsis*. Gene 354: 110–116. https://doi.org/10.1016/j.gene.2005.03.039.

**Leister D (2012).** Retrograde signalling in plants: from simple to complex scenarios. Frontiers in Plant Science. 19;3:135. https://doi.org/10.3389/fpls.2012.00135.

**Liberatore KL, Dukowic-Schulze S, Miller ME, Chen C and Kianian SF** (2016). The role of mitochondria in plant development and stress tolerance. Free Radical Biology and Medicine, Volume 100, Pages 238-256, ISSN 0891-5849. https://doi.org/10.1016/j.freeradbiomed.2016.03.033.

**Livak KJ and Schmittgen TD** (2001). Analysis of relative gene expression data using real-time quantitative PCR and the 2(-Delta Delta C(T)). Methods 25, 402-408. DOI: 10.1006/meth.2001.1262.

**Logan DC** (2006). The mitochondrial compartment. Journal of Experimental Botany, 57(6), 1225–1243. https://doi.org/10.1093/jxb/erj151.

**Logan DC** (2010). Mitochondrial fusion, division and positioning in plants. Biochemical Society Transactions. 38, pp. 789-795. https://doi.org/10.1042/BST0380789.

**Loro G, Drago I, Pozzan T, Schiavo FL, Zottini M and Costa A** (2012). Targeting of Cameleons to various subcellular compartments reveals a strict cytoplasmic/mitochondrial $Ca^{2+}$ handling relationship in plant cells. The Plant Journal, 71: 1-13. https://doi.org/10.1111/j.1365-313X.2012.04968.x

**Loro G, Wagner S, Doccula FG, Behera S, Weinl S, Kudla J, Schwarzländer M, Costa A and Zottini M** (2016). Chloroplast-Specific in Vivo $Ca^{2+}$ Imaging Using Yellow Cameleon Fluorescent Protein Sensors Reveals Organelle-Autonomous $Ca^{2+}$ Signatures in the Stroma. Plant Physiology, Volume 171, Issue 4, Pages 2317–2330, https://doi.org/10.1104/pp.16.00652.

**Manishankar P, Wang N, Köster P, Alatar A and Kudla J** (2018). Calcium signalling during salt stress and in the regulation of ion homeostasis. Journal of Experimental Botany. 69, 4215–4226. https://doi.org/10.1016/j.abb.2008.01.010.

**Maréchal A, Parent JS, Sabar M, Véronneau-Lafortune F, Abou-Rached C and Brisson N** (2008). Overexpression of DNA-associated *AtWhy2* compromises mitochondrial function. BMC Plant Biology, 8:42. https://doi.org/10.1186/1471-2229-8-42.

**Maréchal A and Brisson N** (2010). Recombination and the maintenance of plant organelle genome stability. New Phytologist, 186: 299–317. https://doi.org/10.1111/j.1469-8137.2010.03195.x.

**Matusikova I, Nap JP and Mlynárová L** (1999). Isolation of High Quality DNA and RNA from Leaves of the Carnivorous Plant *Drosera rotundifolia*. Plant Molecular Biology Reporter. 17. 269-277. DOI: 10.1023/A:1007627509824.

**Mhadhbi H, Fotopoulos V, Mylona PV, Jebara M, Aouani ME and Polidoros AN** (2013). Alternative oxidase 1 (*Aox1*) gene expression in roots of *Medicago truncatula* is a genotype-specific component of salt stress tolerance. Journal of Plant Physiology, Volume 170, Issue 1, Pages 111-114,ISSN 0176-1617. https://doi.org/10.1016/j.jplph.2012.08.017.

**Mittler R** (2017). ROS Are Good. Trends Plant Sci. 22, 11–19. https://doi.org/10.1016/j.tplants.2016.08.002.

**Mogensen HL and Rusche ML** (1985). Quantitative ultrastructural analysis of barley sperm. Protoplasma 128:1–13. https://doi.org/10.1007/BF01273229.

**Morley SA and Nielsen BL** (2016). Chloroplast DNA Copy Number Changes during Plant Development in Organelle DNA Polymerase Mutants. Frontiers in Plant Science. Volume 7, pages 57. DOI=10.3389/fpls.2016.00057.

**Mueller SJ and Reski R** (2015). Mitochondrial Dynamics and the ER: The Plant Perspective. Frontiers in Cell and Developmental Biology. DOI=10.3389/fcell.2015.00078.

**Munns R and Tester M** (2008). Mechanisms of salinity tolerance. Annual Review of Plant Biology. 59:651–681. DOI: 10.1146/annurev.arplant.59.032607.092911.

**Mur LA, Kenton P, Lloyd AJ, Ougham H and Prats E** (2008). The hypersensitive response; the centenary is upon us but how much do we know?. Journal of Experimental Botany. 59: 501–520. DOI: 10.1093/jxb/erm239

**Murashige T and Skoog F** (1962). A revised medium for rapid growth and bioassays with tobacco tissue cultures. Physiologia Plantarum 15: 473–497. https://doi.org/10.1111/j.1399-3054.1962.tb08052.x.

**Ng S, De Clercq I, Van Aken O, Law SR, Ivanova A, Willems P, Giraud E, Van Breusegem F and Whelan J** (2014). Anterograde and retrograde regulation of nuclear genes encoding mitochondrial proteins during growth, development, and stress. Molecular Plant: Cell Press. 7, 1075–1093. doi:10.1093/mp/ssu037.

**Ng S, Ivanova A, Duncan O, Law SR, Van Aken O, De Clercq I, Wang Y, Carrie C, Xu L, Kmiec B, Walker H, Van Breusegem F, Whelan J and Giraud E** (2013). A membrane bound NAC transcription factor, ANAC017, mediates mitochondrial retrograde signalling in *Arabidopsis*. Plant Cell. 25(9):3450-71. doi: 10.1105/tpc.113.113985.

**Oldenburg DJ and Bendich AJ** (1996). Size and structure of replicating mitochondrial DNA in cultured tobacco cells. Plant Cell. 8: 447–461. doi: 10.1105/tpc.8.3.447.

**Oldenburg DJ and Bendich AJ** (2001). Mitochondrial DNA from the liverwort *Marchantia polymorpha*: circularly permuted linear molecules, head-to-tail concatemers, and a 50 protein. Journal of Molecular Biology 310:549–562. doi: 10.1006/jmbi.2001.4783.

**Pan R, Jones AD and Hu J** (2014). Cardiolipin-Mediated Mitochondrial Dynamics and Stress Response in *Arabidopsis.* The Plant Cell, Volume 26, Issue 1, Pages 391–409, https://doi.org/10.1105/tpc.113.121095.

**Paradiso A, Berardino R, de Pinto MC, Sanita di Toppi L, Storelli MM, Tommasi F and De Gara L** (2008). Increase in ascorbate-glutathione metabolism as local and precocious systemic responses induced by cadmium in durum wheat plants. Plant and Cell Physiology. 49. doi: 10.1093/pcp/pcn013.

**Paradiso A, Domingo G, Blanco E, Buscaglia A, Fortunato S, Marsoni M, Scarcia P, Caretto S, Vannini C and De Pinto MC** (2020). Cyclic AMP mediates heat stress response by the control of redox homeostasis and ubiquitin-proteasome system. Plant, Cell & Environment. 43. doi: 10.1111/pce.13878.

**Paszkiewicz G, Gualberto JM, Benamar A, Macherel D and Logan DC** (2017). *Arabidopsis* seed mitochondria are bioenergetically active immediately upon imbibition and specialize via biogenesis in preparation for autotrophic growth. Plant Cell. Volume 29, Issue 1, Pages 109–128, https://doi.org/10.1105/tpc.16.00700.

**Pesaresi P, Masiero S, Eubel H, Braun HP, Bhushan S, Glaser E, Salamini F and Leister D** (2006). Nuclear Photosynthetic Gene Expression Is Synergistically Modulated by Rates of Protein Synthesis in Chloroplasts and Mitochondria. Plant Cell, Vol. 18, 970–991. doi: 10.1105/tpc.105.039073.

**Pesaresi P, Schneider A, Kleine T and Leister D** (2007). Interorganellar comunication. CURRENT OPINION IN PLANT BIOLOGY, vol. 10, p. 600-606, ISSN: 1369-5266, doi:10.1016/j.pbi.2007.07.007.

**Pirayesh N, Giridhar M, Ben Khedher A, Vothknecht UC and Chigri F** (2021). Organellar calcium signalling in plants: An update. Biochimica et Biophysica Acta (BBA). Molecular Cell Research, Volume 1868, Issue 4, ISSN 0167-4889. https://doi.org/10.1016/j.bbamcr.2021.118948.

**Polidoros AN, Mylona PV, Pasentsis K, Scandalios JG and Tsaftaris A (**2005). The maize alternative oxidase 1a (Aox1a) gene is regulated by signals related to oxidative stress. Red Rep, 10 (2005), pp. 71-78. DOI: 10.1179/135100005X21688.

**Polidoros AN, Mylona PV and Arnholdt-Schmitt B** (2009). Aox gene structure, transcript variation and expression in plants. Physiologia Plantarum. 137, pp. 342-353. https://doi.org/10.1111/j.1399-3054.2009.01284.x.

**Preuten T, Cincu E, Fuchs J, Zoschke R, Liere K and Borner T** (2010). Fewer genes than organelles: extremely low and variable gene copy numbers in mitochondria of somatic plant cells. The Plant Journal. 64 948e959. doi: 10.1111/j.1365-313X.2010.04389.x.

**Prevost CT, Peris N, Seger C, Pedeville DR, Wershing K, Sia EA and Sia RAL** (2018). The influence of mitochondrial dynamics on mitochondrial genome stability. Current Genetics 64, 199–214. https://doi.org/10.1007/s00294-017-0717-4.

**Qiu QS, Barkla BJ, Vera-Estrella R, Zhu JK and Schumaker KS** (2003). $Na^+/H^+$ exchange activity in the plasma membrane of *Arabidopsis*. Plant Physiology. 132, 1041–1052. doi: 10.1104/pp.102.010421.

**Qiu QS, Guo Y, Quintero FJ, Pardo JM, Schumaker KS and Zhu JK** (2004). Regulation of vacuolar $Na^+/H^+$ exchange in *Arabidopsis thaliana* by the salt-overly-sensitive (SOS) pathway. Journal of Biological Chemistry, 279, 207–215. DOI: 10.1074/jbc.M307982200.

**Ramonell KM, Kuang A, Porterfield DM, Crispi ML, Xiao Y, McClure G and Musgrave ME** (2001). Influence of atmospheric oxygen on leaf structure and starch deposition in *Arabidopsis thaliana*. Plant, Cell & Environment. 24:419–428. doi: 10.1046/j.1365-3040.2001.00691.x.

**Ray JR** (2021). Contribution of Massive Mitochondrial Fusion and Subsequent Fission in the Plant Life Cycle to the Integrity of the Mitochondrion and Its Genome. International Journal of Molecular Sciences 22, no. 11: 5429. https://doi.org/10.3390/ijms22115429.

**Rhoades JD and Loveday J** (1990). Salinity in irrigated agriculture. From the journal Agronomy (USA). ISSN : 0065-4663. pp. 1089-1142.

**Rieu I, Ruiz-Rivero O, Fernandez-Garcia N, Griffiths J, Powers SJ, Gong F, Linhartova T, Eriksson S, Nilsson O, Thomas SG, Phillips AL and Hedden P** (2007). The gibberellin biosynthetic genes AtGA20ox1 and AtGA20ox2 act, partially redundantly, to promote growth and development throughout the *Arabidopsis* life cycle. The Plant Journal. 53:488-504. https://doi.org/10.1111/j.1365-313X.2007.03356.x.

**Rose RJ and McCurdy DW** (2017). New beginnings: Mitochondrial re- newal by massive mitochondrial fusion. Trends in Plant Science, 22(8), 641–643. https://doi.org/10.1016/j.tplan ts.2017.06.005.

**Roy SJ, Negrão S and Tester M** (2014). Salt resistant crop plants. Current Opinion in Biotechnology, 26, 115–124. https://doi.org/10.1016/j.copbio.2013.12.004.

**Sachdev S, Ansari SA, Ansari MI, Fujita M and Hasanuzzaman M** (2021). Abiotic Stress and Reactive Oxygen Species: Generation, Signaling, and Defense Mechanisms. Antioxidants, 10(2), 277. https://doi.org/10.3390/antiox10020277.

**Saha B, Borovskii G and Panda SK** (2016). Alternative oxidase and plant stress tolerance. Plant Signaling & Behavior. 11(12). doi: 10.1080/15592324.2016.1256530.

**Scholz D and Westermann B** (2013). Mitochondrial fusion in *Chlamydomonas reinhardtii* zygotes. European Journal of Cell Biology. 92 (2013), pp. 80-86. DOI: 10.1016/j.ejcb.2012.10.004.

**Scott I, Tobin AK and Logan DC** (2006). *BIGYIN*, an orthologue of human and yeast *FIS1* genes functions in the control of mitochondrial size and number in *Arabidopsis thaliana*. Journal of Experimental Botany, Volume 57, Issue 6, Pages 1275–1280, https://doi.org/10.1093/jxb/erj096.

**Seguı´-Simarro JM, Coronado MJ and Staehelin LA** (2008). The mitochondrial cycle of *Arabidopsis* shoot apical meristem and leaf primordium meristematic cells is defined by a perinuclear tentaculate/cage-like mitochondrion. Plant Physiology. 148:1380–1393. doi: 10.1104/pp.108.126953.

**Smirnoff N and Arnaud D** (2018). Hydrogen peroxide metabolism and functions in plants. New Phytologist. https://doi.org/10.1111/nph.15488.

**Steiner P, Luckner M, Kerschbaum H, Wanner G and Lütz-Meindl U** (2018). Ionic stress induces fusion of mitochondria to 3-D networks: An electron tomography study. Journal of Structural Biology, Volume 204, Issue 1, Pages 52-63, ISSN 1047-8477, https://doi.org/10.1016/j.jsb.2018.06.010.

**Suetsugu N, Higa T, Gotoh E and Wada M** (2016). Light-Induced Movements of Chloroplasts and Nuclei Are Regulated in Both Cp-Actin-Filament-Dependent and -Independent Manners in *Arabidopsis thaliana*. PloS one, 11(6), e0157429. https://doi.org/10.1371/journal.pone.0157429.

**Supriya R and Priyadarshan PM** (2019). Chapter One - Genomic technologies for Hevea breeding. Advances in Genetics, Academic Press, Volume 104, Pages 1-73, ISSN 0065-2660, ISBN 9780128171615, https://doi.org/10.1016/bs.adgen.2019.04.001.

**Taanman JW** (1999). The mitochondrial genome: structure, transcription, translation and replication. ScienceDirect. Volume 1410, Issue 2, Pages 103-123. https://doi.org/10.1016/S0005-2728(98)00161-3.

**Terzaghi WB and Cashmore AR** (1995). Light-Regulated Transcription. Annual Review of Plant Physiology and Plant Molecular Biology. P 445-474, V 46. DOI: 10.1146/annurev.pp.46.060195.002305.

**Unseld M, Marienfeld JR, Brandt P and Brennicke A** (1997). The mitochondrial genome of *Arabidopsis thaliana* contains 57 genes in 366,924 nucleotides. Nature Genetics. 15 57e61. doi: 10.1038/ng0197-57.

**Urao T, Yamaguchi-Shinozaki K, Urao S and Shinozaki K** (1993). An *Arabidopsis* myb homolog is induced by dehydration stress and its gene product binds to the conserved MYB recognition sequence. The Plant Cell, Volume 5, Issue 11, Pages 1529–1539, DOI: https://doi.org/10.1105/tpc.5.11.1529.

**Van Aken O, Zhang B, Carrie C, Uggalla V, Paynter E, Giraud E and Whelan J** (2009). Defining the Mitochondrial Stress Response in *Arabidopsis thaliana*. Molecular Plant, Volume 2, Number 6, Pages 1310–1324. https://doi.org/10.1093/mp/ssp053.

**Van Aken O, Ford E, Lister R, Huang S and Millar** AH (2016). Retrograde signalling caused by heritable mitochondrial dysfunction is partially mediated by ANAC017 and improves plant performance. The Plant Journal. 2016 Nov; 88(4):542-558. doi: 10.1111/tpj.13276.

**Van Aken O** (2021). Mitochondrial redox systems as central hubs in plant metabolism and signaling. Plant Physiology, Volume 186, Issue 1, Pages 36–52. https://doi.org/10.1093/plphys/kiab101

**Vanderauwera S, Vandenbroucke K, Inzé A, van de Cotte B, Mühlenbocka P, De Rycke R, Naouara N, Van Gaevera T, Van Montagua MCE and Van Breusegema F** (2012). AtWRKY15 perturbation abolishes the mitochondrial stress response that steers osmotic stress tolerance in *Arabidopsis*. PNAS, 109 (49) 20113-20118. https://doi.org/10.1073/pnas.1217516109.

**Vigani G, Faoro F, Ferretti AM, Cantele F, Maffi D, Marelli M, Maver M, Murgia I and Zocchi G** (2015). Three-dimensional reconstruction, by TEM tomography, of the ultrastructural modifications occurring in *Cucumis sativus L.* mitochondria under fe deficiency. PLoS ONE, 10(6), 1–13. https:// doi.org/10.1371/journal.pone.0129141.

**Wang DY, Zhang Q, Liu Y, Lin ZF, Zhang SX, Sun MX and Sodmergen** (2010). The Levels of Male Gametic Mitochondrial DNA Are Highly Regulated in Angiosperms with Regard to Mitochondrial Inheritance. The Plant Cell, Volume 22, Issue 7, Pages 2402–2416, https://doi.org/10.1105/tpc.109.071902.

**Wang Y, Berkowitz O, Selinski J, Xu Y, Hartmann A and Whelan J** (2018). Stress responsive mitochondrial proteins in *Arabidopsis thaliana*. Free Radical Biology and Medicine, Volume 122, Pages 28-39, ISSN 0891-5849. https://doi.org/10.1016/j.freeradbiomed.2018.03.031.

**Wang Y, Selinski J, Mao C, Zhu Y, Berkowitz O and Whelan J** (2020). Linking mitochondrial and chloroplast retrograde signalling in plants. Philosophical Transactions of the Royal Society B. 375: 20190410. http://dx.doi.org/10.1098/rstb.2019.0410.

**Wei SS, Niu WT, Zhai XT, Liang WQ, Xu M, Fan X, Lv TT, Xu WY, Bai JT, Jia N and Li B** (2019). *Arabidopsis* mtHSC70-1 plays important roles in the establishment of COX-dependent respiration and redox homeostasis, Journal of Experimental Botany, Volume 70, Issue 20, Pages 5575–5590, https://doi.org/10.1093/jxb/erz357.

**Winter D, Vinegar B, Nahal H, Ammar R, Wilson GV and Provart NJ** (2007). An "Electronic Fluorescent Pictograph" browser for exploring and analyzing large-scale biological data sets. PLoS One. 8;2(8). doi: 10.1371/journal.pone.0000718.

**Woloszynska M and Trojanowski D** (2009). Counting mtDNA molecules in *Phaseolus vulgaris*: sublimons are constantly produced by recombination via short repeats and undergo rigorous selection during substoichiometric shifting. Plant Molecular Biology. 70, 511-521, doi:10.1007/s11103-009-9488-8.

**Woodson JD and Chory J** (2008). Coordination of gene expression between organellar and nuclear genomes. Nature Reviews Genetics. 9(5):383-95. Doi: 10.1038/nrg2348. PMID: 18368053; PMCID: PMC4854206.

**Wu Z, Oeck S, West AP, Mangalhara KC, Sainz AC, Newman LE, Zhang X, Wu L, Yan Q, Bosenberg M, Liu Y, Sulkowski PL, Tripple V, Kaech SM, Glazer PM and Shadel GS** (2019). Mitochondrial DNA stress signalling protects the nuclear genome. Nature Metabolism. https://doi.org/10.1038/s42255-019-0150-8.

**Wu Z, Waneka G, Broz AK, King CR, Sloan DB** (2020). MSH1 is required for maintenance of the low mutation rates in plant mitochondrial and plastid genomes. Proceedings of the National Academy of Sciences. 117 (28) 16448-16455. DOI: 10.1073/pnas.2001998117.

**Xiang D, Venglat P, Tibiche C, Yang H, Risseeuw E, Cao Y, Babic V, Cloutier M, Keller W, Wang E, Selvaraj G and Datla R** (2011). Genome-wide analysis reveals gene expression and metabolic network dynamics during embryo development in *Arabidopsis*. Plant physiology, 156(1), 346–356. https://doi.org/10.1104/pp.110.171702.

**Xu YZ, Arrieta-Montiel MP, Virdi KS, de Paula WBM, Widhalm JR, Basset GJ and Mackenzie SA** (2011). MutS HOMOLOG1 Is a nucleoid protein that alters mitochondrial and plastid properties and plant response to high light. The Plant Cell, 23(9), 3428–3441. https://doi.org/10.1105/tpc.111.089136.

**Yamaguchi-Shinozaki K and Shinozaki K** (1994). A novel cis-acting element in an *Arabidopsis* gene is involved in responsiveness to drought, low-temperature, or high-salt stress. The Plant Cell, Volume 6, Issue 2, Pages 251–264, https://doi.org/10.1105/tpc.6.2.251.

**Yan C, Duanmu X, Zeng L, Liu B and Song Z** (2019). Mitochondrial DNA: Distribution. Mutations, and Elimination. 1, 1–15. https://doi. Org/10.3390/cells 8040379.

**Yu SB and Pekkurnaz G** (2018). Mechanisms orchestrating mitochon- drial dynamics for energy homeostasis. Journal of Molecular Biology, 430(21), 3922–3941. https://doi.org/10.1016/j.jmb.2018.07.027.

**Zhai XT, Wei SS, Liang WQ, Bai JT, Jia N and Li B** (2020). *Arabidopsis* mtHSC70-1 physically interacts with the Cox2 subunit of cytochrome c oxidase. Plant Signaling & Behavior. doi: 10.1080/15592324.2020.1714189.W

**Zhao SY, Wang GD, Zhao WY, Zhang S, Kong FY, Dong XC and Meng QW** (2018). Overexpression of tomato WHIRLY protein enhances tolerance to drought stress and resistance to *Pseudomonas solanacearum* in transgenic tobacco. Biologia Plantarum. 62, 55–68. https://doi.org/10.1007/s10535-017-0714-y.

**Zhu W, Miao Q, Sun D, Yang G, Wu C, Huang J and Zheng C** (2012). The Mitochondrial Phosphate Transporters Modulate Plant Responses to Salt Stress via Affecting ATP and Gibberellin Metabolism in *Arabidopsis thaliana*. PLOS ONE 7(8): e43530. https://doi.org/10.1371/journal.pone.0043530.

**Zottini M, Barizza E, Bastianelli F, Carimi F and Lo Schiavo F** (2006). Growth and senescence of *Medicago truncatula* cultured cells are associated with characteristic mitochondrial morphology. New Phytologist, 172(2), 239–247. https://doi.org/10.1111/j.1469-8137.2006.01830.x.

Received: 10 February 2020 | Revised: 18 April 2020 | Accepted: 24 April 2020

DOI: 10.1002/pld3.229

ORIGINAL RESEARCH

# WHIRLY2 plays a key role in mitochondria morphology, dynamics, and functionality in *Arabidopsis thaliana*

Serena Golin[1] | Yuri L. Negroni[1] | Bationa Bennewitz[2] | Ralf B. Klösgen[2] | Maria Mulisch[3] | Nicoletta La Rocca[1] | Francesca Cantele[4] | Gianpiero Vigani[5] | Fiorella Lo Schiavo[1] | Karin Krupinska[3] | Michela Zottini[1]

[1]Department of Biology, University of Padova, Padova, Italy

[2]Institute of Biology-Plant Physiology, Martin Luther University Halle-Wittenberg, Halle (Saale), Germany

[3]Institute of Botany, Christian-Albrechts University of Kiel, Kiel, Germany

[4]Department of Chemistry, University of Milano, Milano, Italy

[5]Department of Life Science and Systems Biology, University of Turin, Turin, Italy

**Correspondence**
Michela Zottini, Department of Biology, University of Padova, Via U. Bassi 58B, 35131 Padova, Italy.
Email: michela.zottini@unipd.it

**Funding information**
Fondazione Cassa di Risparmio di Padova e Rovigo (Foundation Cariparo); Ministero dell'Istruzione, dell'Università e della Ricerca (MIUR)

## Abstract

WHIRLY2 is a single-stranded DNA binding protein associated with mitochondrial nucleoids. In the *why 2-1* mutant of *Arabidopsis thaliana*, a major proportion of leaf mitochondria has an aberrant structure characterized by disorganized nucleoids, reduced abundance of cristae, and a low matrix density despite the fact that the macroscopic phenotype during vegetative growth is not different from wild type. These features coincide with an impairment of the functionality and dynamics of mitochondria that have been characterized in detail in wild-type and *why 2-1* mutant cell cultures. In contrast to the development of the vegetative parts, seed germination is compromised in the *why 2-1* mutant. In line with that, the expression level of *why 2* in seeds of wild-type plants is higher than that of *why 3*, whereas in adult plant no difference is found. Intriguingly, in early stages of shoots development of the *why 2-1* mutant, although not in seeds, the expression level of *why 3* is enhanced. These results suggest that WHIRLY3 is a potential candidate to compensate for the lack of WHIRLY2 in the *why 2-1* mutant. Such compensation is possible only if the two proteins are localized in the same organelle. Indeed, *in organello* protein transport experiments using intact mitochondria and chloroplasts revealed that WHIRLY3 can be dually targeted into both, chloroplasts and mitochondria. Together, these data indicate that the alterations of mitochondria nucleoids are tightly linked to alterations of mitochondria morphology and functionality. This is even more evident in those phases of plant life when mitochondrial activity is particularly high, such as seed germination. Moreover, our results indicate that the differential expression of *why 2* and *why 3* predetermines the functional replacement of WHIRLY2 by WHIRLY3, which is restricted though to the vegetative parts of the plant.

KEYWORDS

*Arabidopsis thaliana*, mitochondria, nucleoid, seed germination

## 1 | INTRODUCTION

Mitochondria occupy a central place in the metabolic network of eukaryotic cells, with essential metabolic processes occurring within the organelle itself and several other pathways either emanating from or converging on mitochondria. Mitochondria can form dynamic, interconnected networks, regulated by a dynamic equilibrium between fusion and fission events that in turn determine their number, size, shape and functionality. A high motility of mitochondria is required to encounter different energy requirement of the cells in different developmental stages or environmental conditions (Zottini, Barizza, Bastianelli, Carimi, & Lo Schiavo, 2006). The regulation of mitochondrial shape dynamics plays a critical role in energy homeostasis as it responds rapidly and directly to acute metabolic perturbations contributing to energy demand and homeostasis (Yu & Pekkurnaz, 2018). Alterations of the dynamics and shape of mitochondria are also linked to genome instability (Xu et al., 2011). The balance between fission and fusion of mitochondria ensures the integrity of the organelle genome and the equal distribution of DNA among the mitochondria (Arimura, 2018). It has been observed that in the regions of the plant where a high cell division occurs, e.g., in germinating seeds and in shoot apical meristems, mitochondria have an elongated shape due to the dominance of the fusion over the fission process, coincident with an active mtDNA synthesis. Mitochondrial fusion provides indeed an opportunity for recombination of mtDNA fragments occurring during the replication of mtDNA (Arimura, 2018).

WHIRLY2 belongs to a small family of ssDNA binding proteins characteristic for higher plants (Desveaux, Allard, Brisson, & Sygusch, 2002). All WHIRLY proteins have in common the highly conserved WHIRLY domain including the KGKAAL motif implicated in binding to ssDNA (Desveaux, Maréchal, & Brisson, 2005). The crystal structure of the WHIRLY domain was determined by X-ray diffraction analysis (Cappadocia et al., 2010). Such analyses revealed that tetrameric WHIRLIES bind to ssDNA in a sequence unspecific manner. By atomic force microscopy, it has been shown that hexamers of WHIRLY2 tetramers assemble into 24-meric higher-order structures upon binding long DNA molecules, whereby the interactions between the tetramers depend on K67 within the KGKAAL motif (Cappadocia, Parent, Sygusch, & Brisson, 2013). The structure of WHYRLY domain is highly conserved among and different WHIRLY proteins and plants, as revealed by a 3D structure analysis (Akbudak & Filiz, 2019). WHIRLY2, together with other organellar ssDNA binding proteins, plays a key role in the maintenance of integrity of mitochondrial DNA that is an absolute requirement for cell growth and proliferation. Failure in maintaining the stability of the mitochondrial genome would result in the accumulation of mutations and genomic rearrangements that can become deleterious (Gualberto & Kühn, 2014).

While most plants possess two WHIRLY proteins, *Arabidopsis thaliana* and other members of the *Brassicaceae* family have three WHIRLY proteins, which show differential organelle targeting (Krause et al., 2005). WHIRLY1 was imported into chloroplasts, both in *in organello* experiments and after transient expression in protoplasts. WHIRLY2 was instead imported into mitochondria in the transient expression analysis but showed dual targeting into both isolated organelles, chloroplasts and mitochondria. WHIRLY3, on the other hand, was solely analyzed with transient expression assays and showed targeting of the GFP reporter to chloroplasts (Krause et al., 2005).

Arabidopsis plants, lacking either plastid or mitochondrial WHIRLY proteins, accumulate higher levels of microhomology-mediated DNA rearrangements (MHMRs) than wild-type (Cappadocia et al., 2010;Maréchal et al., 2008) indicating that WHIRLY proteins act as components of the organellar DNA repair machinery. It has been proposed that WHIRLY2 prevents the accumulation of abnormal mtDNA molecules by limiting the microhomology-mediated end-joining during double-stranded breaks in mtDNA repair process (García-Medel et al., 2019).

Under standard growth conditions, adult plants of the Arabidopsis *why 2-1* mutant do not show any obvious difference in the phenotype compared to the wild type (Maréchal et al., 2008). However, overexpression of *AtWHIRLY2* in Arabidopsis causes a reduction in mitochondrial transcripts and mitochondrial DNA, translating into lower activities of the respiratory chain complexes as well as earlier senescence (Maréchal et al., 2008). Since WHIRLIES are evidently associated with organellar DNA, tissues having low levels of mtDNA, such as mature pollen of Arabidopsis, lack expression of WHIRLY2 (Cai, Guo, Shen, Wang, & Zhang, 2015). On the other hand, overexpression of *WHIRLY2*, under control of a promoter that is specifically active in pollen vegetative cells, leads to slower growth of pollen tubes paralleled by an increase in mtDNA content of pollen and accumulation of reactive oxygen species (Cai et al., 2015).

Apart from its role in maintaining the integrity of mtDNA and organellar gene expression, information about the role of WHIRLY2 in the modulation of mitochondrial metabolism and morphology is still lacking.

Therefore, in this study, transgenic Arabidopsis plants as well as cultured cells defective in *AtWHIRLY2* expression (*why 2-1* mutant lines) were used to investigate at the cellular level, the impact of WHYRLY2 on the mitochondrial morphology, dynamics and function. Furthermore, we investigate whether the presence of aberrant mitochondria in the *why 2-1* mutant could have consequences for development of the plant. And, finally, we provide indications based on gene expression and immunological analyses together with organelle import assays that the lack of WHYRLY2 in mitochondria can be compensated by WHIRLY3 in a tissue-specific manner.

## 2 | MATERIAL AND METHODS

### 2.1 | Plant materials and growth conditions

All experiments were performed using the Arabidopsis (*A. thaliana*) ecotype Columbia (Col-0). The T-DNA insertion mutant line *why 2-1* (SALK_118900), obtained from the Nottingham

Arabidopsis Stock Centre (http://arabidopsis.org), corresponds to a line previously described as a true knockout mutant (Janicka et al., 2012). T-DNA insertion sites were determined by PCR (*primer WHY2 For 5′-GCATCCTCAAAACCAATGAC-3′*, *primer WHY2 Rev 5′-CATGATGTGTGGAAGAGCAA-3′*, and *primer T-DNA Rev 5′-ATTTTGCCGATTTCGGAAC-3′*) and subsequent sequencing.

The seeds were surface sterilized in 70% (v/v) EtOH and 0.05% Triton X-100, followed by pure EtOH. The seeds were sown onto square Petri dishes containing one-half MS medium (Murashige & Skoog, 1962) supplemented with 0.5 g/L MES-KOH, pH 5.8, 0.8% (w/v) Plant Agar (Duchefa), and 1% (w/v) Suc, stratified for 2 days at 4°C in the dark, and placed vertically in a growth chamber at 22°C with 16-hr day length and PAR of 150 µmol $m^{-2}$ $s^{-1}$. The experiments were conducted at different Arabidopsis growth stages, as defined by Boyes et al. (2001).

Some experiments were conducted with non-embryogenic cell suspension cultures of wild type (WT) and *why 2-1* lines. Suspension cell cultures were grown at 25°C under a long daylight period on a gyratory shaker in liquid MSR2 medium (MS medium supplemented with 2 mg/L glycine; 0.5 mg/L nicotinic acid; 0.1 mg/L thiamine hydrochloride; 0.5 mg/L pyridoxal hydrochloride; 100 mg/L myo-Inositol; 0.5 g/L malt extract; 3% (w/v) Suc; 1 mg/L 6-BAP; and 2 mg/L 2,4-D; pH 5.8). For subculturing, 2 ml of packed cells were transferred into 50 ml fresh medium every 7 days. To determine the growth capabilities of the two suspension cultures, cells were filtered and their dry weight was determined. For the dry weight, the cells were placed in a stove for 24 hr at 40°C. Experiments were performed at 5 days after subcultivation, when cells are in the exponential growth phase.

For the *in organello* protein transport experiments, pea seedlings (*Pisum sativum* var. Feltham First) were grown on soil for 7 days at a 16 hr photoperiod under constant temperature (18–22°C).

## 2.2 | Oxygen consumption measurements

Oxygen consumption was measured using a Clark-type oxygen electrode (Hansatech Instrument, United Kingdom). Respiration of Arabidopsis cell suspension cultures was measured in the dark at 25°C. One ml of a 5-day-old suspension cell culture was placed in the chamber containing 1 ml of MSR2 medium.

## 2.3 | RNA isolation and qRT-PCR

Plants and cells of the WT and *why 2-1* mutant lines were harvested for subsequent analyses. Total RNA was extracted from samples using RNeasy® Plant Mini Kit (Qiagen) according to the manufacturer's instructions. RNA concentration was measured using a Nanodrop ND-1000 spectrophotometer (Nanodrop Technologies). First-strand cDNA synthesis was performed using 2 µg of RNA, oligo(dT) primers, and SuperScript-II Reverse Transcriptase (Invitrogen) according to the manufacturer's instructions. The qRT-PCR reactions were performed with 100 ng of cDNA using the SYBR Green technology of Go Taq® qPCR Master Mix (Promega) in a 7500 Real-time PCR System (Life Technologies). The primers sequences for qRT-PCR are reported in Table S1. The expression levels of each gene were normalized to the expression level of the housekeeping gene *ACTIN-2* (*ACT2*; At3g18780) and analyzed using the ΔΔCT method (Livak & Schmittgen, 2001).

## 2.4 | Confocal laser scanning microscopy

Confocal Laser Scanning Microscopy (CLSM) analyses were performed using a Zeiss LSM700 (Carl Zeiss Microscopy). Cells and seedlings were incubated for 20 min in 0.25 µM of tetramethylrhodamine (TMRM) solution. Samples were washed twice (10 mM MES, 10 mM $CaCl_2$, and 5 mM KCl pH 5.8) and then observed. For TMRM detection samples were excited at 535 and fluorescence was measured at 600 nm. For GFP detection, excitation was at 488 nm and emission between 515/530 nm. For the chlorophyll detection, excitation was at 488 nm and detection over 570 nm. For PI detection, excitation was set at 548 nm and emission 573 nm. Acquired images were analyzed using the Fiji—ImageJ bundle software (http://fiji.sc/Fiji). The experiments were performed at least in triplicate, and each sample set comprised 10 samples.

## 2.5 | Transmission electron microscopy

For ultrastructural analysis, small samples of the first leaves from WT and *why 2-1* mutant were fixed in 2.5% (w/v) glutaraldehyde and 1% (v/v) formaldehyde (prepared from paraformaldehyde) in 0.1 M sodium cacodylate (pH 7.4) at 4°C overnight, and postfixed for 4 hr in buffered 1% osmium tetroxide on ice. Washing was done with 0.1 M sodium cacodylate (pH 7.4). The specimens were dehydrated in a graded series of ethanol and embedded in LR White resin (London Resin Company). Polymerization was in gelatine capsules at 60°C for 48 hr. Ultrathin sections of the specimens were cut with a diamond knife at a Leica Ultracut UCT ultramicrotome and placed on formvar-coated copper grids. Sections were stained with uranyl acetate and with lead citrate (Reynolds, 1963), and subsequently observed in a Philips CM10 transmission electron microscope. Two replicates were analyzed for both WT and *why 2-1* and 30–50 images were analyzed for each replicate.

## 2.6 | Electron tomography

The tomography acquisitions were performed using Zeiss LIBRA 200FE-HR TEM, operating at 200 kV and equipped with an in-column omega filter for energy selective imaging and diffraction. The tomographic series were collected with a Fischione 2040 Dual-Axis Tomography Holder, following the dual-axis strategy. The 3D reconstruction is obtained by using weighted back-projection algorithm

and simultaneous alignment method followed by local refinement, as previously described (Vigani et al., 2015). The 3D reconstruction is obtained by use of weighted back-projection algorithm and simultaneous alignment method according to Cantele, Paccagnini, Pigino, Lupetti, and Lanzavecchia (2010). Segmentation was carried out by using the program JUST to obtain the final tomogram of mitochondrial selected (Salvi et al., 2008). The tracings from all sections are modeled as 3D surfaces and displayed as a 3D model by the program Avizo (FEI, SAS).

### 2.7 | In organello protein transport assay

Radiolabeled precursor proteins of AtWHIRLY3 and the organelle-specific control proteins FNR (chloroplast Ferredoxin-NADP-Oxidoreductase) and mitochondrial Rieske Fe/S protein were obtained by in vitro translation in rabbit reticulocyte lysates in the presence of [35S]-methionine. Incubation with intact mitochondria or chloroplasts isolated from pea leaves followed the protocol of Rödiger, Baudisch, and Bernd Klösgen (2010). Competition experiments were performed as described (Bennewitz, Sharma, Tannert, & Klösgen, 2020).

Gel electrophoresis of proteins under denaturing conditions was carried out according to Laemmli (1970). The gels were exposed to phosphorimaging screens and analyzed with a Fujifilm FLA-3000 (Fujifilm) using the software packages BAS Reader (version 3.14) and AIDA (version 3.25; Raytest). Protein concentration was determined according to Bradford (1976).

### 2.8 | Statistical methods

The data were submitted to Student's *t* test for statistically significant difference ($^{*}p < .05$; $^{**}p < .01$). Results are shown as mean ± *SE* with at least three biological replicates.

## 3 | RESULTS

### 3.1 | WHIRLY2 affects mitochondria morphology in cultured cells

To evaluate the role of WHIRLY2 in Arabidopsis, the *why 2-1* mutant line, previously described as a true knockout mutant (Janicka et al., 2012), harboring the T-DNA insertion in the last intron of *WHIRLY2*, was used.

Cell suspension cultures were generated from both WT and *why 2-1* plants. Such cultures represent an ideal system for detailed analysis at the cellular level, being homogeneous, fast growing, easy to handle, and readily accessible to treatments. WT and *why 2-1* cell cultures were characterized with regard to their dry weight (Figure 1a) showing no considerable differences between the two lines. The expression level of *Why 2* was determined at different stages of culture growth and it appeared to be high in the early subculture phase and decreased during cell culture progression (Figure 1b).

With regard to the mitochondrial localization of WHIRLY2, the impact of *Why 2* disruption on mitochondria morphology, ultrastructure, dynamics, and functionality was investigated. CLSM imaging of cultured cells stained with TMRM allowed to evaluate mitochondria morphology in vivo (Figure 1c). While, in the WT line, mitochondria appear to be spherical or punctiform, mutant lines had an impaired mitochondrial morphology whereby mitochondria appeared as more elongated and sometimes showed a peculiar loop shape (Figure 1c, arrows) that in animal system has been demonstrated to be typically associated with cellular oxidative stress conditions (Jaipargas, Barton, Mathur, & Mathur, 2015). TEM images revealed that disruptive rearrangements have taken place in the mitochondria of *why 2-1* cell lines. While in WT cell lines mitochondria were round or oval, contained several cristae and an electron-dense matrix, mitochondria in the *why 2-1* lines, instead, appeared to be swollen, with a reduced number of cristae and a low electron density matrix that might indicate a low functionality (Logan, 2006;Vigani et al., 2015). Interestingly, a large translucent area (Figure 1c inset) in the center of the organelles is present, where fibrillar structures resembling unpacked DNA are evident.

In order to investigate the ultrastructure of mitochondria in the cells of the *why 2-1* mutant line, representative specimens were selected for tomographic reconstructions as described by Vigani et al. (2015). At the ultrastructural level, mitochondria from the WT cell culture displayed homogenous matrices as well as regular internal cristae (Figure 1c). In contrast, in the mutants, a heterogeneous morphology of mitochondria was observed. While few of them appeared to be only slightly altered, the majority of mitochondria had a lower matrix density and a reduced number of cristae when compared to WT plants. Such ultrastructural alterations were observed in all the examined samples from three independent experiments. The numbers of cristae as well as the sizes of the relative intracristae surface areas were determined on mitochondria randomly selected for each sample (Talbe S2). In the *why 2-1* mutant line, the number of cristae per mitochondrion in cultured cells was reduced by about 20%, while the relative intracristae surface area (intracristae surface area per mitochondrion) was even reduced by about 40% ($p < .05$; Table S2). These data taken together strongly support a key role of WHIRLY2 in nucleoid structure maintenance and in shaping the morphology of the mitochondria.

### 3.2 | WHIRLY2 affects the functionality of mitochondria in cultured cells

The observed changes in the morphology of mitochondria might lead to changes in the functionality of these organelles. Therefore, respiratory efficiencies of WT and mutant cell lines were compared. The total respiration of *why 2-1* cells is reduced by 30% compared to WT (Figure 1d, upper plot). Seventy percentage of the residual oxygen consumption present in the *why 2-1* mutant has to be assigned to the alternative

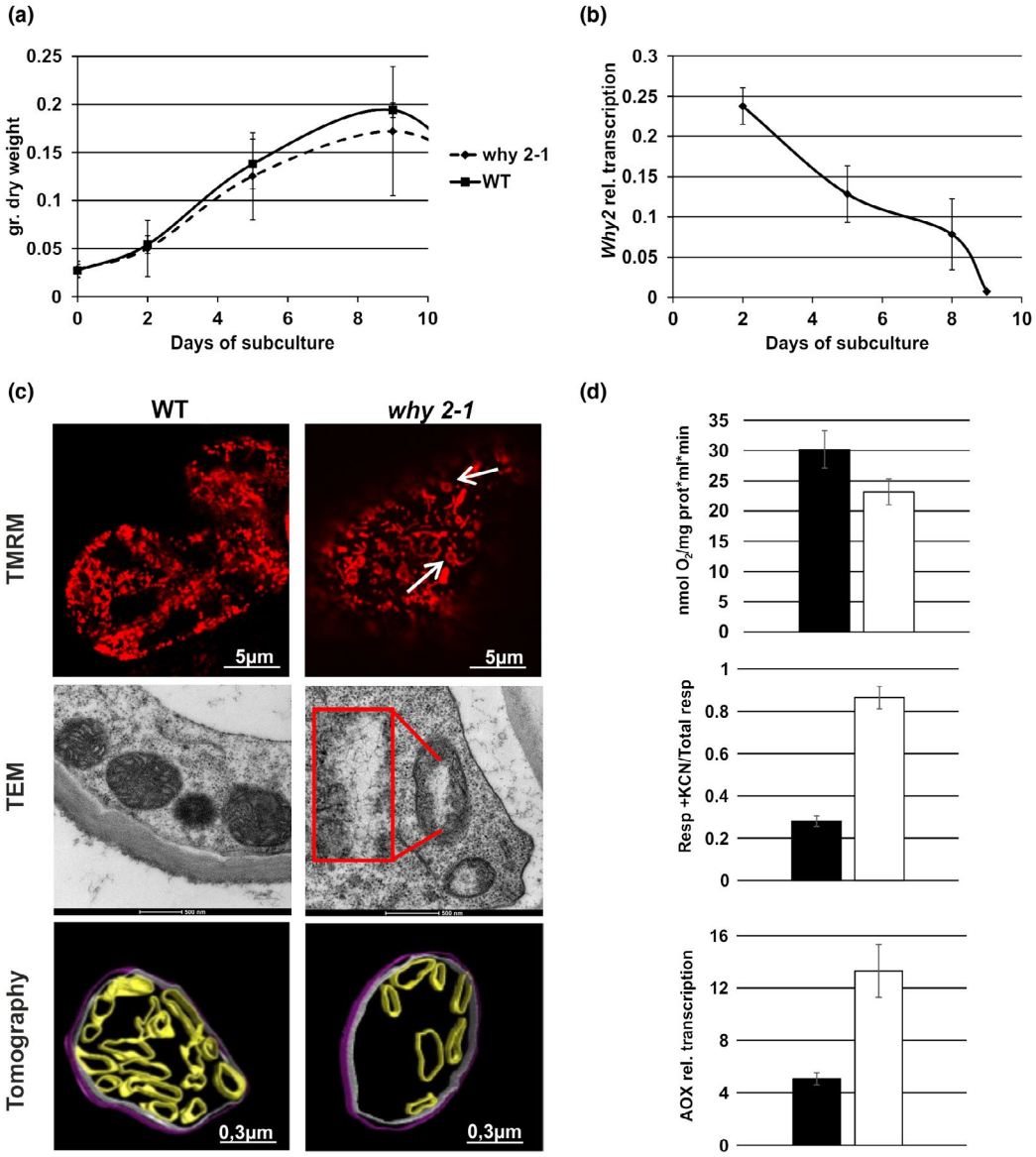


**FIGURE 1** WT and *why 2-1* Arabidopsis suspension cell cultures. (a) Growth curve calculated as dry weight (gr.) at different days after subcultures. (b) *Why 2* expression profile in WT suspension cell cultures at different days after subcultures. (c) Confocal, transmission electron microscope images and tomographic 3D reconstruction model of mitochondria from suspension cell cultures at 5 days after subcultures. Inset magnification 3X. Arrows in the CLSM image indicate mitochondria with peculiar morphology. Different colors were used for the rendering of the different suborganellar structures in the tomographic 3D reconstruction: magenta for inner membranes (IM), blue for outer membranes (OM), and green for cristae. (d) Mitochondria functionality in WT and *why 2-1* suspension cell cultures defined as: Oxygen consumption (upper plot), alternative oxidase capacity (middle plot) of cells treated with 1 mM KCN, relative expression profile of the alternative oxidase (AOX; lower panel). Values represent the mean ± standard deviation of three independent experiments performed in triplicate. The asterisks indicate values that are significantly different from WT cells using the Student's *t* test method (*$p < .05$)

pathway, defined as AOX capacity (Figure 1d, middle plot). AOX capacity is defined as the part of the $O_2$ consumption that is insensitive to the cytochrome (*cyt*) pathway inhibitor KCN, and sensitive to the AOX inhibitor (salicylic-hydroxamic acid, SHAM). This measure of capacity is typically related to the abundance of AOX. Specific AOX gene family members are strongly induced at the transcript and protein level by an insufficient *cyt* pathway capacity downstream of the ubiquinone pool (Vanlerberghe, Martyn, & Dahal, 2016;Yu, 2019). Accordingly, in the *why 2-1* mutant cells, the expression level of the AOX gene is higher than in WT cells (Figure 1d, lower plot), thus supporting the data on an increased AOX capacity observed in the mutant line.

### 3.3 | WHIRLY2 localizes to mitochondria in different plant organs

In order to verify the mitochondrial localization of WHIRLY2 *in planta*, stable transformed Arabidopsis plants harboring the WHIRLY2

coding sequence fused to the GFP gene under control of the 35S CaMV promoter were generated. In stable transformed plants, GFP fluorescence was detected in different organs, in roots (Figure 2a), in leaf (Figure 2b), and in hypocotyl (Figure 2c), as small and highly dynamic punctate structures (Movie S1). In the root, WHIRLY2 appears to be more concentrated at the level of the root tip most likely because of the small size of cells, as compared to elongated cells whose volume is mostly occupied by the vacuole. In Figure 2c, it is shown that WHIRLY2:GFP clearly colocalize with the mitochondria-specific dye TMRM confirming the mitochondrial localization previously determined in transiently transformed protoplasts (Krause et al., 2005). Within the mitochondria, WHIRLY2:GFP fluorescence was not equally distributed but appeared in punctiform spots. It has also been observed that discrete WHIRLY2:GFP spots move between mitochondria during the fusion–fission processes (Movie S1). All these data are consistent with a putative nucleoid association of WHIRLY2, supporting a role in mtDNA packaging/maintenance. Another interesting issue is that WHIRLY2 is not equally present in all the mitochondria stained by TMRM and not even uniformly distributed in the root tip where WHIRLY2 appears to be more concentrated at the level of the tip (Figure 2a).

### 3.4 | *why 2-1* mutant plants have an altered mitochondrial structure

In order to compare the mitochondria morphology in WT and mutant plants in vivo, Arabidopsis roots were stained with TMRM and analyzed by confocal microscopy. In mutant lines, mitochondria appear as elongated organelles (Figure 3 upper panel) characterized by reduced dynamics when compared with those present in the roots of WT plants (Movie S2 and S3). On leaf sections from 3-week-old

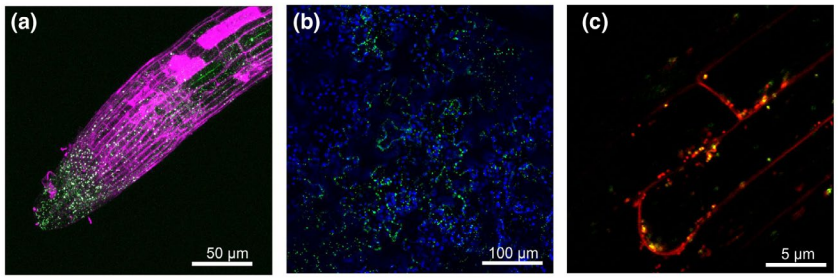


**FIGURE 2** Mitochondrial localization pattern of *35S-WHIRLY2:GFP* in roots (a) stained with propidium iodide (magenta), leaf epidermal cells (b; blue color is due to chlorophyll), and hypocotyl (c) stained with TMRM (red)

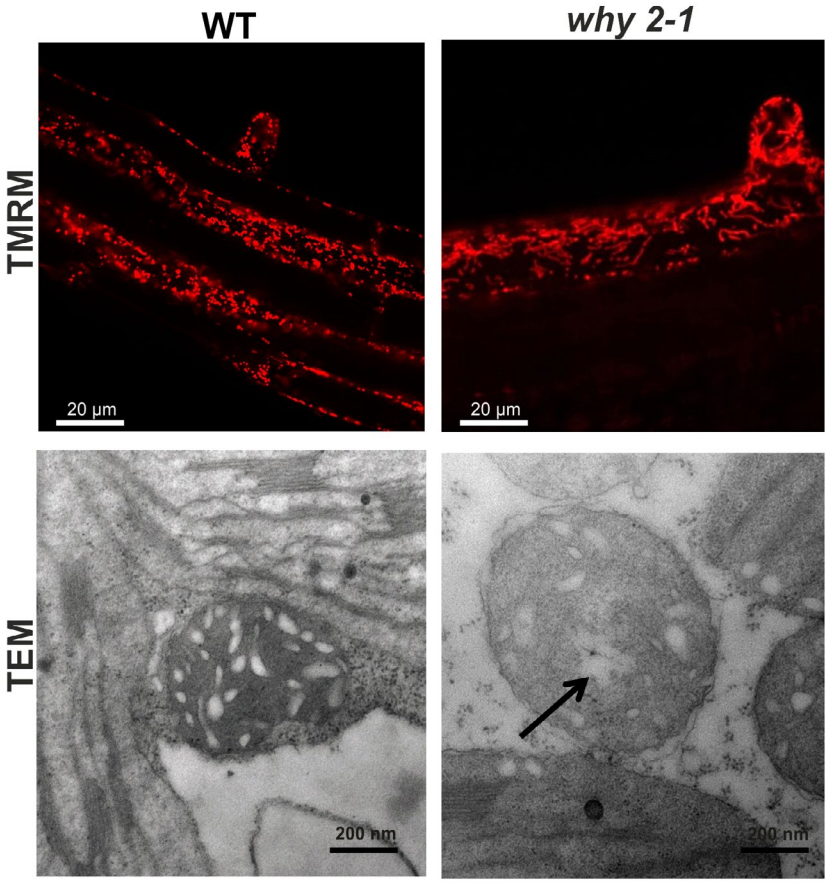


**FIGURE 3** Mitochondria morphology in plant tissues. Upper panel: confocal images of roots of WT and *why 2-1* plants stained with TMRM. Lower panel: transmission electron microscope images of mitochondria from leaf section from 3-week-old WT and mutant plants. Arrow indicates translucent area within mitochondria matrix

plants of Col-0 and *why 2-1* mutant TEM analyses were performed as indicated in Figure 3 (lower panel). In the mutant line, mitochondria resemble those identified in cultured cells confirming the swollen morphology, the reduced number of cristae, and the presence of a translucent area (arrow) within the mitochondrial matrix. Approximately 30% of the mitochondria in leaves of the mutant line exhibited such altered morphology compared with the WT (Figure 3 lower panel). Furthermore, as calculated from TEM images of leaf sections, the relative intracristae surface area decreased by about 40% ($p < .05$) in the *why 2-1* mutant line when compared to the WT (Table S2).

### 3.5 | Seed germination is compromised in *why 2-1* mutants

In Figure 4a, the expression profile of *WHIRLY2* in different developmental phases, from imbibed seeds to flowering stage, is reported. The results show a relatively high level of the expression in 24 hr imbibed seeds, as expected for proteins involved in organelle DNA repair/replication in rapidly growing tissues (Diray-Arce, Liu, Cupp, Hunt, & Nielsen, 2013), with a subsequent drop in expression level.

In order to investigate whether the presence of aberrant mitochondria in the *why 2-1* mutant could have consequences for development of the plant, WT and *why 2-1* plants were compared at different stages of development, starting from seed germination. Sterilized seeds were sown in solid one-half MS medium, stratified for 48 hr, and, then, placed in a growth chamber. Seeds were microscopically analyzed to evaluate the rupture of the *testa* indicating the beginning of germination process (Figure 4b). A clear difference between the two genotypes was detected: *why 2-1* seeds showed a significant reduction (20%) in the percentage of germination compared to the WT (Figure 4c). These data highlight the important role of WHIRLY2 in a phase of plant life characterized by active mtDNA synthesis, such as seed germination (Paszkiewicz, Gualberto, Benamar, Macherel, & Logan, 2017).

### 3.6 | WHIRLY3 mRNA level and protein abundance are enhanced in shoots of the *why 2-1* mutant

The "mild" development-dependent phenotype of the *why 2-1* mutant suggests that in adult mutant plants, where no phenotype is shown, the lack of the WHIRLY2 protein could be compensated, at least in part. A possible candidate for such functional compensation could be another WHIRLY protein. In the absence of WHIRLY2 an increase in the mRNA level of WHIRLY3 was observed at earlier stages of shoot development (Stage 1.02; Figure 4). The low expression level of *WHIRLY3* is, instead, not altered in imbibed seeds. These data suggest a tight coordination between the expression of *Why 2* and *Why 3*.

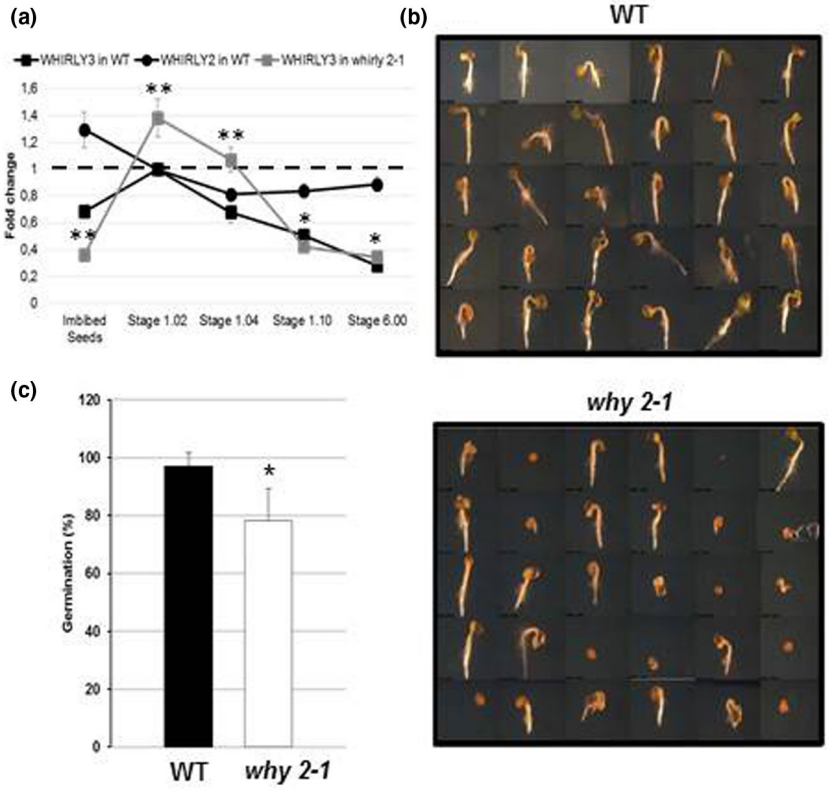


**FIGURE 4** Germination assay of WT and *why 2-1* mutant. (a) Expression profile of *Why 2* and *Why 3* genes in WT and *why 2-1* plants and seeds. The expression was analyzed in 24 hr imbibed seeds and in plants at 1.02, 1.04, 1.10, and 6.00 stages of growth. Data were analyzed using the ΔΔCT method. Values represent the mean ± confidence interval ($p < .05$) of three independent experiments performed in triplicate. (b) Representative stereomicroscope images of WT and *why 2-1* seedlings 4 days after sowing (DAS); (c) Percentage of germinated seed at 4 DAS

### 3.7 | The WHIRLY3 protein is imported into chloroplasts as well as into mitochondria

Functional compensation of absence of WHIRLY2 is also a matter of the correct subcellular localization, i.e., WHIRLY3 must be present in the same subcellular compartments to be capable of compensating the lack of WHIRLY2. However, upon transient transformation of suitable GFP-fusion polypeptides in tobacco protoplasts, the WHIRLY2 protein was shown to accumulate in mitochondria, while WHIRLY3 could be detected solely in chloroplasts (Krause et al., 2005), which makes a functional compensation rather unlikely. On the other hand, *in organello* protein transport experiments performed with WHIRLY2 clearly demonstrated dual targeting properties of the protein, i.e., the authentic precursor is imported into both, chloroplasts and mitochondria, when incubated with isolated intact organelles (Krause et al., 2005). Such complementing *in organello* transport experiments have not been carried out though with WHIRLY3.

Therefore, *in organello* protein transport experiments using intact mitochondria and chloroplasts that were isolated from a single pulping of pea leaves (Rödiger et al., 2010) were performed here with the authentic precursor of WHIRLY3. In addition to WHIRLY3, two control proteins with known organelle localization, namely, chloroplast FNR (Ferredoxin-NADP-Oxidoreductase) and the mitochondrial Rieske-Fe/S protein (mtRi), were analyzed in parallel. For this purpose, freshly isolated intact organelles were incubated with the respective radiolabeled precursor proteins, which were obtained by in vitro transcription of the corresponding cDNA clones and subsequent in vitro translation with reticulocyte lysates in the presence of [35S]-methionine. The two

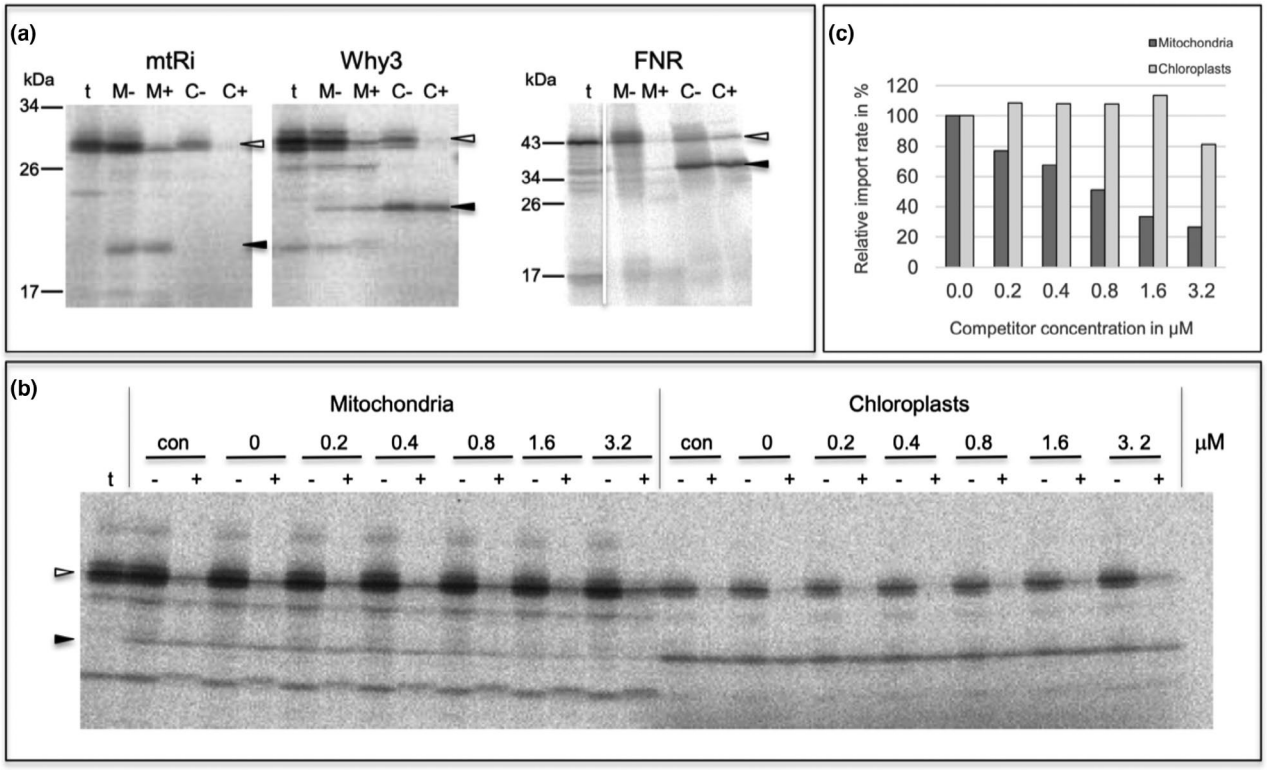


**FIGURE 5** *In organello* protein transport experiments with isolated pea organelles. (a) Radiolabeled precursor polypeptides of mitochondrial Rieske Fe/S protein (*mtRi*), WHIRLY3 (*Why3*), and chloroplast Ferredoxin-NADP-Oxidoreductase (*FNR*) were obtained by coupled in vitro transcription/translation of the corresponding cDNA clones and incubated for 20 min at 25°C with either intact mitochondria (*lanes M*) or chloroplasts (*lanes C*) from pea. After the import reaction, the organelles were recovered by centrifugation and treated with thermolysin (*lanes M+*, *C+*) or mock treated (*lanes M-*, *C-*). Stoichiometric amounts of each fraction corresponding to 50 µg protein (mitochondria) or 12.5 µg chlorophyll (chloroplasts) were separated on a 10%–17.5% SDS polyacrylamide gradient gel and visualized by phosphorimaging. In *lanes t*, 1 µl aliquots of the in vitro translation assays (corresponding to 10% of the protein added to each import reaction) were loaded. The position of precursor and mature polypeptides are indicated by *open arrowheads* and *filled arrowheads*, respectively. The size of molecular marker proteins is given in kDa. (b) Effect of competitor protein on organelle import of WHIRLY3. *In organello* protein transport experiments with the WHIRLY3 precursor protein were performed in the absence (*con*) or presence of increasing amounts of the precursor of mitochondrial Rieske Fe/S-protein which was obtained by heterologous overexpression in *Escherichia coli*. The concentration of competitor protein present in each assay (given in µM) is indicated above the lanes. (c) Bar chart showing the relative amounts of WHIRLY3 accumulating in the organelles of the competition experiment shown in (b). The bands corresponding to mature WHIRLY3 polypeptide in lanes + were quantified and depicted in terms of percentage of mature WHIRLY3 in the control reaction in the absence of competitor (lanes 0)

control proteins showed the expected organelle specificity: mtRi is imported into mitochondria but not into chloroplasts, while FNR shows the reciprocal result, i.e., it is transported into chloroplasts but not into mitochondria (Figure 5). Within the organelles, the two precursor proteins are cleaved by organellar processing peptidases to yield the respective mature proteins. These processing products are resistant to protease added externally to the assays after import, which confirms that they have been internalized into the organelles (Figure 5). In contrast, precursor proteins that are not imported but remain attached to the organellar envelopes in the course of the experiment are largely, although not always completely, degraded under these conditions.

Remarkably, WHIRLY3 is not only imported into chloroplasts but also accumulates in a protease-protected manner also in mitochondria (Figure 5). Within both organelles the protein is processed after membrane transport to a product of approximately 24 kDa, which corresponds well to the size of the mature protein (Isemer et al., 2012). In contrast, the control protein for chloroplast import, FNR, does not show any hint of mitochondrial import in these assays which rules out that the mitochondrial import of WHIRLY3 observed is due to contaminating chloroplasts in the mitochondrial preparation.

This was further confirmed by competition experiments that were performed as a complementary approach to evaluate the dual targeting properties of WHIRLY3. In these experiments, the mitochondrial import machinery was gradually saturated by excess amounts of the mitochondrial control protein, mtRi, which was obtained by overexpression in *Escherichia coli*. With increasing concentration of mtRi precursor in the assay, import of WHIRLY3 into mitochondria decreased gradually (Figure 5). Control experiments showed that the import of WHIRLY3 into chloroplasts remained unaffected in the presence of the competitor protein, which emphasizes the specificity of the competition reaction.

## 4 | DISCUSSION

WHIRLY2 is a member of the small plant-specific family of WHIRLY proteins binding to single stranded DNA and proposed to be key components of the organelle repair machinery (Cappadocia et al., 2010;Marechal et al., 2009). It has been reported that WHIRLY2 and other plant-specific single-stranded DNA binding proteins hinder microhomology-mediated end-joining (MMEj; García-Medel et al., 2019). In the present study, it has been demonstrated that WHIRLY2 deficiency compromises mitochondria ultrastructure, morphology, and functionality. In *why 2-1* mutants, mitochondria contain a low number of cristae and show a reduced functionality if compared to the WT, as evidenced by the reduced respiration activity and the low electron density of the organelles analyzed by TEM. TEM analysis showed that *why 2-1* mutant mitochondria house a peculiar translucent area likely containing filamentous mtDNA. This phenomenon resembles what has been already observed in WHIRLY1 knockdown plants of barley where translucent areas in chloroplasts from WHIRLY1-deficient plants coincide with reduced packaging of nucleoids (Krupinska et al., 2014). The data presented in this study confirm the nucleoid localization of WHIRLY2 but also support a structural role in mitochondria nucleoid organization. The alteration of the shape of mitochondria toward swollen organelles, observed in *why 2-1* plants, is likely due to an impairment in the recruitment of the fission proteins involved in mitochondria division (Yan, Duanmu, Zeng, Liu, & Song, 2019) while the elongation could be attributed to a perturbation of the fusion/fission balance. These data strongly suggest that a tight association exist between nucleoid organization and mitochondria morphology and dynamics. Besides, in mammals, it has been demonstrated that the integrity of mtDNA/nucleoids plays an important role in the remodeling of cristae structures (Ban-Ishihara, Ishihara, Sasaki, Mihara, & Ishihara, 2013). Moreover, it has been suggested that, in plants, mitochondrial dynamics, that reshape organelle morphology through the ongoing fusion and fission events, is an important feature for maintaining mitochondrial plasticity but also to provide a means for promoting recombination of DNA fragments (Arimura, 2018). MMF is likely to facilitate nucleoid transmission, mitochondrial DNA (mtDNA) recombination, and the homogenization of mitochondrial components, thus providing a type of quality control for mitochondrial populations (Rose & McCurdy, 2017).

It has been demonstrated that in *why 2-1* plants the microhomology-mediated DNA rearrangements (MHMRs) occur at higher levels than in the WT. It is likely that the accumulation of DNA rearrangements could be responsible for nucleoid disorder and consequently for the elongated mitochondria. The observed reduced mitochondrial dynamics would in turn favors mitochondria fusion and elongation. The alterations in mitochondrial morphology and functionality observed in the *why 2-1* mutant are expected to have a severe impact on development and growth of the plants. For this reason, an impairment of growth is expected. On the other hand, no obvious phenotype is evident in the *why 2-1* mutant plants during vegetative growth (Maréchal et al., 2008). Indeed a significant decrease in seed germination percentage was observed in *why 2-1* compared to WT background. A possible explanation might be that the impact of WHIRLY2 absence is particularly pronounced when organelle DNA synthesis is active, such as in highly dividing cultured cells and during germination (Arimura, 2018;Cheng et al., 2017).

During germination a metabolic reorganization occurs: the higher expression of WHIRLY2 was observed in the 24h imbibed seeds when reactivation of cellular and mitochondrial metabolism occurs (Paszkiewicz et al., 2017). It must be taken into consideration that mtDNA replication probably takes place by recombination-dependent replication occurring as a result of double-stranded homologous recombination breakage or of double- or single-stranded break repair mechanisms that likely involve WHIRLY2 (Cheng et al., 2017).

The lack of an evident mutant phenotype of the mature plant upon abrogation of *Why 2* expression suggests the presence of functional homologues or the activation of compensating mechanisms in mitochondria. Possible candidates for compensation of WHIRLY2 deficiency in the *why 2-1* mutant are WHIRLY1 and WHIRLY3. WHIRLY1 was shown to be exclusively imported into

chloroplasts both in *in organello* protein transport experiments and after transient transformation of protoplasts (Krause et al., 2005) which precludes a functional role in mitochondria. WHIRLY3 was likewise found solely in chloroplasts after transient expression of a reporter construct (Krause et al., 2005). However, this result was not independently confirmed with a second method which was shown to be essential to prevent potential misinterpretation (Sharma, Bennewitz, & Klösgen, 2018). Indeed, as proven here by *in organello* import as well as competition experiments, WHIRLY3 is dually targeted into both, mitochondria and chloroplasts (Figure 5), which in principle enables the compensation of WHIRLY2 deficiency by WHIRLY3. In line with that, *Why 3* expression is actually higher in the *why 2-1* mutant than in the WT at early stages of development.

In a similar scenario, WHIRLY3 might even compensate for WHIRLY1 deficiency considering the lack of an apparent mutant phenotype of the *why1* knockout mutant (Yoo, Kwon, Lee, & Chung, 2007). In contrast, in plants lacking WHIRLY3 such as maize and barley, WHIRLY1 deficiency leads to a disturbance of chloroplast development (Krupinska et al., 2019;Prikryl, Watkins, Friso, van Wijk, & Barkan, 2008).

Although further efforts are required to elaborate the functional interaction of WHIRLY proteins, these data suggest already that the coordination of the three WHIRLY proteins in *A. thaliana* is required to guarantee the integrity of the organellar genomes in the early phases of seed germination.

## 5 | CONCLUSIONS

In this study, we identify a role of WHIRLY2 in maintaining mitochondria morphology and functionality. In particular, we found that the absence of WHIRLY2 is associated with a disorganization of the nucleoids and the fine ultrastructure of the mitochondria both in cultured cells and in leaf. We demonstrated that the strong mitochondria alterations observed in the *why 2-1* mutant significantly compromise the seed germination process. Experiments by means of an *in organelle* import assay demonstrate that along with WHIRLY2 also WHIRLY 3 can enter the mitochondria, strongly suggesting a compensatory activity of WHIRLY3 in *why 2-1* mutant plants. These results cast new light on the role of the mitochondrial protein WHIRLY2 in plant cells paving the way for further studies on the link between mitochondria structure/morphology and functionality both at the cellular and at the plant level.

### ACKNOWLEDGMENTS

We thank Prof Fanco Faoro, Dario Maffio (University of Milan) and Dr Anna M. Ferretti (National Research Council, Milan) for the assistance in TEM-Eletrocton tomography analysis. Funding: University of Padova, institutional funds to MZ; CARIPARO foundation fellowship to SG; Ministry of Education, University and Research fellowship to YLN.

### AUTHOR CONTRIBUTIONS

MZ and KK conceived the project, MZ designed the experiments and analyzed the data; SG and YLN performed most of the experiments on Arabidopsis plants and cell cultures; NLR and MM performed the TEM experiments; BB and RBK designed and performed the experiments of *in organello* assay; GV with the technical assistance of FC performed the tomography experiments; MZ and KK wrote the article with contributions of all the authors; FLS supervised and completed the writing; MZ agrees to serve as the author responsible for contact and ensures communication.

### ORCID

*Yuri L. Negroni* https://orcid.org/0000-0002-2163-6687
*Ralf B. Klösgen* https://orcid.org/0000-0002-0555-0234
*Nicoletta La Rocca* https://orcid.org/0000-0003-4866-5952
*Francesca Cantele* https://orcid.org/0000-0003-1373-0793
*Gianpiero Vigani* https://orcid.org/0000-0001-8852-3866
*Michela Zottini* https://orcid.org/0000-0001-8930-2969

### REFERENCES

Akbudak, M. A., & Filiz, E. (2019). Whirly (Why) transcription factors in tomato (Solanum lycopersicum L.): genome-wide identification and transcriptional profiling under drought and salt stresses. *Molecular Biology Reports*, *46*(4), 4139–4150. https://doi.org/10.1007/s11033-019-04863-y

Arimura, S. (2018). Fission and fusion of plant mitochondria, and genome maintenance. *Plant Physiology*, *176*(1), 152–161. https://doi.org/10.1104/pp.17.01025

Ban-Ishihara, R., Ishihara, T., Sasaki, N., Mihara, K., & Ishihara, N. (2013). Dynamics of nucleoid structure regulated by mitochondrial fission contributes to cristae reformation and release of cytochrome c. *Proceedings of the National Academy of Sciences of the United States of America*, *110*(29), 11863–11868. https://doi.org/10.1073/pnas.1301951110

Bennewitz, B., Sharma, M., Tannert, F., & Klösgen, R. B. (2020) Dual targeting of TatA points to a chloroplast-like Tat pathway in plant mitochondria. bioRxiv. https://doi.org/10.1101/2020.04.06.026997

Boyes, D. C., Zayed, A. M., Ascenzi, R., McCaskill, A. J., Hoffman, N. E., Davis, K. R., & Görlach, J. (2001). Growth stage-based phenotypic analysis of Arabidopsis: A model for high throughput functional genomics in plants. *The Plant Cell*, *13*(7), 1499–1510. https://doi.org/10.1105/tpc.13.7.1499

Bradford, M. M. (1976). A rapid and sensitive method for the quantitation of microgram quantities of protein utilizing the principle of protein-dye binding. *Analytical Biochemistry*, *72*, 248–254. https://doi.org/10.1016/0003-2697(76)90527-3

Cai, Q., Guo, L., Shen, Z. R., Wang, D. Y., & Zhang, Q. (2015). Elevation of pollen mitochondrial DNA copy number by WHIRLY2: Altered respiration and pollen tube growth in arabidopsis. *Plant Physiology*, *169*(1), 660–673. https://doi.org/10.1104/pp.15.00437

Cantele, F., Paccagnini, E., Pigino, G., Lupetti, P., & Lanzavecchia, S. (2010). Simultaneous alignment of dual-axis tilt series. *Journal of Structural Biology*, *169*(2), 192–199. https://doi.org/10.1016/j.jsb.2009.10.003

Cappadocia, L., Maréchal, A., Parent, J.-S., Lepage, É., Sygusch, J., & Brisson, N. (2010). Crystal structures of DNA-whirly complexes and their role in *Arabidopsis* Organelle genome repair. *The Plant Cell*, *22*(6), 1849–1867. https://doi.org/10.1105/tpc.109.071399

Cappadocia, L., Parent, J. S., Sygusch, J., & Brisson, N. (2013). A family portrait: Structural comparison of the Whirly proteins from

*Arabidopsis thaliana* and Solanum tuberosum. *Acta Crystallographica Section F*, *69*(11), 1207–1211. https://doi.org/10.1107/S1744309113028698

Cheng, N., Lo, Y. S., Ansari, M. I., Ho, K. C., Jeng, S. T., Lin, N. S., & Dai, H. (2017). Correlation between mtDNA complexity and mtDNA replication mode in developing cotyledon mitochondria during mung bean seed germination. *New Phytologist*, *213*(2), 751–763. https://doi.org/10.1111/nph.14158

Desveaux, D., Allard, J., Brisson, N., & Sygusch, J. (2002). A new family of plant transcription factors displays a novel ssDNA-binding surface. *Nature Structural Biology*, *9*(7), 512–517. https://doi.org/10.1038/nsb814

Desveaux, D., Maréchal, A., & Brisson, N. (2005). Whirly transcription factors: Defense gene regulation and beyond. *Trends in Plant Science*, *10*(2), 95–102. https://doi.org/10.1016/j.tplants.2004.12.008

Diray-Arce, J., Liu, B., Cupp, J. D., Hunt, T., & Nielsen, B. L. (2013). The Arabidopsis At1g30680 gene encodes a homologue to the phage T7 gp4 protein that has both DNA primase and DNA helicase activities. *BMC Plant Biology*, *13*(1), 1–11. https://doi.org/10.1186/1471-2229-13-36

García-Medel, P. L., Baruch-Torres, N., Peralta-Castro, A., Trasviña-Arenas, C. H., Torres-Larios, A., & Brieba, L. G. (2019). Plant organellar DNA polymerases repair double-stranded breaks by microhomology-mediated end-joining. *Nucleic Acids Research*, *47*(6), 3028–3044. https://doi.org/10.1093/nar/gkz039

Gualberto, J. M., & Kühn, K. (2014). DNA-binding proteins in plant mitochondria: Implications for transcription. *Mitochondrion*, *19*, 323–328. https://doi.org/10.1016/j.mito.2014.02.004

Isemer, R., Mulisch, M., Schäfer, A., Kirchner, S., Koop, H. U., & Krupinska, K. (2012). Recombinant Whirly1 translocates from transplastomic chloroplasts to the nucleus. *FEBS Letters*, *586*(1), 85–88. https://doi.org/10.1016/j.febslet.2011.11.029

Jaipargas, E.-A., Barton, K. A., Mathur, N., & Mathur, J. (2015). Mitochondrial pleomorphy in plant cells is driven by contiguous ER dynamics. *Frontiers in Plant Science*, *6*, 1–14. https://doi.org/10.3389/fpls.2015.00783

Janicka, S., Kühn, K., Le Ret, M., Bonnard, G., Imbault, P., Augustyniak, H., & Gualberto, J. M. (2012). A RAD52-like single-stranded DNA binding protein affects mitochondrial DNA repair by recombination. *Plant Journal*, *72*(3), 423–435. https://doi.org/10.1111/j.1365-313X.2012.05097.x

Krause, K., Kilbienski, I., Mulisch, M., Rödiger, A., Schäfer, A., & Krupinska, K. (2005). DNA-binding proteins of the Whirly family in *Arabidopsis thaliana* are targeted to the organelles. *FEBS Letters*, *579*(17), 3707–3712. https://doi.org/10.1016/j.febslet.2005.05.059

Krupinska, K., Braun, S., Nia, M. S., Schäfer, A., Hensel, G., & Bilger, W. (2019). The nucleoid-associated protein WHIRLY1 is required for the coordinate assembly of plastid and nucleus-encoded proteins during chloroplast development. *Planta*, *249*(5), 1337–1347. https://doi.org/10.1007/s00425-018-03085-z

Krupinska, K., Oetke, S., Desel, C., Mulisch, M., SchÃ¤fer, A., Hollmann, J., … Hensel, G. Ã¶tZ. (2014). WHIRLY1 is a major organizer of chloroplast nucleoids. *Frontiers in Plant Science*, *5*(August), 1–11. https://doi.org/10.3389/fpls.2014.00432

Laemmli, U. K. (1970). 227680a0. *Nature*, *227*, 680–685.

Livak, K. J., & Schmittgen, T. D. (2001). Analysis of relative gene expression data using real-time quantitative PCR and the 2-ΔΔCT method. *Methods*, *25*(4), 402–408. https://doi.org/10.1006/meth.2001.1262

Logan, D. C. (2006). The mitochondrial compartment. *Journal of Experimental Botany*, *57*(6), 1225–1243. https://doi.org/10.1093/jxb/erj151

Maréchal, A., Parent, J. S., Sabar, M., Véronneau-Lafortune, F., Abou-Rached, C., & Brisson, N. (2008). Overexpression of mtDNA-associated AtWhy2 compromises mitochondrial function. *BMC Plant Biology*, *8*, 1–15. https://doi.org/10.1186/1471-2229-8-42

Marechal, A., Parent, J.-S., Veronneau-Lafortune, F., Joyeux, A., Lang, B. F., & Brisson, N. (2009). Whirly proteins maintain plastid genome stability in Arabidopsis. *Proceedings of the National Academy of Sciences of the United States of America*, *106*(34), 14693–14698. https://doi.org/10.1073/pnas.0901710106

Murashige, T., & Skoog, F. (1962). A revised medium for rapid growth and bioassays with tobacco tissue cultures. *Physiologica Plantarum*, *15*, 473–497.

Paszkiewicz, G., Gualberto, J. M., Benamar, A., Macherel, D., & Logan, D. C. (2017). Arabidopsis seed mitochondria are bioenergetically active immediately upon imbibition and specialize via biogenesis in preparation for autotrophic growth. *The Plant Cell*, *29*(1), 109–128. https://doi.org/10.1105/tpc.16.00700

Prikryl, J., Watkins, K. P., Friso, G., van Wijk, K. J., & Barkan, A. (2008). A member of the Whirly family is a multifunctional RNA- and DNA-binding protein that is essential for chloroplast biogenesis. *Nucleic Acids Research*, *36*(16), 5152–5165. https://doi.org/10.1093/nar/gkn492

Reynolds, E. S. (1963). The use of lead citrate at high pH as an electron-opaque stain in electron microscopy. *The Journal of Cell Biology*, *17*(1), 208–212. https://doi.org/10.1083/jcb.17.1.208

Rödiger, A., Baudisch, B., & Bernd Klösgen, R. (2010). Simultaneous isolation of intact mitochondria and chloroplasts from a single pulping of plant tissue. *Journal of Plant Physiology*, *167*(8), 620–624. https://doi.org/10.1016/j.jplph.2009.11.013

Rose, R. J., & McCurdy, D. W. (2017). New beginnings: Mitochondrial renewal by massive mitochondrial fusion. *Trends in Plant Science*, *22*(8), 641–643. https://doi.org/10.1016/j.tplants.2017.06.005

Salvi, E., Cantele, F., Zampighi, L., Fain, N., Pigino, G., Zampighi, G., & Lanzavecchia, S. (2008). JUST (Java User Segmentation Tool) for semi-automatic segmentation of tomographic maps. *Journal of Structural Biology*, *161*(3), 287–297. https://doi.org/10.1016/j.jsb.2007.06.011

Sharma, M., Bennewitz, B., & Klösgen, R. B. (2018). Dual or not dual? - Comparative analysis of fluorescence microscopy-based approaches to study organelle targeting specificity of nuclear-encoded plant proteins. *Frontiers in Plant Science*, *9*, 1350. (10.3389/fpls.2018.01350)

Vanlerberghe, G. C., Martyn, G. D., & Dahal, K. (2016). Alternative oxidase: A respiratory electron transport chain pathway essential for maintaining photosynthetic performance during drought stress. *Physiologia Plantarum*, *157*(3), 322–337. https://doi.org/10.1111/ppl.12451

Vigani, G., Faoro, F., Ferretti, A. M., Cantele, F., Maffi, D., Marelli, M., … Zocchi, G. (2015). Three-dimensional reconstruction, by TEM tomography, of the ultrastructural modifications occurring in *Cucumis sativus* L. mitochondria under fe deficiency. *PLoS ONE*, *10*(6), 1–13. https://doi.org/10.1371/journal.pone.0129141

Xu, Y.-Z., Arrieta-Montiel, M. P., Virdi, K. S., de Paula, W. B. M., Widhalm, J. R., Basset, G. J., … Mackenzie, S. A. (2011). MutS HOMOLOG1 Is a nucleoid protein that alters mitochondrial and plastid properties and plant response to high light. *The Plant Cell*, *23*(9), 3428–3441. https://doi.org/10.1105/tpc.111.089136

Yan, C., Duanmu, X., Zeng, L., Liu, B., & Song, Z. (2019). Mitochondrial DNA: Distribution. *Mutations, and Elimination.*, *1*, 1–15. https://doi.org/10.3390/cells8040379

Yoo, H. H., Kwon, C., Lee, M. M., & Chung, I. K. (2007). Single-stranded DNA binding factor AtWHY1 modulates telomere length homeostasis in Arabidopsis. *Plant Journal*, *49*(3), 442–451. https://doi.org/10.1111/j.1365-313X.2006.02974.x

Yu, S. B., & Pekkurnaz, G. (2018). Mechanisms orchestrating mitochondrial dynamics for energy homeostasis. *Journal of Molecular Biology*, *430*(21), 3922–3941. https://doi.org/10.1016/j.jmb.2018.07.027

Yu, Y. (2019). Prohibitin shuttles between mitochondria and the nucleus to control genome stability during the cell cycle. *Plant Physiology*, *179*(4), 1435–1436. https://doi.org/10.1104/pp.19.00176

Zottini, M., Barizza, E., Bastianelli, F., Carimi, F., & Lo Schiavo, F. (2006). Growth and senescence of Medicago truncatula cultured cells are associated with characteristic mitochondrial morphology. *New Phytologist*, *172*(2), 239–247. https://doi.org/10.1111/j.1469-8137.2006.01830.x

## SUPPORTING INFORMATION

Additional Supporting Information may be found online in the Supporting Information section.

**How to cite this article:** Golin S, Negroni YL, Bennewitz B, et al. WHIRLY2 plays a key role in mitochondria morphology, dynamics, and functionality in *Arabidopsis thaliana*. *Plant Direct*. 2020;4:1–12. https://doi.org/10.1002/pld3.229